Università degli Studi di Palermo

AREA QUALITÀ, PROGRAMMAZIONE E SUPPORTO STRATEGICO
SETTORE STRATEGIA PER LA RICERCA
U. O. DOTTORATI

Dottorato di Ricerca in Scienze Fisiche e Chimiche
Dipartimento di Fisica e Chimica Emilio Segrè
Settore Scientifico Disciplinare CHIM02

pH-Responsive Cyclodextrin-Surfactant Inclusion Complexes: Thermodynamics and Structural Aspects

IL DOTTORE
Larissa DOS SANTOS SILVA ARAÚJO

IL COORDINATORE
Prof. Marco CANNAS

IL TUTOR
Prof. Giuseppe LAZZARA

EVENTUALE CO TUTOR
Dr. Leonardo CHIAPPISI

Dr. Ralf SCHWEINS

CICLO XXXV
ANNO CONSEGUIMENTO TITOLO 2023

" I stand
on the sacrifices
of a million women before me
thinking
what can I do
to make this mountain taller
so the women after me
can see farther
- legacy "

Rupi Kaur

To my family,
in special, to my beloved parents,
Áurea and Edmundo.

Abstract

This thesis presents the investigation of the multilevel assembly of the alkyl oligoethylenoxide carboxylic acids and cyclodextrins. The aim of the work is to combine the short-range host-guest and long-range electrostatic interactions to form highly-ordered supramolecular complexes. The interactions between the components affect their individual response and their properties; therefore, the knowledge of the nature and the influence of their chemical structure is essential to understand the system's behaviour. Polyoxyethylene alkyl carboxylic acids are an attractive class of surfactants to integrate both inclusion complexes and polyelectrolyte systems due to their pH and thermoresponsiveness.

The complementary combination approach of thermodynamic and structural investigations allowed probing the formation and responsiveness of the complexes. First, the inclusion complexes systems were studied by densitometry and isothermal titration calorimetry and a comprehensive structural investigation was conducted by small-angle neutron scattering, differential scanning calorimetry and microscopy. The spontaneous formation of the host-guest complexes at different pH was evidenced, and their assembly as building blocks of large supramolecular aggregates with rich structural behaviour was verified. Different aspects of these systems were studied, and it was possible to tune the structures by exploring the components' concentration, cyclodextrin-to-surfactant ratio, and the pH response of the surfactants. The charge density plays an important role in directing the assembly into highly-ordered cylindrical structures without drastically changing the thermodynamics of the inclusion complex formation. In addition, the analysis allowed to unveil the effect of the temperature, the chemical structure of the surfactants and the cyclodextrin on the morphology of the aggregates.

Finally, the co-assembly between inclusion complexes and chitosan exploring the long-range electrostatic interactions was assessed in different aspects with a main focus on their structures and directing their assembly by controlling the pH and concentration of the systems.

This thesis delivers a thermodynamic and structural complementary approach that allows designing supramolecular aggregates of the desired properties with potential applications in a variety of formulations. It also highlights the importance of evaluating the impact of the tuning parameters in the hierarchical assembly process from the short to the long-range interactions envisioning their systematic application.

Acknowledgements

I would like to express my gratitude to all the people who helped and supported me through this journey in the Institut Laue-Langevin and Università degli Studi di Palermo. Thank you for contributing to my scientific and personal development.

First, I would like to acknowledge my supervisors Prof. Dr. Giuseppe Lazzara and Dr. Leonardo Chiappisi. Thank you for welcoming me to your research groups in Italy and France and offering me great opportunities over these years. Besides the professional and scientific competencies, thank you for the patience, guidance and for promptly answering my (many) questions.

I would like to thank the Large Scale Structures Group for the great scientific moments, discussions and outings. Special thanks to Lionel Porcar, Sylvain Prévost, Anne Martel, Martina Sandroni and Ralf Schweins for always being so open to answering my questions with very nice discussions. I am deeply thankful to Prof. Christoph Schalley for welcoming me to his Group at Freie Univerität Berlin and for the patience and support offered. Thank you for the many fruitful scientific curiosities and discussions brought to our coffee breaks. I also would like to express my gratitude to Schalley's group members for making my stay in Berlin very pleasant. I am thankful to Beth, Donal, Emily, Audrey, Eoghan and Leonardo for bringing joy to my days in Palermo and for the great friendship.

I would like to thank the PhD community at ILL for the support and partnership for scientific and social matters! I can't thank enough Javier Carrascosa-Tejedor, Andreas Santamaria and Giacomo Corucci for the great times at the office, for the rich discussions trying to solve our scientific problems, for being excited when I got good results and for believing and supporting me through the bad days. Je n'ai peux pas oublier le meilleur café, Le Café Trois Deux Six, for all the coffees, great conversations, beers, scientific and not too scientific discussions, even when we found a way to involve our knowledge in trying to find "the best" coffee recipe! A big THANKS to Mohit Agarwal, Wenke Muller, Moritz Frewein, Xaver Brems, Martha Stando, Xamuel Lund, Sofia Erikson, Sam Winnal and Peter Mills for the great company in this journey! Thank you for being there for the beers, scientific discussions and code debug sessions!

Eu gostaria de agradecer as pessoas que caminharam ao meu lado até aqui, na França, na Itália, no Brasil e na Alemanha. À minha amiga, Ana Luiza Viera Maia, por estar sempre ao meu lado desde as épocas de faculdade e Ouro Preto, mesmo com toda a distância; minhas amigas Luciana Barcelos, Marcela Ferman e Isabela Calaes, por todas as conversas, os bons momentos, todos os poucos encontros que a a distância permite nas minhas idas ao Brasil e todo incentivo ao longo de todo o meu percurso; aos meus queridos presentes do CEFET: Lais Mamão, Jessica Machado,

Thaís do Valle, Julia Vasconcellos, Aryane Amaral e Lívia Lugon, pelos incentivos; minha amiga Luiza Campos, minha companheira de saídas, de momentos descontração e me apoiar desde o meu mestrado em Ouro Preto; à Daiana Silva, minha amiga de todas as horas, que mesmo na distância se fez presente. Um grande danke, à Marjorie Vieira, pela amizade e companheirismo durante a minha estadia em Berlin. Agradeço á Prof. Mônica Teixeira pelos ensinamentos, conselhos e incentivos para iniciar a jornada do doutorado.

Queria expressar a minha imensa gratidão aos meus amigos de Lyon, por me fazerem da França a minha casa e trazerem o Brasil para perto do meu coração; em especial a Indira Medeiros, Felipe Castro, Sueny Santos e Louise Ramos. Obrigada pelas aventuras! Gostaria de agradecer, com todo carinho, àquele que fez a França se tornar casa, com seu amor, companheirsmo e incentivos, Luís Gabriel Alves Rodrigues. Obrigada por todo o carinho e apoio incondicional nessa jornada!

Enfim, gostaria de expressar meu amor e meus maiores agradecimentos à toda a minha família pelo suporte incondicional durante meus estudos e minha vida. Sou extremamente grata aos meus pais, Áurea e Edmundo, pela educação e valores, por acreditarem em mim e me incetivarem a correr atrás dos meus sonhos mesmo que eles estejam há muitos milhares de quilômetros. Agradeço à minha irmã, Melissa, por ser minha companheira de vida, me apoiar, me ensinar e me oferecer seu abraço sempre que preciso! Obrigada por me darem forças e amor para continuar a minha caminhada e ir fazendo das pedras, o meu caminho. Essa conquista também é de vocês.

Contents

List of Figures

List of Tables

List of Symbols and Abbreviations

α	Surfactant's degree of ionization
C_p	Specific heat
ΔG	Free Energy Gibbs
ΔH	Enthalpy change
ΔS	Entropy change
λ	Wavelength
K	Binding constant
n	Stoichiometry
M_w	Molecular weight
a_h	Surfactant's head group area
l_c	Surfactant's hydrocarbon length
υ	Surfactant's hydrocarbon chain volume
q	Modulus of the scattering vector
P	Packing parameter
T	Temperature
ρ	Density
m	Molality
V_ϕ	Apparent molar volume
ΔV^{CD}	Volume of transfer
Ω	number of states of a system
k_b	Boltzmann constant
S(q)	Structure factor
F(q)	Form Factor
Y	Cyclodextrin -to surfactant molar ratio
Z	Glucosamine units in chitosan to surfactant molar ratio
θ	Scattering angle
ρ_p	Scattering length density of the particle
ρ_s	Scattering length density of the solvent
αCD	α-cyclodextrin
βCD	β-cyclodextrin
γCD	γ-cyclodextrin

$C_{12}E_5CH_2COOH$	Pentaoxyethylene dodecyl ether carboxylic acid
$C_{12}E_{10}CH_2COOH$	Decaoxyethylene dodecyl ether carboxylic acid
AEC	alkyl ethoxy carboxylic acids
CD	Cyclodextrin
Cryo-EM	Cryogenic Electron Microscopy
CTAB	Cetyl trimethylammonium bromide
DSC	Differential Scanning Calorimetry
ILL	Intitut Laue Langevin
ITC	Isothermal Titration Calorimetry
NMR	Nuclear Magnetic Resonance
PSCM	Partnership for Soft Condensed Matter
SANS	Small-angle Neutron Scattering
SAXS	Small-angle X-ray Scattering
SDS	Sodium dodecyl sulfate
TEM	Transmission Electron Microscopy

Chapter 1

Introduction

"Le vrai point d'honneur [d'un scientifique] n'est pas d'être toujours dans le vrai. Il est d'oser, de proposer des idées neuves, et ensuite de les vérifier."

Pirre-Gille de Gennes

Organization is a ubiquitous concept in nature. This is evident from many perspectives and different scales when we observe from the minimum atomic disposition to constitute a molecule to the social organizations. In society, we tend to organize ourselves in groups, given a specific aim, function, interpersonal interactions or due to a balance of all of them. When a biological perspective is assumed, the functional organization of lipids, proteins, water, etc, involving a complex balance of interactions leads to spontaneous and functionally oriented assembly to build the living systems. This self-organization phenomenon is universal in nature, and in chemistry, the spontaneous organization of molecules in motion into ordered entities in a variety of forms via non-covalent interactions is defined as ***self-assembly***.

More complex systems involving multilevel assembling with particles of distinct spatial scales, in which primary elementary molecular units assemble into ordered secondary structures acting as a building block to more complex superstructures are also achieved. This form of assembly is named ***hierarchical self-assembly***. Such assemblies can present ordered structures on molecular, nanometric, and micrometric scales. Viruses' capsids are good examples of this type of assembly since their rigid structures are a result of directional and specific interactions between the protein units and unspecific interactions with the genetic material they transport [1].

The great potential exhibited by the hierarchical assembly to build functional

materials inspired by biological structures and exploring the combination of intermolecular and supramolecular interactions has raised the interest of soft matter scientists. The infinite number of molecules available and the possible shapes and geometries become a playground field, also with the aim of understanding the interplay of forces to be able to modulate them.

Cyclodextrins host-guest complexes have been thoroughly studied since the 1950s [2], and their ability to form highly-ordered structures has been extensively investigated in the last two decades. Cyclodextrins' complexation ability is given by their physicochemical properties playing a very important role in controlling the assembly of amphiphiles and in modulating interactions of other soft systems. Both prospects are addressed in this work involving a neglected class of surfactants with remarkable potential, the alkyl ethoxy carboxylic acids.

Polyoxyethylene alkyl carboxylic acids are an attractive class of surfactants due to their molecular architecture (Fig.1.1). The molecule contains a hydrophobic alkyl chain, that can vary in length and saturation, the thermoresponsive ethylene oxide units (EO) and the terminal carboxylic group, which provides pH responsiveness. Structurally, the alkyl chain and the carboxylic acid resemble the fatty acids (C_iCOOH), which respond to pH alterations and had the solubility improved with the "simple" insertion of EO in the fatty acids molecules. The alkyl chain and the EO units resemble the nonionic alkyl ethers (C_iE_j), which are temperature-sensitive and present a rich phase diagram. The combination of these properties in one single molecule widens applications in fundamental and applied research.

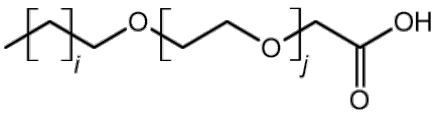

FIGURE 1.1: General molecular structure of alkyl ether carboxylates.

Hereafter, aiming to investigate the number of ethyelene oxide units' effect on the CD-surfactant complexation, emphasis will be given to pentaoxyethylene dodecyl ether carboxylic acid ($C_{12}E_5CH_2COOH$) and decaoxyethylene dodecyl ether carboxylic acid ($C_{12}E_{10}CH_2COOH$) surfactants. They are commercially available under the trade names AKYPO RLM45CA (444 g mol^{-1}, 92% purity) and AKYPO RLM100 (686 g mol^{-1}, 90% purity) (KAO chemicals), respectively. Both present a mixture of C_{12} and C_{14} in the hydrophobic alkyl chains and a Gaussian distributed number of ethylene oxide units around an average of 4.6 and 9.6 ethylene oxide units [3]. The polidispersity of the alkyl chain and polyethylene block hindered the fitting of the scattering data due to the complexity of the systems and influence of these

parameters in the inclusion complexation. However, the essential information extracted from SANS coupled with the broad suite of techniques used was effective in their characterization. The polydispersity also led to an attempt at the surfactants' synthesis at Freie Universität Berlin in the group of Prof. Christoph Schalley.

Alkyl oligoethylene oxide carboxylic acids have also great potential to compose polyelectrolyte-surfactant systems. Such potential has been demonstrated by their enriched structures with chitosan at interfaces and in solutions [4, 5], tuned by the molecular architecture of the surfactant and their degree of ionization. The chitosan presents the degree of acetylation and the molecular weight as possible parameters to control the complexation. The attractive versatility of these systems is given by the polysaccharide biocompatibility and the possibility of controlling the assembly by exploiting different prospects. The synergy of the surfactant's surface activity and the rheological properties provided by the polymer are demanded in many formulations, in particular, in pharmaceutical, home and personal care industries, paintings and coatings.

The surfactant's ability to interact with both cyclodextrin and chitosan molecules motivates the co-assembly of alkyl ethoxy carboxylic acids, chitosan and cyclodextrins. The system combines the long-range electrostatic interaction between the surfactant and polyelectrolyte and short-range host-guest interactions of the surfactant and cyclodextrin to form well-defined supramolecular complexes. The proposition of ternary systems as the ones investigated in this research can provide improvements to their respective conventional binary systems application, although their investigation is rarely mentioned in the literature.

This thesis is divided into four chapters based on the publications resulting from the activities carried out in this PhD project. **Chapter 2** is dedicated to covering general points of surfactant and cyclodextrin inclusion complexes and the parameters influencing their multilevel assembly.

The **Chapter 3** covers the inclusion complexation process. The energetic processes involved in the general cyclodextrin-guest complexation are firstly described. The thermodynamics of the inclusion complexation between the weakly anionic alkyl ether carboxylic acids formation is further addressed by isothermal titration calorimetry and volumetric investigations. In this context, it provides insights into the formation of the inclusion complexes, which will serve as building blocks of the supramolecular assemblies probed in this work.

The **Chapter 4** focuses on the investigation of the ability of the cyclodextrin-surfactant inclusion complexes to assemble into ordered aggregates. The influence of the concentration, cyclodextrin-to-surfactant ratio, and the molecular architecture of

the surfactant and the different cyclodextrins on the structural features of the assemblies were examined and demonstrated to affect their structures. The responsiveness of the structures to the charge density of the surfactant and temperature were probed by small-angle neutron scattering and optical and electronic microscopy. Additional differential scanning calorimetric studies confirmed the stability and crystalline nature of the ionized surfactant inclusion complexes.

Chapter 5 ties the ability of alkyl ether carboxylates to form complexes with cyclodextrins and with polymers, in special the bio-based polymer, chitosan [5]. The ternary systems' structural properties were evaluated as a function of the chitosan and cyclodextrin concentrations and pH. Similarities and differences between the complex systems could be drawn. The effect of cyclodextrin addition to the polyelectrolyte-surfactant system and the influence of chitosan in the inclusion complexes systems were assessed.

Finally, the **Chapter 6** summarizes the main achievements and conclusion presented in this thesis. Future perspectives are also identified, and their potential is discussed accordingly.

1.1 List of publications

This thesis is based on the following publications:

- ***Paper I***: Cyclodextrin/surfactant inclusion complexes: An integrated view of their thermodynamic and structural properties. Larissa dos Santos Silva Araújo, Giuseppe Lazzara, Leonardo Chiappisi. Advances in Colloid and Interface Science, **2021**, 289, pp. 1–11. ISSN: 00018686. DOI: 10.1016/j.cis.2021.102375

- ***Paper II***: Hierarchical assembly of pH-responsive surfactant-cyclodextrin complexes. Larissa dos Santos Silva Araújo, Leah Watson, Daouda Traore, Giuseppe Lazzara, Leonardo Chiappisi. Soft Matter, **2022**, 18, pp. 6529–6537. ISSN: 17446848. DOI: 10.1039/d2sm00807f.

- ***Paper III***: Thermoresponsive behavior of cyclodextrin inclusion complexes with weakly anionic alkyl ethoxy carboxylates. Larissa dos Santos Silva Araújo, Giuseppe Lazzara, Leonardo Chiappisi. Soft Matter, **2023**, 19; pp. 17– 19. ISSN: 1744-683X. DOI: 10.1039/d2sm01621d.

- ***Paper IV***: Ternary alkyl oligoethylene oxide carboxylic acids - cyclodextrin - polysaccharide complexes
  In preparation.

Chapter 2

Cyclodextrin-surfactant inclusion complexation: An overview

Published in *Adv. Colloids and Interfaces, 2021, 289, 102375, 1-11.*

Almost all aspects of life are engineered at the molecular level, and without understanding molecules, we can only have a very sketchy understanding of life itself.

Francis Crick

2.1 Cyclodextrins

Cyclodextrins (CDs) are a class of cyclic oligosaccharides formed by α-(1-4) linked D-glucopyranose units. The most common ones are α-, β- and γ-cyclodextrins, with six, seven, and eight glucoside units, respectively. They generally present a truncated cone shape with internal cavity size ranging from 4 to 8 Å, depending on the number of units in the macrocycle. The smaller rim is often designated as the primary rim of the structure or head, and the wider one as the secondary rim or tail. In the structure, hydroxyl groups located at the rims confer hydrophilic properties, while the C-H directed inwards configure a relatively hydrophobic cavity. The non-bonding electron pairs of the oxygen atoms also pointing inward the cavity increases the electronic density providing it with a Lewis base character [6]. The molecular representation and the intrinsic properties of cyclodextrins are depicted in Figure 2.1.

The singular structure of these macrocycles provides unique physicochemical properties and the ability to form **inclusion complexes**, also denominated host-guest

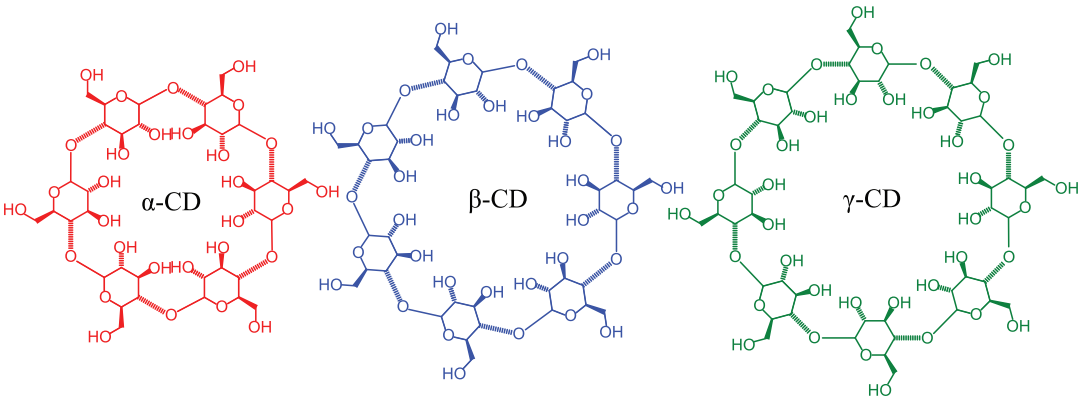

	α-CD	β-CD	γ-CD
Glucopyranose units	6	7	8
Chemical formula	$C_{36}H_{60}O_{30}$	$C_{42}H_{70}O_{35}$	$C_{48}H_{80}O_{40}$
Molar mass [g/mol]	972	1134	1296
Solubility in water [g / kg]	129.5	18.4	249.2
Outer diameter [nm]	1.52	1.66	1.77
Cavity height [nm]	0.78	0.78	0.78
Cavity diameter [nm]	0.45 – 0.53	0.6 – 0.65	0.75 – 0.83
Cavity volume [nm³]	0.174	0.262	0.427
Bound water molecules	6.4	9.6	14.2
Water molecules inside the cavity	3.6	6.3	8.9
Density [g / cm³]	1.48	1.44	1.52

FIGURE 2.1: Chemical structure of α, β and γ-cyclodextrins and their physicochemical properties. Data are reported from Refs. [7, 8]. *Figure adapted from Ref. [9] with permission of Elsevier.*

complexes. Besides the hydrophobic cavity and hydrophilic rims domains, the presence and further release of high-energy water molecules inside the cavity drives the complexation [6, 10]. The inclusion complexation affects the chemical potential of the guest molecule [11], and can consequently promote the solubility [12], and control of volatilization [13], for example.

Many molecules are reported to form host-guest complexes with cyclodextrins, such as essential oils, dyes, drugs, polymers, and surfactants. The biocompatibility and low toxicity extend the possible suitable applications to pharmaceutical [14, 15], medical [16, 17] and cosmetic industries [18, 19].

This work emphasizes α-cyclodextrin (αCD) and β-cyclodextrin (βCD) inclusion complexes, as it allows the evaluation of their different cavity sizes in the dynamics of complexation and in the structural aspects arising from it.

The availability of βCD expands their application in research, and its well-known complexation ability reported in the literature comprises a variety of guest molecules. Although the broad usage, βCD solubility is a major limiting factor. The extra unit glucopyranose unit favors the formation of intramolecular hydrogen bonds preventing the interactions within the surrounding water molecules [20]. In αCD, the hydrogen intramolecular bonding is incomplete due to a slight distortion of the structure, and the hydrogen bonding is embedded in the water network resulting in a higher solubility [21].

Due to the multiple reactive hydroxyl groups available at the cyclodextrin rims, modified cyclodextrins are easily obtained through chemical modifications – the most common being the hydroxypropylation or hydroxymethylation [22–24]. Cyclodextrin derivatives are broadly used as an alternative to conventional ones due to the properties provided to the molecule by the attached group. In inclusion complexes, the groups demonstrated to offer extra cavity effects that contribute to the stabilization of guests. On the other hand, the drawback of chemical substitutions is the possible inhibition of the complexes assembly process due to the disruption of the hydrogen bonding network between neighbouring cyclodextrins [25, 26].

2.2 Surfactants: an infinite world of possibilities

Surfactants are one of the most versatile molecules in colloidal sciences. Their amphiphilic nature provides them with interesting properties when in aqueous solutions. They are often used as stabilizers (or the opposite), detergents, and solubilizing agents, for example. The physicochemical properties such as critical micelle concentration, interfacial activity, and foamability strongly depend on the molecular architecture, hydrophobic and hydrophilic groups. The endless combinations of the headgroups and hydrophobic moieties and their responsiveness are a playground for colloidal science. Recently, their direct use in the spontaneous formation of complex materials as building blocks and their direct application in cosmetic, pharmaceutical, and medical formulations has received great attention.

A large number of cyclodextrin inclusion complexes with a variety of surfactants have been reported in the literature. Multiple anionic, cationic, zwitterionic and nonionic surfactants have been studied as guest candidates to integrate the complexes. The complexation between sodium dodecyl sulfate (SDS) [27–31] and n-alkyl trimethylammonium bromide (C_xTAB) [29, 32, 33] are the most extensively

systems investigated in terms of thermodynamics and structural aspects, often with β-cyclodextrin or its derivatives. They are usually used as a reference for the study of their ionic corresponding classes.

From the nonionic class of surfactants, polyethylene oxide-based surfactants with different hydrophobic chains can be highlighted as they provide the easy variation of the hydrophobic moiety and the number of ethylene oxide units in the PEG block. Studies with p-tert-octylphenyl ethers (commercially known as Triton X surfactants [34, 35], polyoxyethylene oxide n-alkyl ethers (Brij surfactants) [36], polyoxyethylene sorbitol esters (named Tween) [37] with αCD and βCD are also reported.

Double-tailed and gemini surfactants [38–40] widen the possibilities of inclusion complexes investigations due to the presence of more than one surfactant tail in one molecule, which is generally the common CD binding site. The extra hydrophobic chain changes the stoichiometry of the inclusion complexes, and so the dynamics of the complexation. Although the weak surface activity, bolaform surfactants are also interesting guest candidates due to the possibility of varying the hydrophobic and hydrophilic moieties [41, 42]. Clearly, these surfactants present more tuning parameters. In addition, the complexation of the bolaform and the spacer in the gemini surfactants resemble the structure of a rotaxane and configure different properties to the complexes.

The infinite possibilities in surfactants' molecular architectures allow probing of the inclusion complexation and the evaluation of the guest's role, as well as the effect of their properties in the assembly process. The impact of the alkyl length effect has been largely studied and probed with different headgroups. However, the investigations concerning the headgroups generally neglect the effect of the charge density as either nonionic or ionic surfactants are often selected as guests. By employing weakly acidic surfactants, such as polyoxyethylene alkyl ether carboxylic acids, the charge density can be systematically varied by pH adjustment. In this manner, its effect on the inclusion complexation process and the morphology of the assemblies can be resolved.

2.2.1 Polyoxyethylene alkyl ether carboxylic acids

Polyoxyethylene alkyl ether carboxylic acids, also generally named alkyl ethoxy carboxylic acids (AECs), are prepared by Williamson's synthesis (Fig. 2.2). The synthesis consists of the reaction of nonionic alkyl ether and halogen acetic acids, usually chloro or bromoacetic acid, in the presence of a strong base, with a yield of approx. 90% [43, 44]. Industrial technical AECs are largely available at low cost with diverse alkyl chain lengths and ethoxylate units, generally polydispersed.

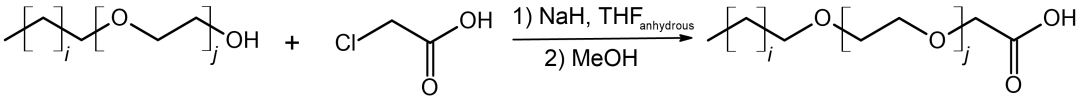

FIGURE 2.2: Synthesis of alkyl ether carboxylic acids from the alkyl ethers.

In solution, AECs phase behaviour strongly depends on the pH, concentration, and temperature [45]. Their *cmc* depend on pH and can vary from 20 to 400 μmol L^{-1} [46]. The different aggregates formed results from geometrical constraints described by the packing parameter (Eq. 2.1) [47]:

$$P = \frac{\upsilon}{a_h l_c}, \tag{2.1}$$

where υ is the hydrocarbon chain volume, a_h, the area of the headgroup and, l_c the hydrocarbon length.

Accordingly, systems exhibiting small packing parameters tend to form spherical micelles, and larger P values point to larger aggregates with smaller curvature [47, 48].

In the case of AECs, the headgroup area, mostly for small headgroups, relies on the protonation of the carboxylic group. As predicted by P, the different aggregates upon the increase of the surfactant's degree of ionization at various pH are comprehensively characterized in the literature [45, 49]. Small-angle neutron scattering (SANS) measurements revealed that the surfactant molecular architecture (Fig. 1.1), specifically the number of ethylene oxide units, strongly influences their assembly behaviour. Upon increasing the pH, the $C_{12}E_5CH_2COOH$ assemblies evolve from planar structures to a mixture of polydisperse vesicles and small micelles, whereas ellipsoidal aggregates becoming spherical with pH increase are observed for $C_{12}E_{10}CH_2COOH$ [49, 50].

The temperature-related behaviour of the polyoxyethylene alkyl ether carboxylic acids follows the same as observed for their nonionic correspondent alcohols. The hydration of the ethylene oxide headgroup is gradually modified in response to the temperature changes [45]. The increase in temperature promotes the dehydration of the EO units and leads to phase separation at a given temperature (Cloud point) and concentration. Then, a surfactant-rich phase and a surfactant-poor phase are obtained. Different types of structures are found in the systems as a result of entropy maximization and steric repulsion minimization, which relates to the microscopic description of entropy by the Boltzmann equation [51, 52].

The two surfactants investigated in this research present different thermoresponsive properties remarkably dependent on the pH. In pH inferior to 4.1, $C_{12}E_5CH_2COOH$ solutions are turbid and the formation of precipitates at 25°C was

verified by Renoncourt et al. [45]. If heated up to 55°C, the precipitation of the surfactant and a clear supernatant are obtained. At pH 5 and temperatures superior to 20°C, slight micellar growth is reported and a macroscopically transparent bluish solution is reported. A further increase in pH provides the formation of small micellar structures [49]. $C_{12}E_{10}CH_2COOH$ solutions at low pH present cloud point at 68°C. Differently from the previously mentioned surfactants with fewer EO units, the pH increase does not trigger the micellar growth.

Polyoxyethylene alkyl ether carboxylic acids are very versatile surfactants in pure solutions and permit modulation of their properties by exploring stimuli responsiveness and chemical modifications. Hence, the novelty of this work lies in employing such interesting surfactants as guests in inclusion complexes with cyclodextrins.

2.3 Inclusion complexes

Cyclodextrin-surfactant inclusion complexation is driven by non-covalent interactions, Van der Waals, electrostatic, charge transfer, hydrophobic and hydrogen interactions, and other steric effects [6, 10]. The intrinsic properties resulting from the nature and architectural constraints of the species involved in the interactions play an important role in the process. Still, other tunable variables are also significant for the complexation itself and the inclusion complexes assembly.

The relative **cyclodextrin-to-surfactant molar ratio** (Y) of host and guest is one of the most relevant parameters directing the complexation. Stoichiometry is controlled by the number of available binding sites in the guest molecule and host concentration in an energetically favoured process involving or not mechanisms of cooperativity.

Size-match compatibility can anticipate the interactions, but the exact stoichiometry must be evaluated case by case. The 1:1, 2:1 and 1:2 stoichiometries (CD:surfactant), as shown in Figure 2.3, are common for these complexes, but mixtures of them can also be observed. In general, surfactants with short alkyl chain lengths are able to accommodate only one cyclodextrin, while a 2:1 stoichiometry is favoured for surfactants with 12 or more carbon units. α and βCD cavities are not expected to form 1:2 complexes with surfactants due to the size of the cavity, but due to the larger cavity, γCD is able to host two alkyl chains. In some cases, the excess of surfactant with respect to cyclodextrin concentration can also provide 2:1 complexes [53]. Isothermal titration calorimetry is the most used method to accurately determine the complex's thermodynamic properties, including stoichiometry, at a constant temperature [54]. NMR [55], potentiometry, density [53], speed of sound

[33, 56] and tensiometry [39] are also widely used to probe the thermodynamics of the inclusion complexes formation.

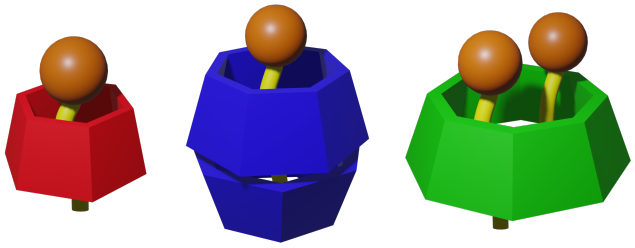

FIGURE 2.3: Schematic representation of inclusion complexes formed with stoichiometries of 1:1, 2:1, 1:2, from left to right. Sketches are not at scale. *Reproduced from Ref. [9] with permission of Elsevier.*

The threading of one or two cyclodextrins to the surfactant molecule is a parameter driving the further assembly behaviour into ordered aggregates, in which partial structures are formed, or the coexistence of more than one type of aggregate can occur, and it will be further discussed.

The **concentration** of the surfactant and CD, consequently the mixtures' total concentration, affect the multiple equilibria involved in the process and the behaviour of the assemblies. Above the critical micellar concentration, surfactant molecules assemble into micelles in solution, and free molecules are also present. Clearly, the surfactant's micellization and activity are affected by the presence of cyclodextrin. The formation of inclusion complexes with CD can be a strategy to control the surfactant self-assembly, as it is for lipids and polymers, and the coexistence of the complexation and micellization equilibriums results in an interesting scenario. The competitiveness of the two processes leads to the overall speciation determined by the different equilibrium constants. The concentration also determines the supramolecular growth of the alkyl ether carboxylic acid assemblies, as demonstrated in Chapter 4 (Fig. 4.8).

The supramolecular growth and structure of the assemblies are also concentration dependent. Directed by the water-mediated hydrogen bonds between adjacent cyclodextrins, the rich phase behaviour of such systems is often explored as a function of concentration ranging from few Angstrom to multiple μm. The general structural trend is the predominance of monomers at very low concentrations followed by different aggregates with increasing concentration. In these systems, vesicles, cylinders, tubular and lamellar structures are commonly found despite the type of the surfactant and are directed by the cyclodextrin type. The sodium dodecyl sulphate-βCD system is a good example for understanding the critical aggregation concentration, in which monomers can be found at very low concentrations (inferior to 0.5%wt), vesicles are predominant up to 6%wt, cylindrical structures prevailing between 6 and 25%wt,

and lamellas at higher concentrations [27, 57]. Driven by the minimization of the energies of the systems and by entropy's maximization, the inclusion complexes assembly will be further addressed in Chapter 4.

Temperature is a very convenient tool to strategically modulate molecular assembly in the short and long-range due to the non-covalent nature of the driving forces. It is also one of the well-known parameters to influence thermodynamics and affects the complexation process, entropy, enthalpy, and binding constants. Thermodynamic quantities and magnitudes are directly associated with the host and guest properties, but discrete ΔG° are observed over enthalpy-entropic compensation since significant heat capacities resultant from the inclusion are expected.

Rising the energy of such systems increases the thermal motion and has also been demonstrated to influence cyclodextrin-cyclodextrin and cyclodextrin-water interactions in the spatial ordering of the lattice and strongly affect the structural phase behaviour. Combining the concentration and temperature behaviours, a very descriptive phase diagram can be constructed to illuminate the highly-ordered arrangement of the inclusion complexes and establish a link between interaction potential, stability, and thermodynamics.

The **host and guest's molecular architecture** also determines interaction aspects. The alkyl chain and the head nature play an important role in the inclusion complexes for amphiphilic guests. The influence of the headgroup on thermodynamics is expected, especially for the cases of proximity with the threaded CD. However, for the same alkyl length, complexes with different anionic headgroups can be slightly more stable than the ones with cationic, but the interactions of inclusion complexes with nonionic surfactants require a careful evaluation. The hydrophilic part frequently contains a variable number of ethylene oxide units, which can also be threaded by groups of two in the CD cavity [30]. In addition, changes in the solvation dynamics of the units upon threading also contribute to the thermodynamic events.

Although the clear differences in the complexation foreseen from the surfactant's headgroup nature, the unveiling of contributions from the electrostatic interactions is yet to be better understood. By using a surfactant that allows controlling the headgroup's **charge density**, as the alkyl ethoxy carboxylates, it was possible to have an insight into the importance of such interactions in the thermodynamics of the complexation and structural features, as it has been demonstrated to drive specific structural arrangements.

In turn, host molecules can vary in cavity size. As previously mentioned, it provides selectivity and can also direct stoichiometry when the cavity is wide enough to complex two guests. In addition, through water-mediated, strong, and highly directional bonds between neighbouring cyclodextrins, the inclusion complexes assemble

forming large organized structures in a lattice assembly process. Laterally, the lattice arrangement relies on the cyclodextrin rotational axis found hexagonal for αCD, rhomboidal for βCD, and squared packed for γCD. Vertically, the channel lattice is the only reported for CD/surfactant inclusion complexes, despite the CD type [58–60].

Another strategy to control the assembly and grant additional properties to the supramolecular aggregates is adding a third component to the system, usually a surfactant or a polymer. Such combinations are very rich in possibilities and structures since the CD can be used in the natural or in a polymeric form, and oppositely charged surfactants and polymers are employed. It is important to emphasize that in anticipating a surfactant-based system, both polymer and cyclodextrin can be assumed to play a controlling role in their self-assembly. In the case of a mixture of surfactants, the addition of CD can modulate the interaction between them and induce phase transition [61, 62]. In CD/surfactant systems, the polymer can be added as a modulator, stabilizing and configuring specific rheological properties [63]. Differently from adding a surfactant, the addition of a polymer aims to explore both inclusion complexation and electrostatic interactions. However, ternary systems involving the inclusion complexation are yet to be further investigated.

The host-guest association is at the heart of the full understanding of the complexation and assembly process. Numerous techniques have been used to characterize surfactant-cyclodextrins complexes' properties. The methods commonly used for thermodynamics assessments are nuclear magnetic resonance (NMR), conductivity, potentiometry, spectrophotometry, isothermal titration calorimetry, density, and speed of sound. The accessibility of a few techniques already inserted in the laboratory routine reflects their usage, as, for example, the conductivity and potentiometry that had been widely applied in the determination of the surfactants aggregation, critical micellar concentration, and the counter ion binding to complexes by direct determination. They are frequently used without sample pretreatment or special technical requirements and simple data analysis. However, the use of both techniques is limited to ionic surfactant complex systems.

NMR is also commonly used to elucidate the binding constants and stoichiometry of the complexation by analyzing the signals or diffusion coefficients of the free molecules and complexes, limited by the clear distinction and resolution of CD and guest signals. Spectrophotometry measurements rely on the evaluation of the absorption spectrum and its possibility to decompose the bands to determine the binding constants and stoichiometry. It is also widely applied in IC studies involving the dye's complexation by the CD and their encapsulation by the CD/surfactant inclusion complexes. The applications of spectrophotometric methods are restricted to

matrices where the signals can be distinguished and correctly assigned.

Density and speed of sound measurements are usually coupled for the determination of the molar volumetric quantities and adiabatic compressibilities to assess the modifications in the nature and hydration state of the molecules upon complexation. The limited number of publications involving these techniques underestimate the simplicity of conducting the measurements and extracting the information from the collected data.

Isothermal titration calorimetry (ITC) is a well-established method that allows the direct determination of the thermodynamic parameters simultaneously. The robustness of the method and the data modeling properties according to the specific characteristics of the evaluated systems provide precise quantitative information on the systems' ΔH, ΔG°, stoichiometry, and binding constant.

Scattering techniques are typically employed for a complete characterization in the structural investigation. Dynamic and static light scattering [64], X-ray and neutron scattering [38, 60, 65–67], X-ray diffraction [68, 69] are usually complemented by atomic force microscopy [70–72], NMR [40] and microscopy techniques [72, 73] for a complete investigation.

Another difficulty pointed by Valente et al. is the usual differences in binding constants for the same systems reported in the literature depending on the technique applied, although a certain agreement at least in magnitude was expected [6]. The mentioned techniques present many advantages and can provide valuable information if their limitations are observed, the experiments are correctly designed, and the data is appropriately modelled. These are particularly critical for the thermodynamic parameters, in which more processes are occurring concomitantly to the complexation, and the detection of subtle quantities may be related to the inclusion complexation.

In the research of cyclodextrin inclusion complexes, the tendency to emphasize the systems' thermodynamics or structural aspects limits the full understanding of the cyclodextrin complexation. The thermodynamics of the inclusion complexation and the structures arising from their assembly will be discussed in Chapter 3 and 4. The multi-scale approach, evaluating from the formation to the inclusion complexes' assembly, triggering parameters and energy quantities associated, contributes to the comprehension of the guest role and to the smart application of such systems.

Chapter 3

Host-guest complexes formation

Published in *Soft Matter, 2022, 18, 6529-6537.*

Almost all aspects of life are engineered at the molecular level, and without understanding molecules, we can only have a very sketchy understanding of life itself.

Francis Crick

3.1 Interactions between cyclodextrin and surfactant

Understanding the cyclodextrin and surfactant inclusion complexation is essential to comprehend their properties and further designing their assemblies. The complementary approach of the geometric match often represented by the lock-and-key model is important, but the balance of multiple interactions drives the binding. This chapter approaches the thermodynamics description of the complexation process.

The knowledge of the complexes' properties requires performing a quantitative analysis of the thermodynamic parameters involved in the process. This includes determining the binding constant, stoichiometry, changes in enthalpy and entropy, and various derivatives of the Gibbs free energy that occur during the interaction between cyclodextrin (CD) and guest molecules. Having this knowledge is necessary to accurately predict and comprehend the general behaviour of the CD-guest complex.

The definition of the occurring events relies on the suitable arrangement and on the maximization of attractive forces while minimizing the repulsive ones between guest and host [74]. However, it is rather difficult to separate and follow the process in terms of successive steps. For better understanding, the process can be divided into stages/events taking place, which are represented in Figure 3.1:

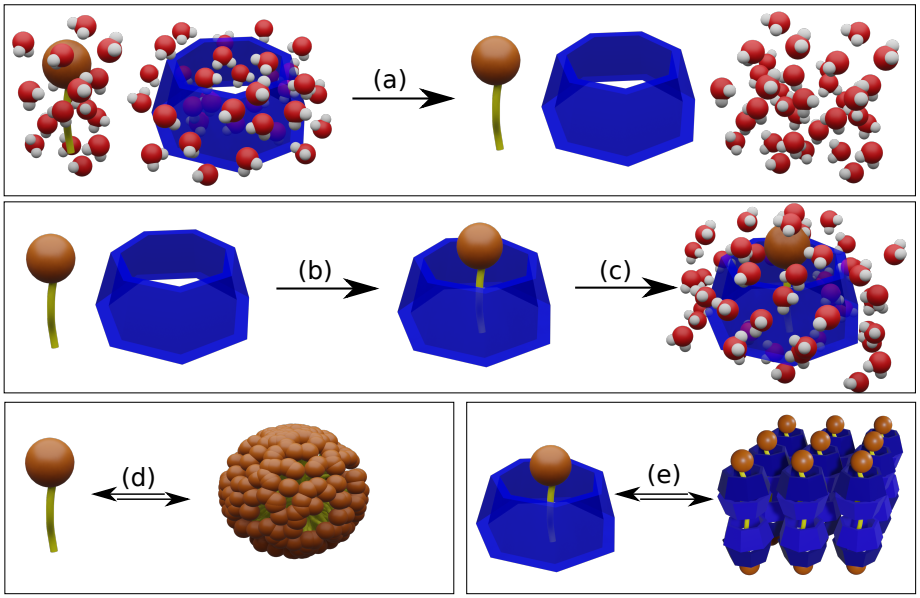

FIGURE 3.1: Schematic representation of the complex formation between surfactants and cyclodextrins in the steps it can be divided: (a) host and guest molecules are dehydrated; (b) the insertion of the surfactant molecule into the CD cavity takes place; (c) the CD/surfactant complex is, then, hydrated. In addition to these essential steps, the equilibrium (d) between the free surfactant and the ones in the micelles and (e) between the inclusion complexes and their assemblies has to be considered. Representation is out of scale. *Reproduced from Ref. [9] with permission of Elsevier.*

- ***Dehydration of guest and host*** (Fig. 3.1(a)): The hydration of the surfactant and cyclodextrin has an important role in the process. The release of high-energy water from the cavity and the rearrangement of the structured water surrounding the surfactant is entropically advantageous, and it also drives the assembly of surfactant and cyclodextrin. In an aqueous solution, the cyclodextrin cavity is occupied by water molecules energetically frustrated due to their imposed distorted hydrogen-bonded network shaped by the molecule's geometry [75]. It is noticeable by the different heat capacities at a constant pressure of the high-energy water in the cavity. For αCD, the C_p is, approximately, 60 J K^{-1} mol^{-1}, while closer values to the liquid water (71 J K^{-1} mol^{-1}) are found in βCD and γCD [76]. As previously mentioned, the number of water molecules inside the cavity and the solubility do not follow a linear proportionality with the number of glucopyranose units as a result of the less theoretically possible four hydrogen bonds. This is a result of the structural distortion and the participation of the water molecules in the network with the hydroxyl groups of the rims. Accordingly, the excess hydrogen bond in the solvation shell around the surfactants stabilizes the hydrophobic chain in the solution. Similarly to the water release from the host, the alkyl chain removal

from the aqueous environment and the rearrangement of the high-energy water molecules also contributes to the energetic quantities of the complexation process.

- ***CD/surfactant interaction*** (Fig. 3.1(b)): The inlet of the surfactant in the CD cavity is stabilized by various Van der Waals interactions, and it is often correlated to the binding strength and specific structures of the species involved in the complexation [10]. The structural aspects are correlated to the molecular size and electron density. With respect to the cyclodextrin cavity size, a narrower cavity as in αCD tends to accommodate tightly a methylene group with a diameter of approximately 0.4 nm, while it can fit loosely in the β or γCD cavity because of their larger size. In a sufficiently ample cavity, the fit of two surfactant molecules occurs in a cooperative process as often seen in γCD inclusion complexes, or no complexation is observed. The complexation in a larger cavity also allows an increased number of possible conformations of the surfactant threaded, which leads to an energetic increase, and decreases the interactions' strength between host and guest. Along the CD threading to the surfactant alkyl chain, the vicinity of the head group and the CD rim can also provide interesting interactions and contribute to the stabilization of the complex.

- ***Hydration of the complex*** (Fig. 3.1(c)): The final rearrangement of the water molecules displaced upon complexation and the hydration shell of the complex is established.

The thermodynamic evaluation requires a careful investigation of more processes occurring concomitantly. In the case of the surfactant-CD complexation, the equilibrium between free surfactant molecules and micellar structures must be considered if surfactants with very low critical micellar concentrations are employed (Fig. 3.1(d)). This equilibrium is knowingly affected by the addition of cyclodextrin in the system and is known to compete with the inclusion complexation process. This proven competitiveness is often used to modulate the assembly of amphiphiles as the activity of the free molecule involved in the micellization is lowered and shifts the *cmc* to higher concentrations [57].

Another process concerning inclusion complexes and their spontaneous organization in highly-ordered supramolecular structures (Fig. 3.1(e)) will be further addressed in Chapter 4.

Essentially, considering the main process involved in the cyclodextrin-surfactant inclusion complexation, it is possible to summarize the process as follows:

$$hH_2O \cdot aCD + bG \cdot gH_2O \rightleftharpoons CD_a \cdot G_b \cdot (g+h-i) + iH_2O \tag{3.1}$$

where a and b are the stoichiometric coefficients of cyclodextrin and surfactant, respectively, h and g are the number of water molecules hydrating the host and guest, and i is the net displaced water upon complexation [54, 77].

The solvent nature also plays a role in the inclusion complexation and evidences the role of the hydrophobic effect in the process. The binding strength of the CD is usually weakened by the addition of an organic co-solvent, usually short-chain alcohols, due to the simple stabilization of the hydrophobic alkyl chain in the medium [32, 78, 79]. In contrast, when not competing with the complexation, the addition of inert salts can strengthen the affinity due to an increase in the polarity, which also strengthens the hydrophobic interactions [10]. By exchanging H_2O for D_2O or by a mixture of the two solvents, the binding affinity increases, and, over a certain concentration, the assembly of the inclusion complexes into aggregates is also favoured [80].

In order to understand the inclusion complexation from a molecular perspective, the thermodynamic parameters evaluation by isothermal titration calorimetry for the determination of the free energy of Gibbs (ΔG°), enthalpy (ΔH) and entropy change (ΔS) and binding constants (K) is discussed in 3.1.1 and the rearrangement of the hydration shell is described by the investigation of the volumes of transfer in section 3.1.2. It is noteworthy that the thermodynamics determinations are influenced by the polydispersity present in the number of carbons in the chain and the number of ethylene oxide in the surfactant.

The ITC experiments and the volumetric studies at low pH were performed by Leah Watson at the ILL during the Master Thesis.

3.1.1 Thermodynamics of inclusion complexation

Many techniques have been applied to quantitatively access the thermodynamics of cyclodextrin complexation from a molecular perspective and the fundamental parameters involved in the interaction between host and guest. Calorimetry is the only one that allows the direct measurement of the heat (q) involved in the process. There are many reasons for the great use of calorimetry, but the high sensitivity and energetic transfer magnitude range can be highlighted to provide the ability to cover all the chemical and biological processes. [81]

Isothermal titration calorimetry is often used in the investigation of thermodynamics of surfactant interactions [81]. The technique's fundaments lie in measuring the heat produced or absorbed upon the interaction between host and guest. The

TABLE 3.1: Prediction of thermodynamic parameters of different surfactant-cyclodextrin complexes.

Ionic character	n	CD	$\Delta H/kJmol^{-1}$	$T\Delta S/kJmol^{-1}$	$\Delta G/kJmol^{-1}$	Reference
1:1						
$C_xSO_4^-$	8 - 12	αCD	- - -	-	- -	[30, 31]
C_xTAB	8 - 14		- -	-	- -	[30, 82]
$C_xSO_4^-$	6	βCD	-	+	-	[29, 83]
	8 - 12		-	+	- -	
C_xTAB	8 - 16		-	+	- -	[83]
2:1						
$C_xSO_4^-$	8	αCD	- - - -	- - -	- -	[30, 31]
	10 - 12		- - - -	- - -	- - -	
C_xTAB	16		-	+	- -	[82]

The signs correspond to the following numeric intervals $0 \leq + \leq 15; 16 \leq ++ \leq 30; 31 \leq +++ \leq 45$ and $46 \leq ++++ \leq 60$. The intervals are analogous to the negative values. Detailed numerical values can be found in the references. *Reproduced from reference [9] with permission of Elsevier.*

direct simultaneous determination of the stoichiometry, enthalpy change (ΔH) and binding constant allows the calculation of the free energy of Gibbs (ΔG°) and entropic change (ΔS). In addition to the mentioned advantages, the use of this technique in the investigation of inclusion complexation is in the important wide range of binding constants, from 10^{-1} to 10^{-8} M^{-1}, *i.e.*, from low to high affinity, in which is possible to accurately determine the thermodynamic parameters [11, 54].

Inclusion complexes investigations employing ITC measurements have been able to resolve the effect of the nature of the headgroup and alkyl chain length of the surfactants on thermodynamic parameters of many α and β-cyclodextrin complexes [29, 30, 83]. Generally, the enthalpy changes and the binding affinity increase with increasing alkyl chain length. The headgroup of the surfactant has a slight impact on the thermodynamics, depending on stoichiometry. This headgroup effect is mainly noticeable in cationic surfactants. Table 3.1 provides a general thermodynamic prediction for the two most studied series of ionic surfactants. Although the interactions and the thermodynamics specificities for each complex system, a general prediction approach can be useful in exploring new systems.

Figure 3.2 presents a schematic representation of an ITC experiment. The ITC apparatus is represented in Fig. 3.2(a). The reference cell is filled with the solvent, the surfactant is placed in the sample cell and the cyclodextrin is added by the injection of aliquots into the sample cell from a syringe inserted on it. After the injection of each aliquot, a heat pulse is detected by the instrument and the raw data graph is obtained Fig. 3.2(b). The heat exchange detected is associated with the cyclodextrin

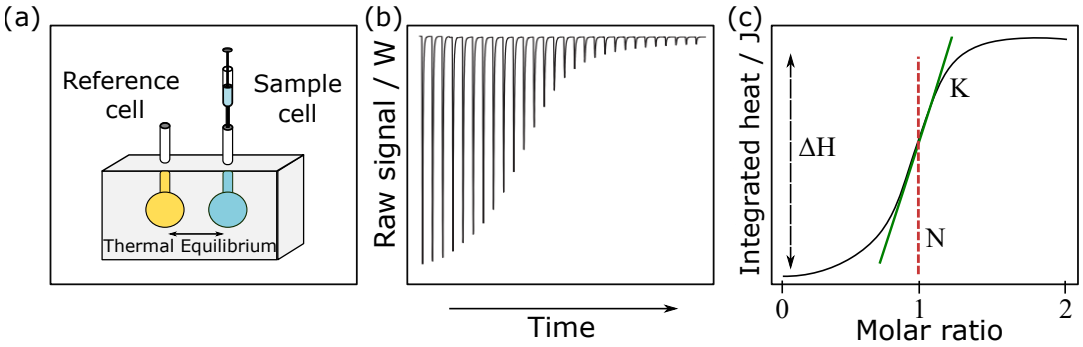

FIGURE 3.2: (a) ITC instrument representation; (b) Raw data (dq/dt) obtained after baseline correction. (c) Integrated power from which enthalpy (ΔH), binding constant (K) and stoichiometry (N) are determined. *Adapted from Ref.[9] with permission of Elsevier.*

and surfactant binding in addition to the other process occurring. The raw signal obtained is processed as described in **Paper I** and the thermodynamic parameters are determined as shown in Fig. 3.2(c).

The technically simple experiment requires the careful preparation of solutions in adequate concentration, buffer, and temperature control. Nonetheless, the modeling to fit the obtained results using the suitable binding model is decisive for interpreting the data.

ITC was used at constant pressure to determine the heat involved in adding the cyclodextrin aqueous solution to the surfactant solution to probe the energetic parameters of their association. The calorimetric curves and fits for the titration of $C_{12}E_5CH_2COOH$ and $C_{12}E_{10}CH_2COOH$ with αCD and βCD at pH 3, 4 and 5 are depicted in Fig. 3.3. The heats of interaction were calculated assuming that each surfactant molecule has n independent and equal binding sites. The heat of cyclodextrin dilution and the demicellization of the surfactants were assessed and proven to be negligible. The resulting heat is ascribed to be associated with the inclusion complex formation. It is important to remark that the experiments were carried out in concentrations above the *cmc*, and the interaction of the host with micelles is also verified.

As a primary experimental observation of the experiment, the heat integration is equivalent to the enthalpy change (ΔH), and the measurement as a response of the systems' total composition provides the determination of the binding constant K and stoichiometry n. From the fit, the free energy of Gibbs of the complexation (ΔG°) using equation 3.2 and, with all obtained parameters, the entropy change (ΔS) can be calculated by the Gibbs-Helmholtz, as in equation 3.3. Table 3.2 presents the results obtained for thermodynamic parameters; the values of ΔH and TΔS are indicated as a function of moles of surfactant.

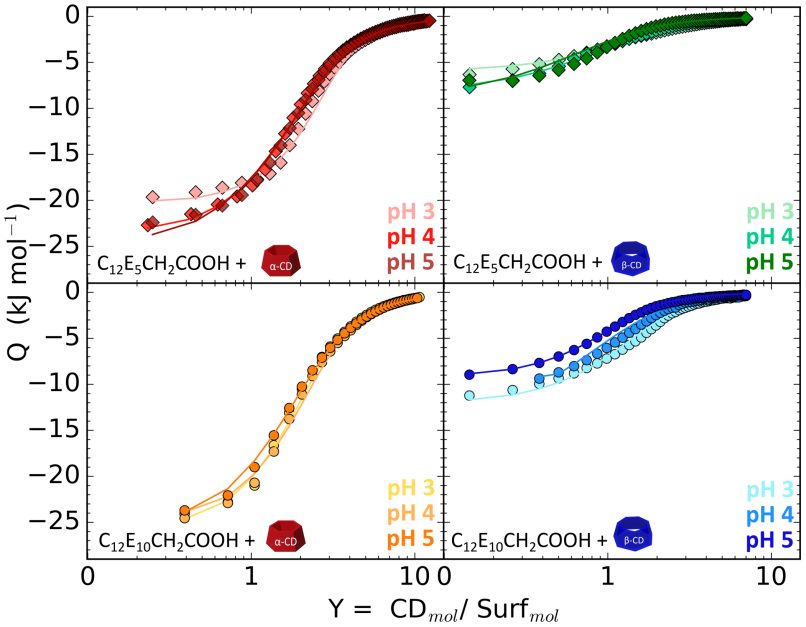

FIGURE 3.3: Titration curves of $C_{12}E_{10}CH_2COOH$ with (a) αCD and (b) βCD and $C_{12}E_{10}CH_2COOH$ (c) αCD and (d) βCD. Solid lines are the best fits according to one-to-one fit. *Adapted from Ref. [84] with permission.*

$$\Delta G^{\circ} = -RT \ln K \tag{3.2}$$

$$\Delta S = \frac{\Delta H - \Delta G^{\circ}}{T} \tag{3.3}$$

The negative values of (ΔG°) indicate the spontaneity of the inclusion complexation between the surfactants and both cyclodextrins at all pH values evaluated. Enthalpic and entropic changes present negative values, but the greater contribution of enthalpy allows characterizing the inclusion complexation as an enthalpically driven process.

From Fig. 3.3, the curves and the thermodynamic parameters also show a very straightforward dependence on the cyclodextrin type. The distinction between αCD and βCD systems entropy changes are related to the cavity size and the water network within it and their release upon complexation. Along with the significant entropic contribution, the release of these molecules upon complexation also provides an enthalpic contribution. As a result of the distortion in the structured water inside αCD, unfavoured and greater entropic contributions of the surfactant systems with this cyclodextrin are observed.

The pH evaluation is motivated by the presence of the terminal carboxylic group in the surfactants molecule headgroup. At pH 3, the nonionic form is predominant ($\sim$ 85%); at pH 4, the nonionized molecules are not predominant ($\sim$ 35%); and at

TABLE 3.2: Thermodynamic parameters of different surfactant-cyclodextrin complexes obtained from the ITC fit.

Systems	*Thermodynamic parameters*	pH 3	pH 4	pH 5
$C_{12}E_5CH_2COOH$-αCD	K	6.3 ± 0.5	5.01 ± 0.1	3.5 ± 0.1
	n	2.44 ± 0.1	1.7 ± 0.1	1.5 ± 0.1
	ΔH ($kJ\ mol^{-1}_{surf}$)	-63.3 ± 1.68	-58.5 ± 1.3	-62 ± 2.6
	$T\Delta S$ ($kJ\ mol^{-1}_{surf}$)	-0.12 ± 0.1	-0.14 ± 0.1	-0.15 ± 0.1
$C_{12}E_5CH_2COOH$-βCD	K	5.9 ± 0.1	7.2 ± 0.1	10 ± 0.9
	n	1 ± 0.1	0.5 ± 0.2	0.4 ± 0.1
	ΔH ($kJ\ mol^{-1}_{surf}$)	-11.4 ± 0.5	-11.2 ± 0.5	-4.5 0.2
	$T\Delta S$ ($kJ\ mol^{-1}_{surf}$)	-0.1 ± 0.10	-0.2 ± 0.1	-0.2 ± 0.1
$C_{12}E_{10}CH_2COOH$-αCD	K	7.6 ± 0.3	7.4 ± 0.5	5.4 ± 0.2
	n	1.7 ± 0.1	1.9 ± 0.1	1.4 ± 0.1
	ΔH ($kJ\ mol^{-1}_{surf}$)	-69.3 ± 3.4	-70.7 ± 3.8	-68.2 ± 4
	$T\Delta S$ ($kJ\ mol^{-1}_{surf}$)	-0.2 ± 0.2	-0.2 ± 0.1	-0.2 ± 0.1
$C_{12}E_{10}CH_2COOH$-βCD	K	8.5 ± 1	8.3 ± 0.7	15 ± 0.3
	n	1 ± 0.1	0.6 ± 0.2	0.9 ± 0.1
	ΔH ($kJ\ mol^{-1}_{surf}$)	-21.9 ± 1.4	-19.2 ± 1	-12.1 ± 0.2
	$T\Delta S$ ($kJ\ mol^{-1}_{surf}$)	-0.1 ± 0.1	-0.1 ± 0.1	0 ± 0.1

pH 5, up to 75% of the surfactant molecules are ionized, depending on the surfactant. Surprisingly, minor effects of the pH are observed and hint towards the non-inclusion of the carboxylic group in the cyclodextrin cavity. Moreover, the differences in the hydration shell of the distinct number of ethylene oxide units in the ionized and non-ionic molecules would also provide contributions to the energetic process that would indicate their threading by the CD. Thus, it interestingly suggests the complexation of the alkyl chain.

Fatty acids with alkyl chain lengths between 11 and 13 carbons also form inclusion complexes with α-cyclodextrin and present similar enthalpically driven mechanisms at pH 10 [85]. Pereira, Valente and Södermann probed the effect of pH in the octanoic acid and determined a stronger binding to octanoate compare to its conjugate. In addition, their investigations pointed to an entropically driven complexation [86]. The two mentioned studies highlight the relevance of the guest's length of the alkyl chain since the vicinity of the cyclodextrin rims and headgroup can provide energetic contributions as a result of their interactions.

3.1.2 Hydration and solvent rearrangements

Volumetric and compressibility properties reflect the degree and nature of hydration of the species in solution. Many volumetric studies have provided useful information on solvent's role in biochemical and physicochemical processes, such as protein folding [87, 88] and the micellization and solubilization in surfactant systems [89]. The geometrical aspect and the hydration rearrangements are important factors in the surfactant-CD complexation. The extensive desolvation of the guest and host and the resolvation of the complex itself contains information about the volume changes occurring in the complexation and can provide a better comprehension of the relative roles of solute-solute and solute-solvent interactions. In spite of all the possible information that volumetric studies can provide, which also includes the possibility of extracting information on stoichiometry, its application in the CD inclusion complexes investigation is limited, given the simplicity of measurements and data analysis.

As previously mentioned, the versatility of the alkyl ethoxy carboxylic acids surfactants is offered by the ending carboxylic group. In order to explore the two possible scenarios, where the majority of species are either ionized or nonionized, the effect of the solvation by density measurements was evaluated at low and high pH, *i.e.*, $\alpha = 0$ and $\alpha = 1$.

The investigation relies on the density (ρ) measurements by means of a vibrating U-tube Anton Paar density meter (DMA 5000M) at the desired temperature. The calibration of the device is conducted with distilled water and dry air. From the densities of the inclusion complexes solutions (ρ) and solvent (ρ_0), the apparent molar volume of the CD (V_ϕ) can be calculated as:

$$V_\Phi = \frac{M_w}{\rho} - \frac{10^3(\rho - \rho_0)}{m \cdot \rho \cdot \rho_0} \tag{3.4}$$

where M_w and m are the cyclodextrin molecular weight (g mol^{-1}) and molality (mol kg^{-1}), ρ as the density of inclusion complexes solutions (g cm^{-3}) and ρ_0 is the correspondent surfactant solution (g cm^{-3}), as previously mentioned.

The volume of transfer (ΔV^{CD}) is then obtained by the difference between the apparent molar volume calculated for the CD in each sample and in water. A python code was used to perform the one-to-one fit of the data.

The strength of the complexation process, as depicted in eq.3.1, is expressed by the binding affinity (K). According to Young's model for one-to-one binding [90], the V_ϕ^{CD} can be expressed with reference to the volumes of the species in solution:

$$V_\Phi^{CD} = V \cdot \frac{m_{CD-S}}{m_{CD}} + (1 - \frac{m_{CD-S}}{m_{CD}}) \cdot V_0 \tag{3.5}$$

where the m_{CD} and m_{CD-S} are the concentration of the free CD and the CD involved in the inclusion complexes, V is the volume in the complex, and V_0 is the non-complexed volume of the CD.

The volume of transfer (ΔV^{CD}) was calculated by the difference of the apparent molar volume of the cyclodextrin in pure aqueous solution and in the surfactant solution and are depicted in Fig. 3.5. The calculated transferred volumes of the CD from water to the surfactant present a monotonic trend of reaching a plateau, indicating the saturation of the available cavities after a first maximum from where the stoichiometry can be extracted.

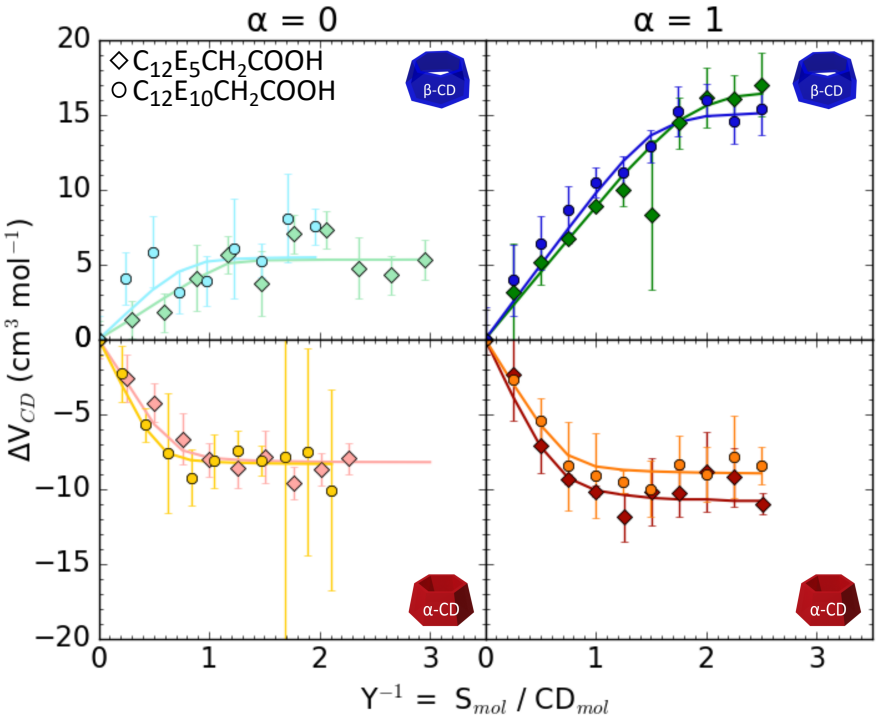

FIGURE 3.4: Volume of transfer (ΔV^{CD}) of α-cyclodextrin and β-cyclodextrin from water to aqueous solution of $C_{12}E_5CH_2COOH$ ($\diamond$) and $C_{12}E_{10}CH_2COOH$ ($\circ$). Solid lines are the best fit according to Eq. 3.5. *Adapted from Ref. [84] with permission of the Royal Society of Chemistry.*

The reported values obtained from the fit, depicted in Table 3.3, align with those obtained from the ITC experiments. Despite the surfactant, the straightforward observation is the opposite signal of the ΔV^{CD} for the different cyclodextrins. The differences occasioned by one extra glucopyranose unit in these molecules are beyond the solubility and intramolecular interactions. In solution, the wider cavity of βCD can accommodate more water molecules, but the incomplete hydrogen bonding network, especially in the narrower cavity of αCD, is highlighted by the different C_p, as previously discussed. The negative values of αCD indicate the predominance of the Van der Waals interactions [91] and the reduced number of water molecules

TABLE 3.3: Thermodynamic parameters of different surfactant-cyclodextrin complexes obtained from the volumetric fit.

Surfactant	**CD**	α **= 0**			α **= 1**		
		n	K (10^3 kg mol $^{-1}$)	ΔV (cm^3 mol $^{-1}$)	n	K (10^3 kg mol $^{-1}$)	ΔV (cm^3 mol $^{-1}$)
$C_{12}E_5CH_2COOH$	αCD	1.17 $\pm$ 0.1	6.23 $\pm$ 0.46	-8.16 $\pm$ 0.1	1.50 $\pm$ 0.1	3.49 $\pm$ 0.12	-10.67 $\pm$ 0.23
$C_{12}E_{10}CH_2COOH$		1.71 $\pm$ 0.2	7.62 $\pm$ 0.31	-8.29 $\pm$ 0.1	0.54 $\pm$ 0.2	5.76 $\pm$ 0.2	-8.87 $\pm$ 0.16
$C_{12}E_5CH_2COOH$	βCD	0.8 $\pm$ 0.1	5.68 $\pm$ 0.08	5.30 $\pm$ 0.1	1.47 $\pm$ 0.1	11.25 $\pm$ 1.04	14.45 $\pm$ 1.93
$C_{12}E_{10}CH_2COOH$		1 $\pm$ 0.1	8.50 $\pm$ 0.96	5.34 $\pm$ 0.3	0.85 $\pm$ 0.1	15.1 $\pm$ 0.42	14.16 $\pm$ 1.13

expelled from the cavity, in addition to a strong contribution of the gauche conformations of alkyl chains involving negative volumes [89, 92]. The positive values obtained for βCD are mostly related to the increased number of water released and to a reduced geometrical constraint of the guest in the cavity. The positive values are also reported for others βCD inclusion complexes containing fluorinated surfactants [93], alkanoates [89], homologous trimethylammonium surfactants of different alkyl chain lengths [33, 94], nicotinic acid [95], dicarboxylates [96] and amino acids [97]. The magnitude of the volumes is evidently specific to each inclusion complex system.

The apparent molar volumes and the transfer volumes calculated depend on the binding affinity, stoichiometry, the inclusion of the guest in the host, and the physicochemical properties. In this case, although a contribution of the EO units of the head was expected to be evidenced by a clear difference in Δ V^{CD}, the distinction was not possible.

Different perspectives associated with the inclusion complexation and the changes in the volumes observed are also reported in the literature exploring the possible flexibility of the cyclodextrins molecules. Such flexibility is assigned to the possible conformations of the α-1,4 linkage connecting the glucosidic units resulting in a tilt of the molecular structure and altering the proximity of the units. The phenomenon is described as more critical for αCD, in which the disruption of the hydrogen bonding network, either by substitution or by guest inclusion, provides certain structural adaptability [11, 98]. The small molecular adjustment was verified in methanol-αCD complexes [99]. Nonetheless, the volumetric contribution of the hydration and the hydrogen bonding upon complexation is still present. The opposite is not commonly addressed, though, as the similarities in the conformation and symmetry of the free and complexed βCD have been examined by X-rays [93, 100, 101].

Chapter 4

Inclusion complexes self-assembly

Published in *Soft Matter, 2022, 18, 6529-6537*
and *Soft Matter, 2023, 19, 1523-1530.*

"Entropy is the price of structure."

Ilya Prigogine

4.1 Hierarchical self-assembly: a multilevel perspective

Entropy is the key energetic parameter in the self-assembly process and challenges the perception of the disorder. Often described in terms of order and disorder concepts, the quantification of a system's entropy is not limited to it. The process relies on the organization as a result of the free energy's minimization and maximization of the entropy. The general definition of entropy is given by the equation 4.1.

$$S = k_B \log \Omega \tag{4.1}$$

where the k_B is Boltzmann constant, and Ω is the number of states or volume phase space accessible to the system [52]. Entropy can be further divided into translational, rotational and vibrational contributions, which relate to the arrangements due to the translational degree of freedom, particle's orientation and vibrational motions, respectively. Shapes and conformations are also directing the assembly, so they directly impact the translational and rotational entropic contributions [52, 102].

The entropic force is not an intrinsic property of the particles but a property of the self-assembling systems. In addition, it increases with increasing the contact area between two particles, *i.e.*, with the increase in concentration. The thermodynamics stability is then a function of the volume in phase-space associated with the states of the system. The ordering arises from the maximization of such volume [52, 102].

Self-assembly is a universal concept in nature. The spontaneous organization of atoms, molecules, ions, and clusters into more complex structures in chemistry, material and biological systems have been the centre of investigations in science. The assembly relies on non-covalent interactions, such as hydrogen bonds, electrostatic interactions, $\pi - \pi$ interactions, dispersion hydrophobic effect, host-guest interactions or metal coordination, for example. In nature, one can find many examples of assembled structures. Micelles and vesicles are classic examples of one-step assembled systems arising from surfactants; in living organisms, the assembly of phospholipids into soft membranes can be cited. Understanding the similarities and differences and so as the triggering parameters of the assembly processes are extremely important to explore the phenomena to design novel materials efficiently [9, 103].

Interesting examples of hierarchical assemblies are provided by cyclodextrin-surfactant systems. The assembly of inclusion complexes into ordered structures is driven by highly directional water-mediated hydrogen bonding between adjacent cyclodextrins and modulated by the repulsion forces provided by the guest molecules [26, 59]. The importance of hydrogen bonding in the process and structures is evidenced by the inhibition of the assembly if substituted cyclodextrins are employed in the complexation [25, 26].

Different packing types are reported in the literature depending on the cyclodextrin type and guest (Fig. 4.1). Channel, cage and brick-type packings are the most common arrangements along their rotational axis. The cage-type lattice is common in small, neutral guests complexes assemblies with αCD and βCD, where they are organized in a herring-bone pattern, as shown in Fig. 4.1(a) [104]; common in small aromatic guests with αCD, the brick-type is exhibited when the complexes are organized in layers of alternating head-tail sequence of cyclodextrins, slightly shifted to each other by approximately half cyclodextrin diameter (Fig. 4.1(b)) [59]; and, in the channel lattice (Fig. 4.1(c)), the complexes are stacked forming a channel, in which the guest is located. The latter is the most common arrangement of the native cyclodextrins in solution and the cyclodextrins-surfactant complexes. Generally, they are organized in dimers, where a tail-to-tail configuration is found in the complexes, and a head-to-head configuration is verified in their vertical assembly [105, 106].

For CD/surfactants assemblies, only channel-type packing is reported despite the macrocycle type. However, the lateral assembly of the complexes is strongly dependent on their cavity size and symmetry. The crystalline structures of αCD present a hexagonal arrangement (Fig. 4.1(d)) [107, 108]; βCD inclusion complexes are arranged in a rhomboidal unit cell [27, 69] (Fig. 4.1(e)); and, although rarely reported, a squared lattice γCD is reported for the native host and small guests in solution (Fig. 4.1(f)), which supports the possible arrangement in CD/surfactant systems.

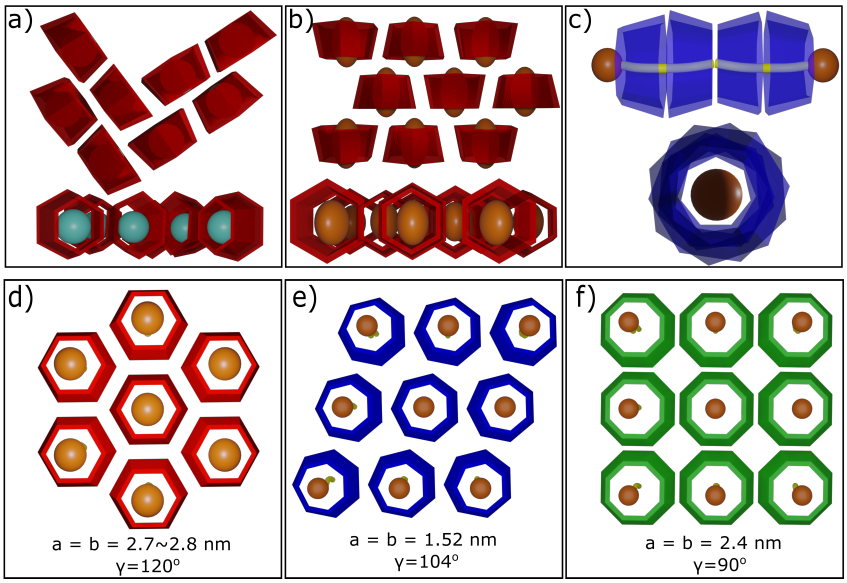

FIGURE 4.1: Schematic representation of the typical lateral assembly found in cyclodextrins and their inclusion complexes. *Figure adapted from [9] with permission of Elsevier.*

In CD/surfactant complexes hierarchical assemblies in aqueous solutions, the first level of assembly consists of the inclusion complexation and the further steps occur depending on the concentration, mixing ratio and temperature. The organization into crystalline membranes, hydrogels, fibers, vesicles, lamellar and tubular structures have been reported in the literature for systems with SDS, polyoxyethylene sorbitol esters and dodecyl trimethylammonium bromide.

Among the systems containing ionic surfactants, the structures arising from the SDS-β-cyclodextrin inclusion complexes self-assembly are largely investigated as a function of their concentration. Reversible phase transitions are reported for a vesicular phase in concentrations between 4 and 6 %wt, tubular assemblies are found in concentrations between 6 and 25 %wt and a lamellar phase is obtained at higher concentrations [66]. For the nonionic surfactant systems, vesicles and lamellas are the most common phases for the complex systems investigated so far [109, 110]. Notwithstanding, structural investigations with either ionic or nonionic surfactants have been conducted. The systematic evaluation of the charge density role, maintaining the chemical architecture of the guest and host, has only been addressed, up to now, by the present investigations with the weakly anionic alkyl ethylene oxide carboxylic acids.

4.1.1 Structural investigation

A comprehensive investigation of the supramolecular assemblies' structure may require the use of a series of techniques. Scattering techniques (light, neutrons and

X-ray scattering) [38, 65, 111–113], nuclear magnetic resonance [114, 115], and other imaging techniques, such as optical microscopy, atomic force microscopy and electron microscopy [73] are frequently used to probe the structural features of complexes' assemblies.

The combination of several techniques allowed a comprehensive structural characterization of the systems described in this thesis. ***Small-angle neutron scattering (SANS)*** was used to characterize the internal structure of the supramolecular assemblies covering their nanometric range. In order to overcome the encountered limitation in the micrometre-scale of the assemblies, optical and electron ***microscopy*** was a suitable technique able to probe the morphology of the assemblies. ***Differential scanning calorimetry*** studies were performed to understand the heat changes associated with physical and chemical transitions in the alkyl ethoxy carboxylates, given their multiple responsiveness and rich phase behaviour.

Small-angle neutron scattering (SANS)

Neutron and X-ray scattering are excellent techniques that provide detailed insight into the shape, size, volume, molecular weight and arrangement of single molecules and multi-component complex systems. Small-angle scattering, either neutron or x-ray scattering, is a powerful technique applied to characterize amphiphilic systems and their complexes. X-ray scattering provides high resolution and brilliance suitable for time-of-flight and experiments requiring high resolution. In turn, neutrons offer high penetrability due to the lack of charge, and the sensitivity to different isotopes provides the possibility of exploiting the selective isotopic labelling of certain elements or the contrast variation to probe the internal structure of the system without changing the molecular architecture of the investigated specimen [116, 117].

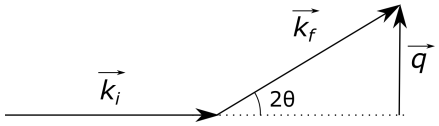

FIGURE 4.2: The vector diagram for elastic scattering $|k_i| = |k_f|$ through a 2θ angle.

Small-angle neutron scattering is based on the coherent and elastic scattered neutrons from the nuclei. The scattering of a neutron by a sample is described by the resultant change in its momentum, as shown in Figure 4.2. So, the neutron beam hits the sample with a wave vector $\vec{k}_i$ and is scattered with the wave vector $\vec{k}_f$. Quantum mechanics allows the expression of the momentum transfer by:

$$\vec{q} = \vec{k}_i - \vec{k}_f \tag{4.2}$$

The no-exchange energy fundamental assumption of elastic scattering: $|\vec{k}_i| = |\vec{k}_f|$, fulfilling the condition that the wave vector modulus and wavelength λ are not changed upon scattering leads to $\vec{k} = 2\ \pi/\lambda$. The simple trigonometry application results in the definition of the modulus momentum transfer by:

$$q = |\vec{q}| = \frac{4\pi \sin\theta}{\lambda} \tag{4.3}$$

The intensity detected is proportional to the number of neutrons reaching the detector at different angles (in the case of a monochromatic beam) or the energy/counts of reaching the detector at the same time (time of flight) and is the Fourier Transform of real-space shapes. The scattering intensity as a function of the scattering vector q is given by :

$$I(q) = N_p V_p^2 (\rho_p - \rho_s)^2 F(q) S(q) + B \tag{4.4}$$

where N_p is the number of particles per volume unit, V_p is their volume, ρ is the scattering length density of the particle (ρ_p) and solvent (ρ_s), F(q) is the form factor, S(q) is the structure factor, and B is the background (with contributions of the incoherent scattering).

The form factor (F(q)) refers to the shape description of the scattering object.

The structure factor (S(q)) describes the contribution of the local ordering of the particles in the sample, which is defined by the interaction between the particles. In very dilute systems, in which the inter-particle distance is high, we assume S(q) = 1.

This technique is used to probe structural details on a length scale between 1 and a few hundred nanometers. A typical SANS scattering curve is represented in Fig. 4.3 and allows the structural characterization of the systems.

From the SANS data, it is possible to approach a model-free analysis, which allows the assessment of a few features of the system without a model fit, and the fitting of the curves to a model that fully describes the system. In general, the following information can be obtained from the SANS curves:

- The zero-q intercept, if the concentration is known, the particle mass can be determined;
- The presence of a plateau at low-q followed by a monotonic decrease provides information about the Radius of gyration (R_g) and the size of the particles;
- Power law modeled towards high-q region indicates the mass fractal dimension, which is related to the shape of the particle;

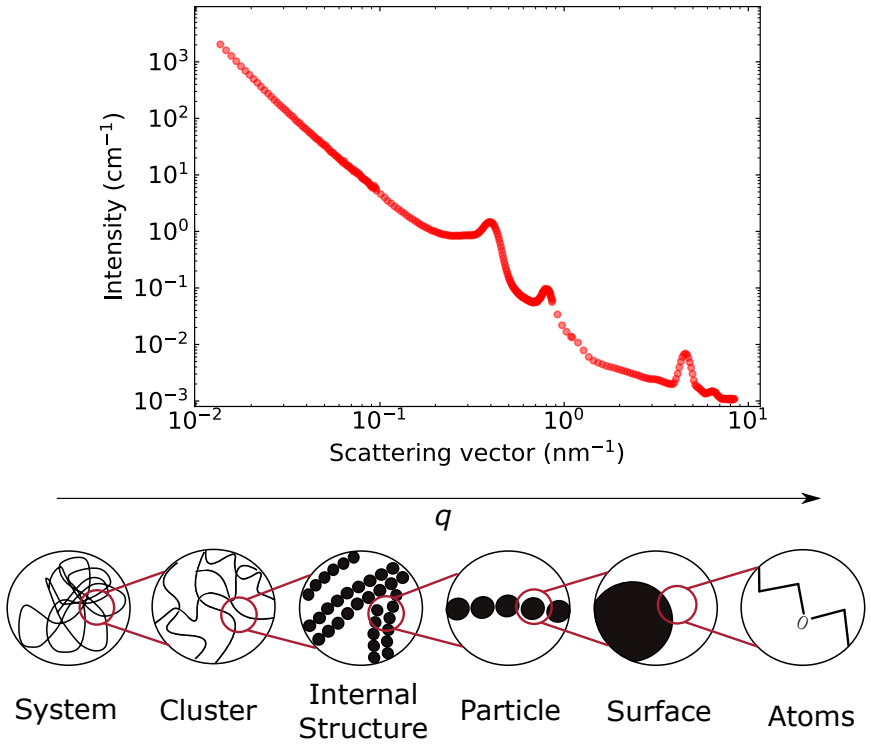

FIGURE 4.3: Schematic representation of a SANS curve and the possible structural features determination. Data depicted are the SANS curve profile of the $C_{12}E_5CH_2COOH$-αCD system at high pH (D22@ILL).

- At mid-q, it is also possible to determine the microstructure if any feature is present, as a result of the structure factor S(q). For example, the peaks shown in Figure 4.3 are a signature of highly-ordered multilayered structures;

- The features from mid to high-q values provide information on the surface area and surface fractal dimension through the Porod approximation.

The presence of micrometer-length structures, as in the case of the cyclodextrins-polyoxyethylene alkyl ether carboxylic supramolecular assemblies, and the lowest achievable q for the system is greater than R_g, *i.e.*, the lack of the Guinier domain. Hence, the determination of the scattered unit's size is precluded. The scattering curves and the characterization are, then, limited to the aggregates' microstructure. In these cases, if the full characterization of the system is aimed, other techniques as microscopy, for example, should also be applied.

The SANS experiments were performed at D11 [118] and D22 [119] instruments at Institut Laue-Langevin (Grenoble, France). The experiments were conducted as described in **Papers II** and **III** [84, 120].

Microscopy

Optical and electron microscopy analyses were performed in order to characterize the morphology of the inclusion complexes' assemblies. Optical microscopy was used as a first exploratory approach and revealed the main structures. Polarized optical microscopy was then applied to verify the ordering of these structures. A higher resolution of the assemblies was provided by transmission electron microscopy (TEM) and cryogenic electron microscopy (cryo-EM).

Optical microscopy is based on generating magnified images from a specimen by the transmitted or reflected visible light travelling through a system of lenses. Polarised optical microscopy offers the possibility of using a polarized plate to convert visible light into polarized light by orienting it at 90° to the illumination. The method provides the assessment of the sample's anisotropic properties by the identification of the phases and out of phases through the recombination of the polarized light travelling in different directions in the sample and the second polarizing filter. A final high-contrast image is obtained, allowing the identification of the ordered phases of the sample [121, 122]

TEM and cryo-EM rely on a concentrated electron beam emitted through a vacuum focused by electromagnetic lenses in a fine beam towards the sample. Bright-field imaging is based on the contrast of the scattered incident electrons depending on compositional density and crystal orientation and the non-scattered electrons. The latter provides a "shadowed" image in which shades vary according to the density of the sample. The image is built from the electrons passing through the analyzed specimen. Tomography can also be provided by obtaining multiple images upon rotation of the sample [121]. The key difference between conventional TEM and cryo-EM is the sample preparation method. Cryo-EM uses the freezing principle to create a specimen avoiding the use of chemical fixation and staining approach typical in TEM. By freezing without additional sample treatments, the structure of macromolecular complexes is preserved and allows their investigation with higher resolution [123].

Sample preparation for the microscopic analyses is described in **Paper II** [84]. Optical microscopy was performed at the ILL, with PSCM support; TEM was performed at IBS with the support of Dr. Daouda Traore and Cryo-EM was performed at BioSupramol Microscopy Core with the support of Dr. Kai Ludwig and Prof. Christoph Schalley.

Differential Scanning Calorimetry (DSC)

Differential scanning calorimetry is a powerful thermoanalytical technique to measure the heat transferred to or from a sample associated with a physical or chemical

change. The straightforward data analysis, the relative simplicity in performing the experiment and low cost of the equipment widen the application of DSC to the investigation in numerous fields [124, 125]. The experiment's purposes vary from quality control aims (purity determinations, for example) to kinetic or safety investigations. In research of soft systems, it is often applied to extract information about the enthalpy change (ΔH), aiming at the evaluation of a system's phase. However, a substantial amount of information can be extracted from the DSC curves by performing the data analysis [124, 125].

An essential step in the data analysis is the correct interpretation of the baseline since it indicates the disparities in sample and reference heat capacities. The enthalpy change is determined by the integration of the apparent heat capacity in the transition-identified temperature range after the subtraction of a proper baseline [124, 125]. For the determination of the enthalpy of the inclusion complexes assemblies, the pyDSC was used to perform the analysis, as described in **Paper III**.

DSC experiments were performed at ILL, with Partnership for Soft Condensed Matter.

4.2 Alkyl ether carboxylic acid and cyclodextrins: a multi-responsive system

The complex interplay of interactions governing the self-assembly process of CD-surfactant inclusion complexes into supramolecular aggregates is a widely exploited strategy to design responsive materials relying on environmental conditions. The dynamic nature of the non-covalent interactions offers the possibility of controlling the system's behaviour and the outcome structures formed in the assembly process via tuning the interactions involved in the assembly.[103]

Inclusion complexes responsive to light [126–128], pH [84], redox potential [129–131], solvent exchanges [32, 37] and temperature [132, 133] have been reported in the literature aiming to explore the stimuli-responsive properties in the design of new materials.

The pH-responsive systems either contain protonable groups, such as the alkyl ethoxy carboxylate, or chemical bonds that cleavage occurs under pH manipulation [103]. The architectural change promoted by this simple change can be very valuable in formulations and systems requiring controlled substance release, such as drug delivery. The pure alkyl ethoxy carboxylates aqueous systems themselves are a good example of pH-adaptable systems and vesicles, flat structures and micelles can be

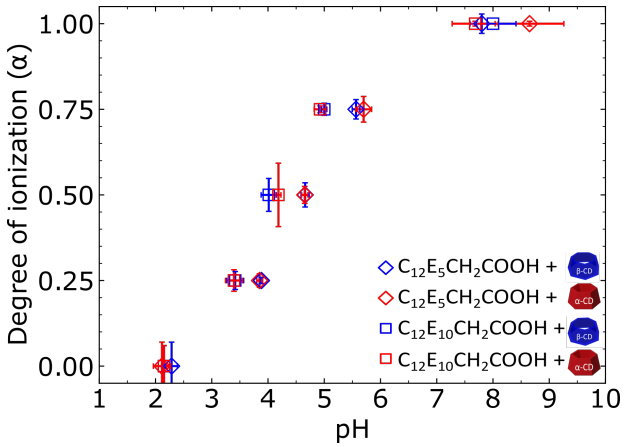

FIGURE 4.4: Degree of ionization of the cyclodextrin-surfactant systems as a function of pH. *Adapted from Ref. [120] with permission of the Royal Society of Chemistry.*

found depending on the number of ethylene oxide units in the headgroup and pH. [49].

Temperature is one of the most exploited stimuli in soft systems to control the self-assembly process due to its great effect on solubility, molecular vibrational states and interactions' strength. In cyclodextrin complexes, vesicles, lamellas, microtubes and hydrogel thermo-switchable phases have been identified in the literature. The thermoresponsive behaviour of SDS@2βCD in the reversible microconfinement of particles within the assemblies along with a co-assembly process has demonstrated the great phase dependency potential application of cyclodextrin systems [134, 135].

The fact that the weakly anionic alkyl ether carboxylic acids is affected by both pH and temperature motivates the investigation of their inclusion complexes with αCD and βCD in terms of the effect of the charge density and their thermoresponsiveness.

As previously mentioned, the ability to assemble into ordered aggregates is one of many interesting features of cyclodextrin-surfactant inclusion complexes. The investigations were conducted in order to probe the effect of the **concentration**, **CD-to-surfactant ratio (Y)**, **degree of ionization** (α), **molecular architecture of the surfactant and CD** and **temperature** on the aggregates' morphology.

The addition of sodium hydroxide in a molar ratio with the surfactant allowed us to systematically control the degree of ionization of the surfactant. The degree of ionization as a function of the pH of the systems is shown in Fig. 4.4.

The CD-to-surfactant mixing ratio had shown to strongly affect the aggregation behaviour, and, in a few systems, it was demonstrated to prevent the assembly or direct their morphology. Macroscopically, as depicted in Fig. 4.6, the assembly was not precluded at Y = 1 in alkyl ethoxy carboxylic acids inclusion complexes,

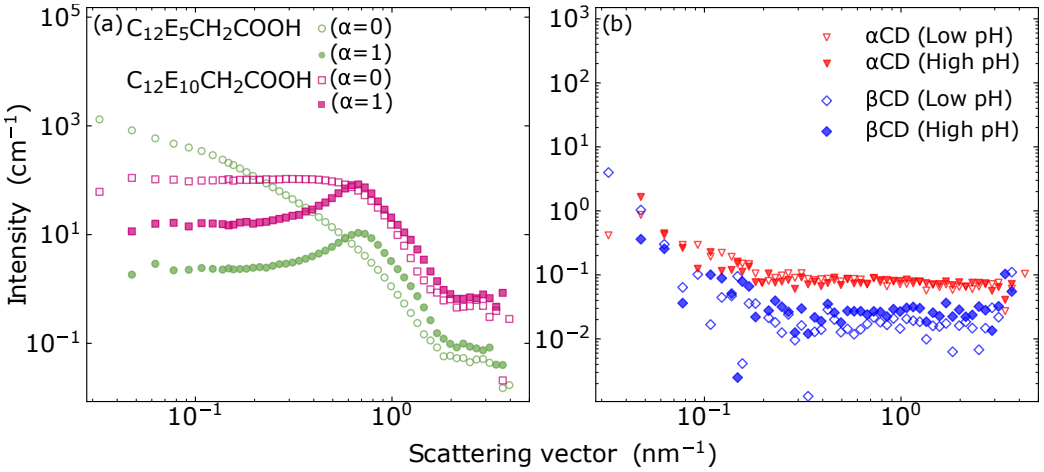

FIGURE 4.5: SANS curves of (a) $C_{12}E_5CH_2COOH$ and $C_{12}E_{10}CH_2COOH$ at 5%wt surfactant concentration and (b) α-cyclodextrin and β-cyclodextrin (saturated solutions) at $\alpha = 0$ (open symbols) and $\alpha = 1$ (closed symbols). Curves of the different surfactants are scaled by successive factors of 10 for readability. Data measured at ZOOM@ISIS. *Adapted from Ref. [120] with permission of the Royal Society of Chemistry.*

but variation in the viscosity of the solutions was observed for αCD despite the ionization. For those, a gel behaviour is verified for the highest ratio, whereas less viscous samples are obtained with a ratio equal to 1. The phase separation into a clear supernatant and a white phase was observed for βCD aggregates after 48 hours and more evident in $C_{12}E_{10}CH_2COOH$. In the ionized systems ($\alpha = 1$) regardless of the surfactant headgroup or cyclodextrin cavity size, the birefringence is a remarkable feature as a result of the ordered aggregates, and it is strongly present in Y = 2. The features verified in these systems are not referent to the surfactants structure or the cyclodextrin aggregates in solutions as demonstrated by their pure solutions SANS measurements depicted in Fig. 4.5 and reported in literature [24].

The SANS data measured for the systems of $C_{12}E_5CH_2COOH$ and $C_{12}E_{10}CH_2COOH$, with mixing ratio [CD]/[Surf] = 1, are depicted in Fig. 4.7, respectively with αCD (a and c) and βCD (b and d) and, with mixing ratio [CD]/[Surf] = 2, are depicted in Fig. 4.8, respectively at different concentrations (a and c) and degrees of ionization (b and d).

The comparison of the SANS curve profiles of Y = 1 and Y = 2 systems at the same concentration indicates the presence of more ordered aggregates for the higher ratio. The presence of peaks at Y = 1 curves at compatible positions with the ones present at Y = 2 points to a limited ordering of the aggregates. The lower mixing ratio leads to an incomplete formation of the structure and a mixture of assemblies of different morphologies as a result of a reduced presence of the directive CD-CD hydrogen bonding network.

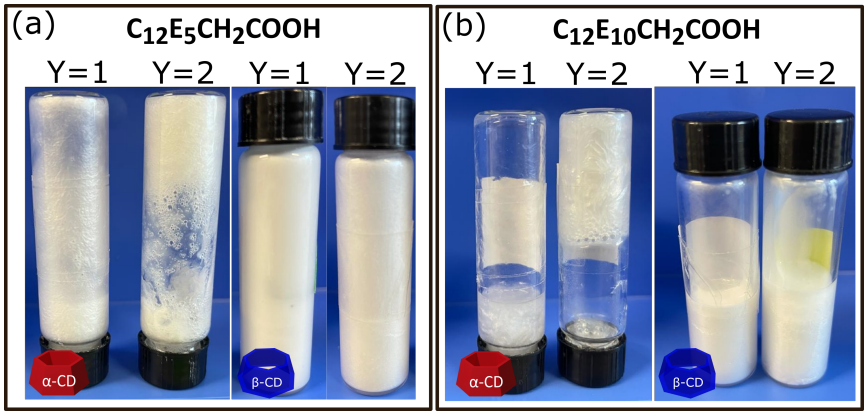

FIGURE 4.6: Figures of $C_{12}E_5CH_2COOH$ and $C_{12}E_{10}CH_2COOH$ samples with αCD and βCD at different CD/Surfactant mixing ratio.

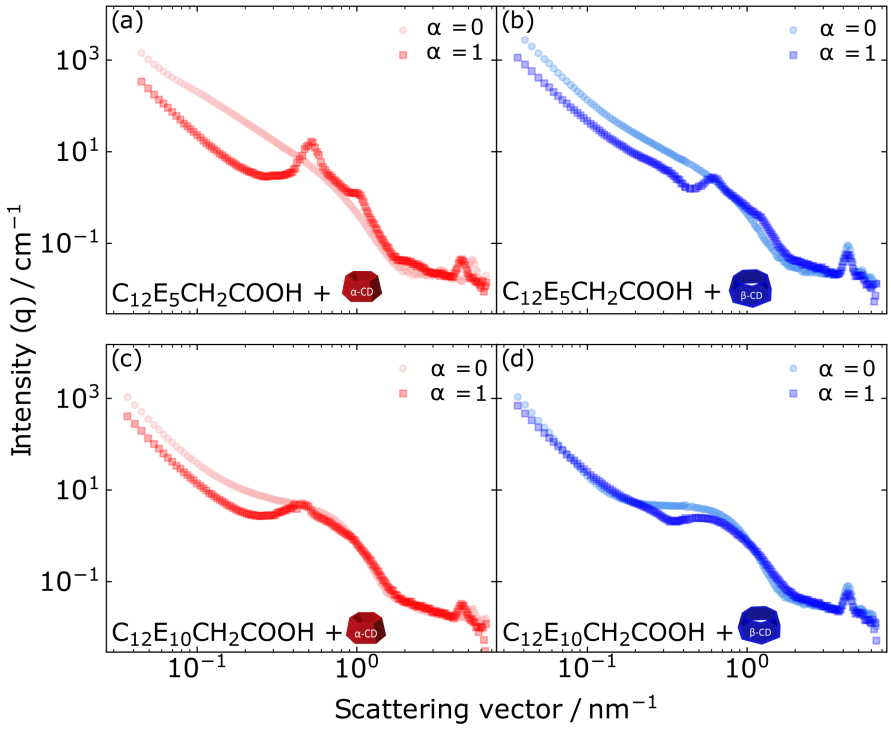

FIGURE 4.7: SANS curves profiles of $C_{12}E_5CH_2COOH$ (a and b) and $C_{12}E_{10}CH_2COOH$ (c and d) αCD and βCD. SANS intensity is expressed as a function of the scattering vector (q). *Adapted from Ref. [84] with permission of the Royal Society of Chemistry.*

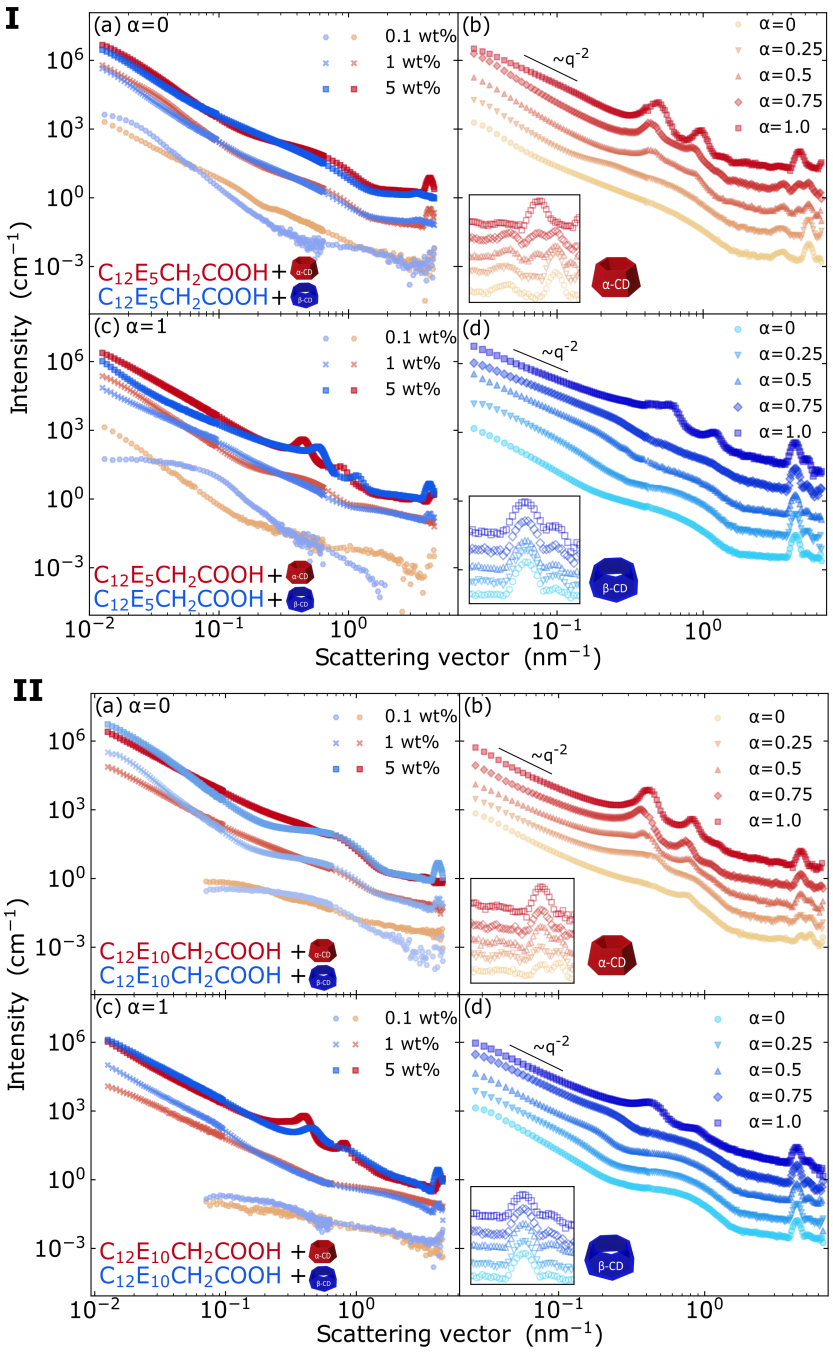

FIGURE 4.8: SANS curves profiles of $C_{12}E_5CH_2COOH$ (I) and $C_{12}E_{10}CH_2COOH$ (5 %wt surfactant) (II) with αCD and βCD. SANS intensity is expressed as a function of the scattering vector (q). The measurements at (a) $\alpha = 0$ and (c) $\alpha = 1$ and the different degrees of ionization for (b) αCD and (d) βCD. Curves are scaled by successive factors of 10 to improve readability. The insets represent an enlargement of the high q region. Data were acquired at D11@ILL and the degree of ionization, at the D22@ILL.

Adapted from Ref. [120] with permission of the Royal Society of Chemistry.

The supramolecular aggregates present a clear **concentration** dependency evidenced by the macroscopic changes upon dilution. At 0.1 %wt of surfactant, transparent systems are observed; at 1 %wt, a white fluid is obtained, while a viscous fluid, with a gel aspect, is obtained in concentrations superior to 3.5 %wt. Although macroscopically visible, the SANS curves evidenced this feature, pointing to a higher level of organization for concentrated samples (5 %wt surfactant). By increasing the concentration of the systems from an inclusion complex solution to an assembled system, the transition to more compact structures is entropically favoured. The enriched microstructure is observed for ionized systems ($\alpha = 1$) (Fig. 4.8 c and d), in which the presence of peaks for the concentrated systems is not cyclodextrin type related and the features are present in both of them with slight differences.

The phase diagrams present in **Paper II** (Fig.1) suggest an effect of the degree of ionization and the CD/S mixing ratio on the aggregates' molecular weight. The impact of the charge density on the structures of most concentrated systems was verified by the evaluation of the SANS curves at different degrees of ionization (Fig. 4.8 and (c) and (d). The ionic systems ($\alpha = 0$) present a -2 power law at low-q and the second-order peaks with a $q_1 / q_2 = 2$ position in the mid-q region. These are the signature characteristics of the occurrence of periodic lamellar structures. Such features are not present in the nonionic surfactant complexes systems and reveal their softer nature.

The impact of ethylene oxide units number in the surfactants' headgroup is highlighted in the comparison of the ionic systems of the two surfactants with the same CD in Fig. 4.9. The data extracted from the peaks are shown in Table 4.1. The shift of $C_{12}E_5CH_2COOH$ peaks towards slightly higher q for both CD evaluated points out compact layers for these systems. $C_{12}E_{10}CH_2COOH$ systems present peaks with αCD at q ≈ 0.4 and 0.82 nm^{-1} and with βCD complexes peaks at $q \approx 0.6$ and 1.2 nm^{-1} probe the periodicity of structures of 15.8 and 10.5 nm, respectively. From the SANS data is also possible to extract the higher structural ordering as a result of the extra ethylene oxide units verified by the third order peak arising in the $C_{12}E_{10}CH_2COOH$-αCD ionized system with $\alpha > 0.5$.

TABLE 4.1: Spacing distances of the ionic inclusion complexes supramolecular assemblies obtained by SANS.

SANS Data / **System**	**Peak position** $\approx$ q (nm^{-1})	**Repeating** distances (nm)
$C_{12}E_5CH_2COOH$-αCD	0.40	14.8
$C_{12}E_5CH_2COOH$-βCD	0.60	10.5
$C_{12}E_{10}CH_2COOH$-αCD	0.40	15.8
$C_{12}E_{10}CH_2COOH$-βCD	0.45	14.2

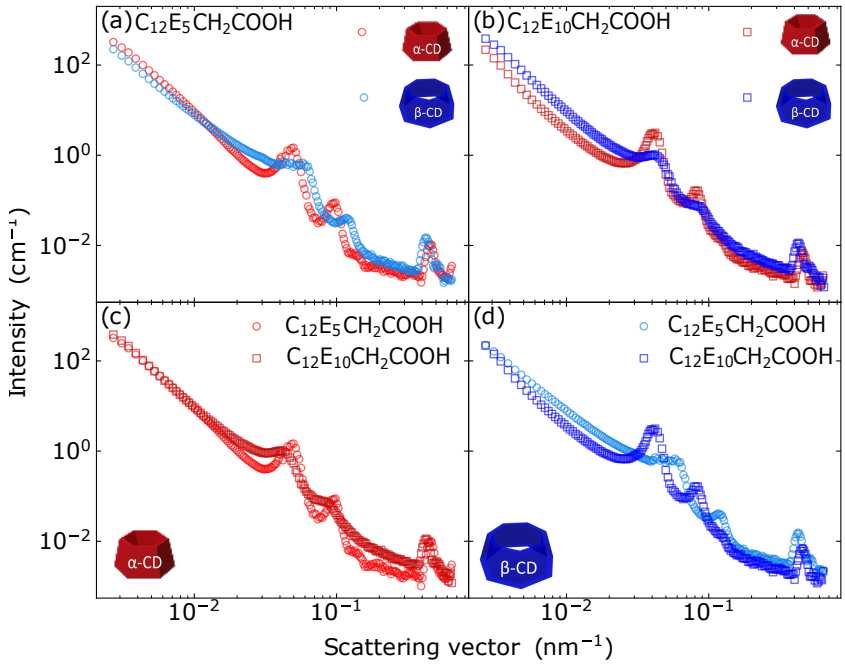

FIGURE 4.9: SANS curves profiles of ionized $C_{12}E_5CH_2COOH$ and $C_{12}E_{10}CH_2COOH$ with αCD and βCD. SANS intensity is expressed as a function of scattering vector (q). *Adapted from Ref.[84] with permission of the Royal Society of Chemistry.*

Finally, the molecular architecture effect of the CD on the packing of the inclusion complexes assemblies in terms of its cavity size is evidenced by the peaks at high-q, highlighted in the insets of (c) and (d) of the Figures 4.8. For βCD, the CD rearrangement upon the increase of the surfactants' degree of ionization is not observed, and a single peak is verified at q $\approx$ 4.31 nm^{-1}, whereas a restructuring on the CD packing is observed in αCD systems. In the latter, the presence of two peaks in the nonionic systems at q $\approx$ 3.45 and 5.25 nm^{-1} unfold to a single signal at the same position of βCD mixtures. The area of αCD molecule (1.8 nm^2) is comparable with the area per molecule of the charged $C_{12}E_{10}CH_2COOH$ at air/water interface ($\approx$ 1.3 nm^2). Then, the increase of the headgroup area and the changes in the hydration shell can be ascribed to direct the αCD packing rearrangement. This behaviour is not verified in βCD assemblies due to a larger spacing primarily directed by the wider cavity, with an approximate area (2.16 nm^2) greater than the surfactant's headgroup.

In the same way, the assembly into supramolecular aggregates is not prevented at low degrees of ionization, where a unilamellar structure is predominant. Hence, the charge density does not affect the assembly process of the inclusion complexes but has an essential role in directing it by providing the electrostatic repulsion required to build the periodicity to the multilayered structures.

The noticeable lack of Guinier domain in all the SANS curves prevents the

full characterization of the assemblies' morphology. Nonetheless, the use of microscopy techniques was able to unveil it. The acquired images of the morphologies of $C_{12}E_5CH_2COOH$ assemblies with αCD and βCD are presented in Fig. 4.10. The aggregates (Fig. 4.10 a and b) evidence the two different morphologies obtained for nonionic and ionic systems with βCD. TEM images allowed the observation of rhomboidal assemblies compatible with the 2D βCD crystallization lattice (Fig. 4.1(e)) and common to many other surfactant systems with the same macrocycle [26, 37, 65, 112]. Ionized surfactant systems with both cyclodextrins exhibit interesting well-ordered hollow cylinders (Fig. 4.10 b-g). A detailed analysis of the tube edge of $C_{12}E_5CH_2COOH$-βCD image obtained by Cryo-EM confirms the multilayered nature of the cylindrical structures with the periodicity described by the SANS measurements of $\approx$ 10 nm (Fig. 4.10(e)).

The statistical distribution of the cylinders conducted from the optical microscopy images indicates the monodispersity of the cylinders' diameters. An average of 2.7 μm ($\pm$ 0.24) was confirmed for the βCD cylinders, and 1.5 μm ($\pm$ 0.25), for αCD. Interestingly, the different cavity diameters do not influence only the lattice but also impact the rigidity of the assemblies. Remarkable straight rigid tubes are verified for βCD and entangled/bending tubes are αCD characteristic.

The formation mechanism of the tubular structures and their nature are yet not fully resolved. The non-linear association of the nucleation and concentration is described by Landmann and collaborators for SDS@2βCD assemblies, in which increasing the concentration would provide the formation of concentric cylinders assigned to the consecutive confinement of lamellas in the first enclosed formed cylindrical layers, providing an internal growth of structures [27, 60]. Their investigations report a certain competition between the bond formation and the bending free energy that leads to the coalescence of the two edges. Another formation mechanism of the tubes reported in the literature is based on the bending in the length of the lamellar structure into the tubular shape and slightly relates to the bending energy [112, 136, 137]. However, the analysis of the cyclodextrin inclusion complexes with alkyl ether carboxylic acids could not resolve the formation mechanism of the tubes observed in the ionized systems.

Assemblies built with hydrogen bonds are often reported to be affected by temperature. The phase transitions triggered by **temperature** change is a common characteristic of cyclodextrins inclusion complexes assemblies [80, 109]. In the inclusion complexes evaluated, the phase diagrams reported in Fig. 1 of **Paper I** hinted at a shift in the phase boundaries upon heating the systems for one hour at 70°C. In order to gain insight into structures involved in the phase transition process, the SANS measurements of the nonionized ($\alpha = 0$) and ionized ($\alpha = 1$) $C_{12}E_5CH_2COOH$

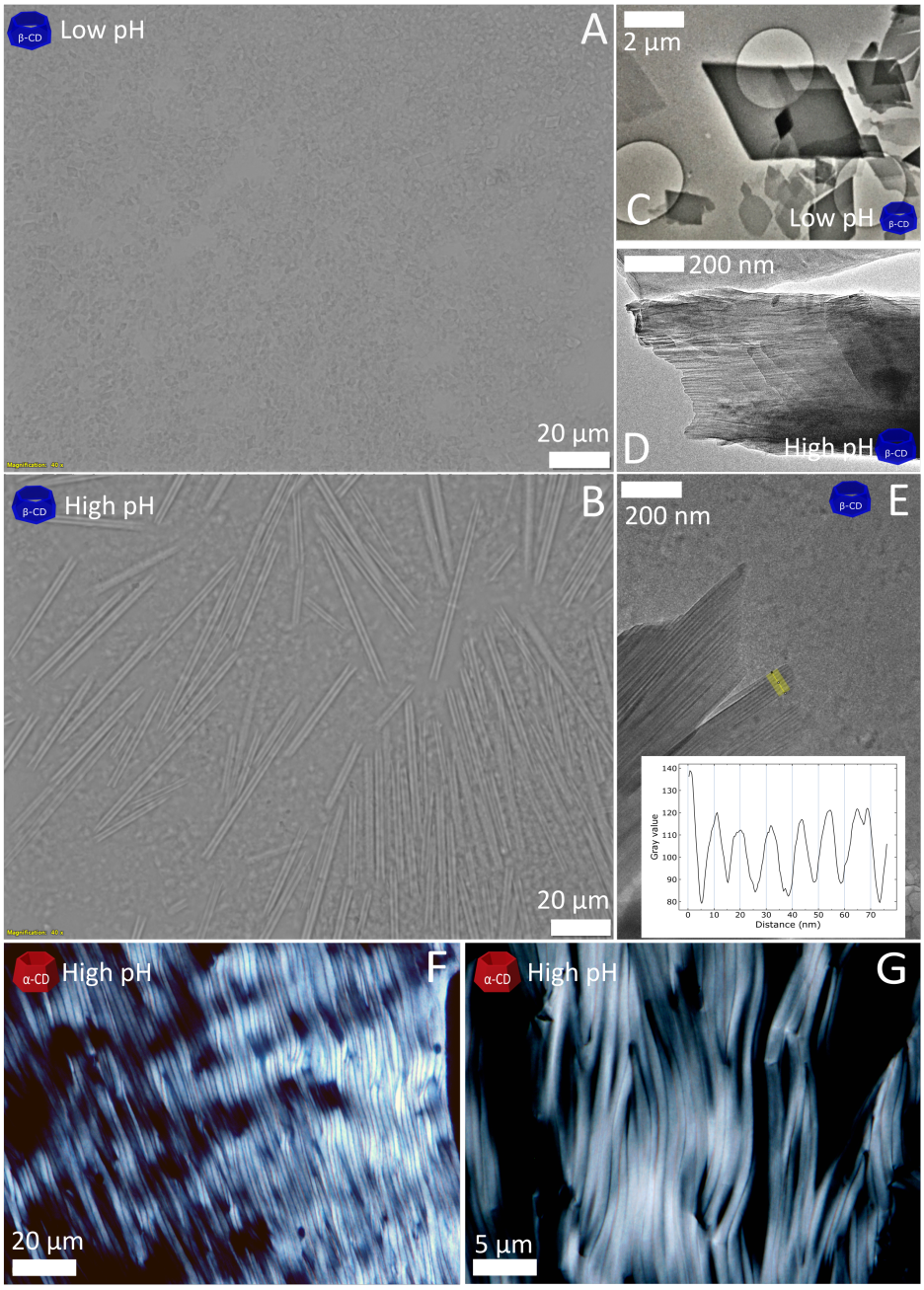

FIGURE 4.10: Morphology of the inclusion complexes aggregates observed by microscopy. Aggregates verified for $C_{12}E_5CH_2COOH$-2βCD inclusion complexes. Optical microscopy overview of the assemblies obtained at (a) $\alpha = 0$ and (b) $\alpha = 1$ (scale bar: 20 μm). (c) TEM image of the rhombic structures from the assembly with the nonionic surfactant (scale bar: 2 μm). (d) Cryo-TEM pictures of the tubular structure edge obtained from $\alpha = 1$ (scale bar: 200 nm) and (e) Cryo-EM picture zoom-in of the multi-layered tube wall (scale bar: 200 nm). Polarized optical microscopy images of αCD systems: (f) Ionized $C_{12}E_5CH_2COOH$-αCD (scale bar: 20 μm) and **(g)** Ionized $C_{12}E_{10}CH_2COOH$-αCD (scale bar: 5 μm). *Reproduced from Ref. [84] with permission of the Royal Society of Chemistry.*

(Fig. 4.11.I and III) and $C_{12}E_{10}CH_2COOH$ (Fig. 4.11.II and IV) systems performed at 15, 25, 45 and 70 °C are shown in Fig. 4.11, as reported in **Paper III**.

At α = 0, the temperature responsiveness of the $C_{12}E_5CH_2COOH$-αCD is an exception. Up to 45°C, the nonionic systems are not affected by thermo-stimuli with a q^{-2} power law, exhibiting a decrease in the scattering intensity at 0.6 nm^{-1}. The curves profiles point to the presence of the cyclodextrin-decorated surfactant vesicles and similarities with the scattering curves of pure aqueous surfactant.

At 70°C, the $C_{12}E_5CH_2COOH$-αCD display a correlation peak at q $\approx$ 1 nm^{-1}, which corresponds to a distance of 6.4 nm equivalent to the surfactant alkyl chain length in real space. Such observation in this system drives our attention to the pure surfactant solution in order to have a better insight into the thermal behaviour of the complex system. The aqueous solutions of $C_{12}E_5CH_2COOH$ also exhibit a correlation peak at q $\approx$ 1 nm^{-1} arising from their densely-packed structures and a liquid-liquid phase separation is observed above 55°C. On the contrary, thermo-stimuli structural changes of βCD mixtures with the same surfactant are not verified up to 70°C.

The thermoresponsiveness of ionized systems' ordered multilayers is noticeable by the broadening of the peaks and their shifts in a few cases. The increase from 15 to 45°C induced broadening of the peaks is characteristic of a reduction in the long-range ordering or in the number of layers, provided, for example, by the increase in the flexibility of the layers. The repeating distances verified for the systems are shown in Table 4.2.

$C_{12}E_5CH_2COOH$-βCD and $C_{12}E_{10}CH_2COOH$-αCD ionized systems heated up to 70°C surprisingly disclose a correlation peak at q $\approx$ 0.36 and 0.44 nm^{-1}, with equivalent inter-particle distance of 18 and 14 nm. These findings indicate a phase transition from multilayered to unilamellar aggregates. Temperature-triggered phase transitions from microtubes to disks or vesicles are also described for SDS@2βCD [64], dodecane@2βCD [109], nonionic phytosterol ethoxylates and perfluoroether-carboxylic acid complexes with αCD.[138, 139].

Temperature also highlights the responsiveness of the αCD lattice in ionized mixtures of both surfactants. It was revealed to provide the opposite charge density effect in the CD packing. The heat in the CD-CD and CD-water interactions causes the single peak in high-q to unfold into two at the same positions found in the nonionic systems, as observed in the insets of Fig. 4.11(b). The effect of the extra number of ethylene oxide units of the $C_{12}E_{10}CH_2COOH$ is also marked in the high-q region of its α-cyclodextrin complex. The lattice phase transition of this nonionic system is similar to the transition verified in the ionized ones (Fig. 4.11. II (a)), while such behaviour is not observed for $C_{12}E_5CH_2COOH$.

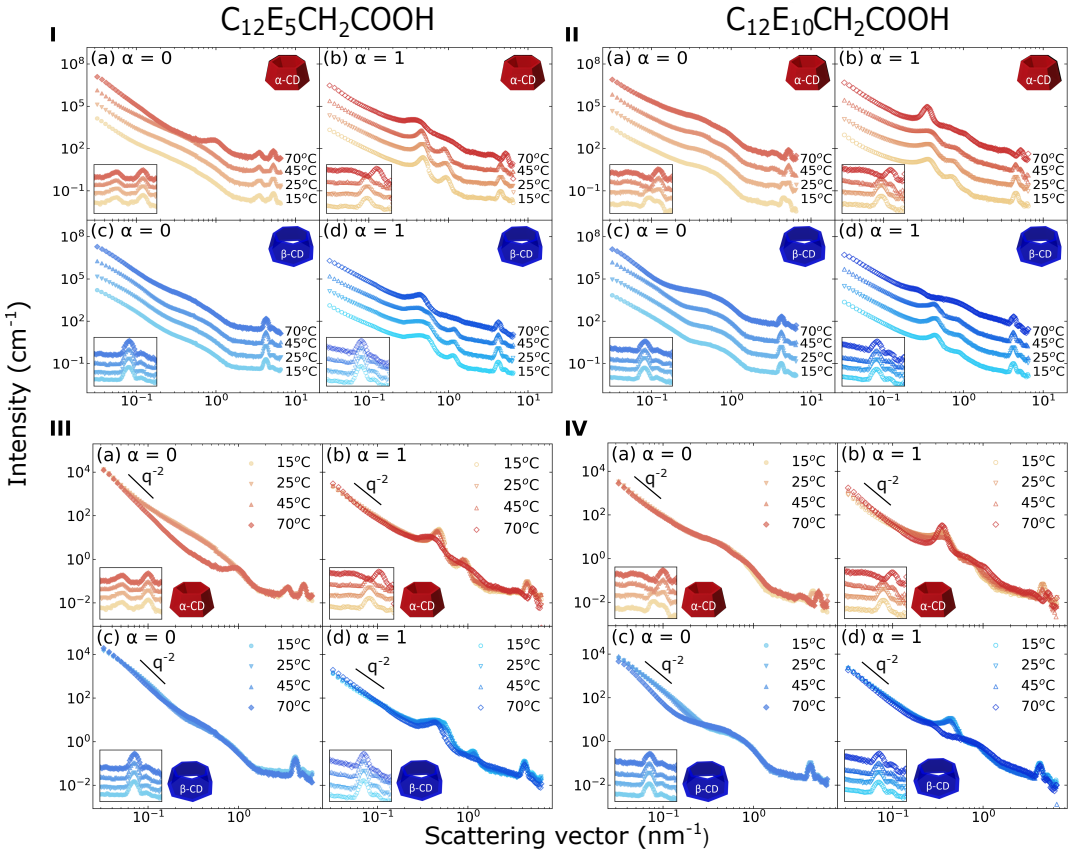

FIGURE 4.11: SANS intensity as a function of scattering vector (q) covering 0.03 - 6.5 nm^{-1}. The measurements of (I) $C_{12}E_5CH_2COOH$ systems and (II) $C_{12}E_{10}CH_2COOH$ systems at $\alpha = 0$ and $\alpha = 1$ with αCD (a and b) and βCD (c and d) were performed at 15, 25, 45 and 70 °C, at ratio CD/Surfactant = 2, (Surfactant = 5%wt). Curves are scaled by successive factors of 10 to improve readability. Non-scaled SANS curves are depicted in III and IV. The insets represent an enlargement of the high q region. *Reproduced from Ref. [120] with permission of the Royal Society of Chemistry.*

Differential scanning calorimetry allowed us to extend the characterization of the structural reorganization observed by small-angle neutron scattering. The thermograms of the systems are depicted in Fig. 4.12 and the enthalpy changes (ΔH) with the temperature of the transitions are shown in Fig. 4.13.

The increase of ΔH with the degree of ionization is the general trend observed in the complex system. These findings corroborate the increased crystallinity found in the aggregates of alkyl ethoxy carboxylates and cyclodextrins complexes. Enthalpy changes vary from almost undetectable values to an average of 40 J K^{-1} g^{-1} surfactant. The endothermic peak of nonionic $C_{12}E_{10}CH_2COOH$-αCD is an exception and indicates the presence of ordered aggregates.

The analysis of calorimetric experiments and the results obtained from SANS allowed us to correlate the energetic events detected in DSC with the structural rearrangements occurring in the microstructure, *i.e.*, 10-20 nm scale. The structural

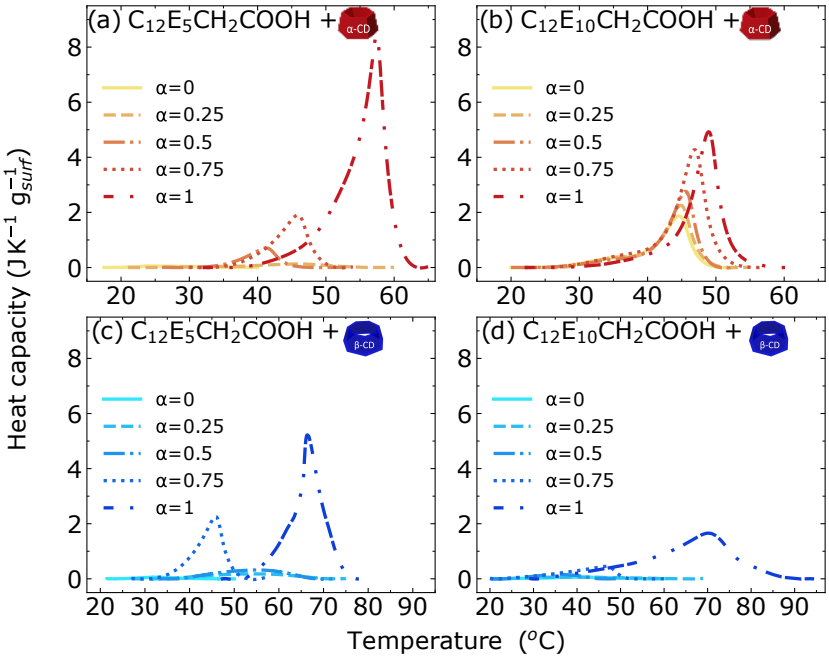

FIGURE 4.12: Thermograms of systems with a CD/Surfactant = 2, ΔH (J $K^{-1}g^{-1}$) corresponding to the inclusion complexes supramolecular aggregates containing 5%wt surfactant with αCD: (a) $C_{12}E_5CH_2COOH$, (b) $C_{12}E_{10}CH_2COOH$ and βCD (c) $C_{12}E_5CH_2COOH$ and (d) $C_{12}E_{10}CH_2COOH$ (Exo ↓). *Adapted from Ref.[120] with permission of the Royal Society of Chemistry.*

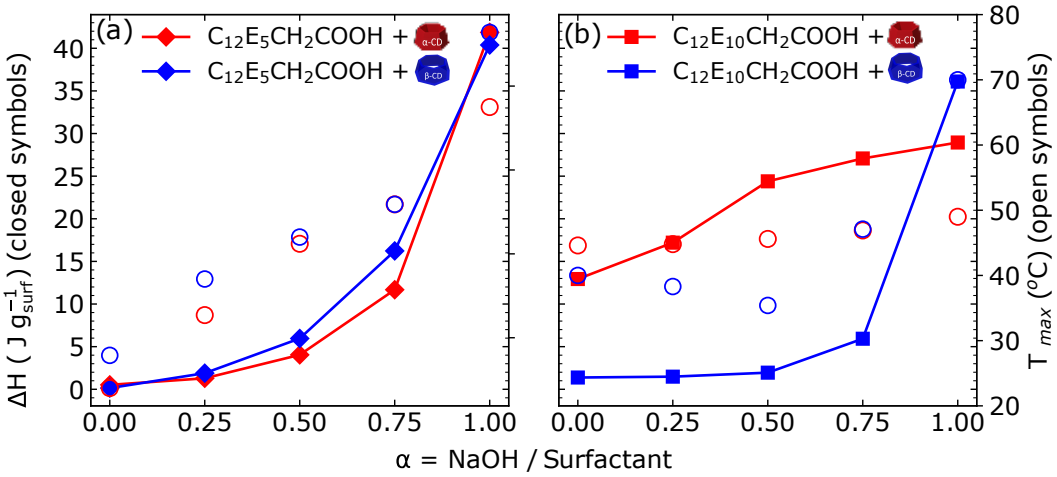

FIGURE 4.13: The enthalpic changes ΔH (J g^{-1}_{surf}) as a function of the surfactant's degree of ionization for (a) $C_{12}E_5CH_2COOH$ (♦) and (b) $C_{12}E_{10}CH_2COOH$ (■) systems and the temperature of the melting peak (◯) corresponding to the assembled systems containing 5%wt surfactant with αCD (red) and βCD (blue). *Adapted from Ref. [120] with permission of the Royal Society of Chemistry.*

TABLE 4.2: Spacing distances of the inclusion complexes supramolecular assemblies obtained by SANS measurements performed at different temperatures (nm).

Systems \ Temperature		15 °C	25 °C	45 °C	70 °C
$C_{12}E_5CH_2COOH$-αCD	$\alpha = 0$	-	-	-	6.5
	$\alpha = 1$	13.0	13.2	13.7	17.1
$C_{12}E_5CH_2COOH$-βCD	$\alpha = 0$	-	-	-	-
	$\alpha = 1$	17.3	17.3	17.3	17.8
$C_{12}E_{10}CH_2COOH$-αCD	$\alpha = 0$	-	-	-	-
	$\alpha = 1$	17.3	17.3	17.5	17.8
$C_{12}E_{10}CH_2COOH$-βCD	$\alpha = 0$	-	-	-	-
	$\alpha = 1$	14.3	14.3	14.3	24.2

Adapted from Ref. [120] with permission of the Royal Society of Chemistry.

stability of $C_{12}E_5CH_2COOH$-αCD increases with the increase of the surfactant's charge density, and so is the melting temperature of the structures, whereas ≈ 40 to 50°C is found for $C_{12}E_{10}CH_2COOH$ with the same cyclodextrin. The fact that the same peak onset, apart from the fully ionized system peak slightly shifted towards greater temperatures, demonstrates that the energy of the crystal is not being modified but evidences the increase in the amount of melting structure. The effect of the surfactant's molecular architecture reinforces the importance of the charge location in the crystallization process and the choice of the guest in the inclusion complexation process.

The investigation of systems containing a mixture of cyclodextrins is not the focus of conventional research on host-guest complexes and not as common as the guest mixtures. The mixing approach can be extremely relevant in the selective complexation of molecules relying on their binding affinity and/or size compatibility or in the enhancement of properties, such as increasing the solubility of guests and complexes. Thermodynamically, there are clear differences due to the different binding affinities, depending on the architectural features of the guest, but the packing parameters of complexes assemblies of the same host with different guests are not drastically affected to prevent the formation of the structures [136, 137, 140].

One of the few studies suggesting and assessing the effect of the macrocycles' mixtures reports the synergy of β-cyclodextrin and γ-cyclodextrin mixture in solubilizing dexamethasone [141]. The solubility properties were pointed to be additive in some cases, but the synergistic effect is assumed in other cases. γCD mixture with its hydroxypropyl derivative also exhibited the tendency with dexamethasone and hydrocortisone [142]. Depending on the concentration, ordered assemblies arise

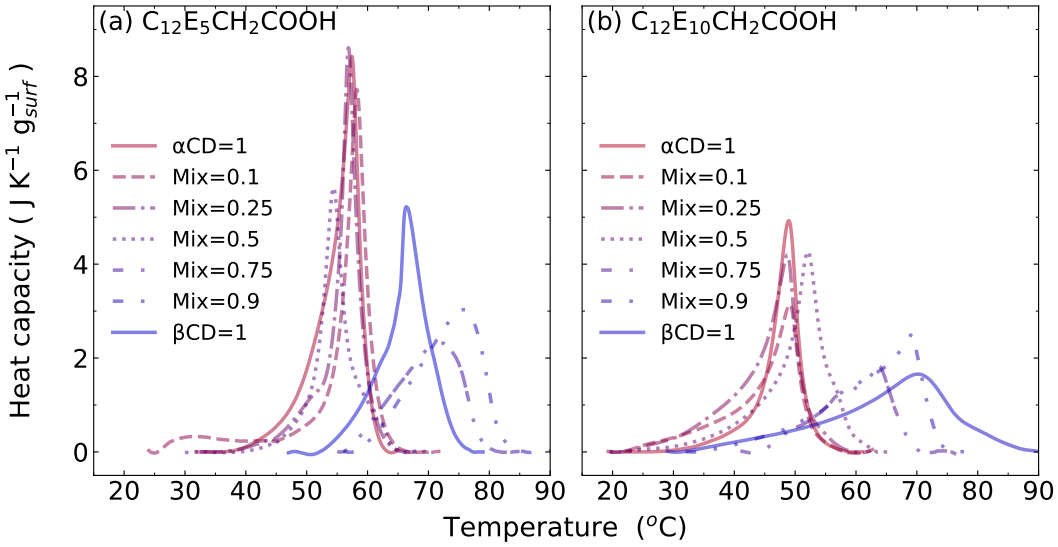

FIGURE 4.14: Thermograms of systems with a CD/Surfactant = 2, ΔH (J $K^{-1}g^{-1}_{surf}$) corresponding to the inclusion complexes supramolecular aggregates containing 5%wt surfactant with mixtures of αCD and βCD: (a) $C_{12}E_5CH_2COOH$ and (b) $C_{12}E_{10}CH_2COOH$. Mixtures are reported as a βCD:αCD molar ratio to equivalent total moles of CD for a Y = 2. (Exo ↓). *Unpublished data.*

from the systems.

Another different application of the CDs mixtures is the synthesis of novel cyclodextrin copolymers. The synthesis of αCD and βCD, βCD and γCD and αCD, βCD and γCD with a poly-carboxylic acid cross-linker copolymers, as well as their derivatives, are claimed in a patent [143]. In addition to the pharmaceutical application related to the previous example for the mixtures, applications in separative chemistry, biology, diagnostics, food and cosmetics can be mentioned.

As the precipitation of the aggregates is observed in those systems at a certain concentration, the main question in the CD/surfactant systems regards the disturbance of the lattice arrangement by the assembly of complexes with different cyclodextrins. In order to investigate the effect of mixed αCD and βCD inclusion complexes with alkyl ethoxy carboxylates, DSC measurements were performed. The analysis was focused on the ionized systems (α = 1) due to their higher ordering structural tendency. The thermograms are depicted in Figure 4.14 and the parameters in Figure 4.15.

For both $C_{12}E_5CH_2COOH$ and $C_{12}E_{10}CH_2COOH$, the presence of the peaks indicates the ordered nature of the supramolecular aggregates in the mixed cyclodextrin systems. The general tendency is the predominance of the cyclodextrin arrangement in greater quantity and is evidenced by the shift of the melting temperatures accordingly. Such changes are observed when equimolar quantities of the two cyclodextrins are mixed (Mix=0.5).

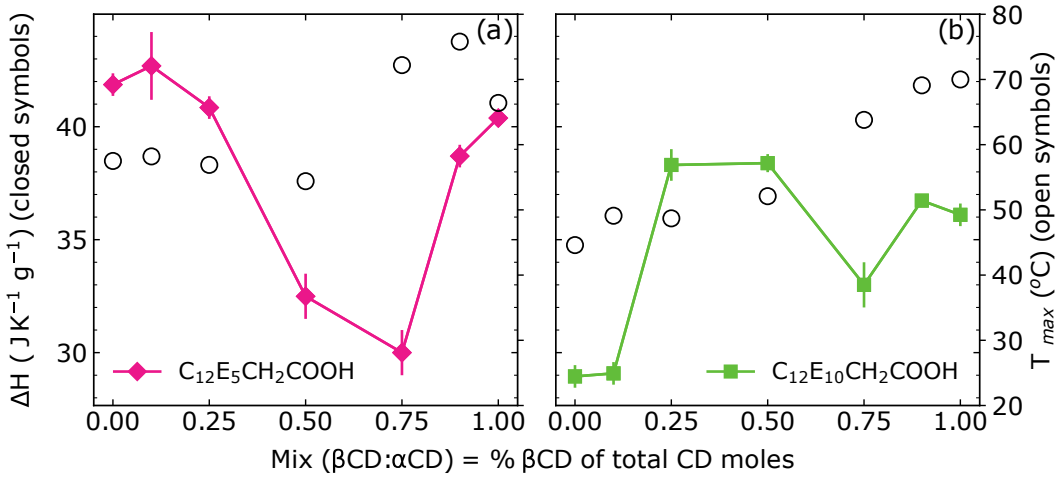

FIGURE 4.15: Enthalpy ΔH (J K^{-1}g$^{-1}_{surf}$ and temperature transitions extracted from thermograms of the $C_{12}E_5CH_2COOH$ and $C_{12}E_{10}CH_2COOH$ with α-cyclodextrin and β-cyclodextrin and their mixtures. *Unpublished data.*

The melting temperatures slightly varying in the 54-60°C range verified for the αCD transitions and the small ΔH variation upon increasing the βCD content demonstrate that α-cyclodextrin structures are still stable and present a small disruption resulting from the presence of the host with a larger cavity. In the predominance of βCD, however, the melting peaks at the same temperature as their correspondent degree of ionization (Fig. 4.12), mainly $C_{12}E_5CH_2COOH$ systems are found.

The enthalpy changes (ΔH) also present a general trend of a small decrease as the content of the other macrocycle increase. The presence of a single peak and the slight variation of the melting enthalpy of mixed systems compared to their pure systems points out the adaptability of the structures to accommodate the complexes with a different host.

Chapter 5

Polyelectrolyte-surfactant-cyclodextrin complexes

"Complexity is the prodigy of the world. Simplicity is the sensation of the universe. Behind complexity, there is always simplicity to be revealed. Inside simplicity, there is always complexity to be discovered."

Gang Yu

Polyelectrolyte-alkyl ethoxy carboxylates complexes are well-described systems in the literature. Between many factors influencing their interactions, the electrostatic interactions and the cooperative interactions of the surfactant alkyl chains direct the assembly can be cited. The pH responsiveness provided by the carboxylic group is able to provide charge density control and, consequently, allows tuning the electrostatic interaction. Further assembly's control is the modulation of the tails by the inclusion complexation properties displayed by this class of surfactants, which were extensively discussed in the previous chapters. Moreover, the polymer addition to the host-guest systems also presents the possibility of controlling their assembly.

Hence, this chapter presents a double possibility of assembly process control involving the short and long-range control of interactions.

5.1 Surfactant-polyelectrolyte interactions

Surfactants, in aggregates or in their monomeric form, can strongly associate with oppositely charged polyions in aqueous media. Their assembly and phase behaviour have been actively investigated over the years [144–146]. As in the inclusion complexes, the diversity of surfactants and polyelectrolytes provides an infinite number

of combinations of polyelectrolyte-surfactant systems. The responsiveness to different stimuli expands the possible fields of application of each class of molecules alone and of their complexes. They can be found in soft materials, particles or surface layers structures in food, cosmetics, drug delivery and home and care products.

The mixed solutions of nonionic surfactant and polymers or the mixture of co-solutes of the same charge usually do not result in complexes formation, but it may lead to a segregative phase separate due to the lack of attractive surfactant-polymer interaction in some cases [146]. The main driving force directing the oppositely surfactant and polyelectrolyte interaction is the attractive-repulsion balance of forces in the assemblies and a consequent entropic gain associated with the release of counterions and water molecules rearrangement [145–147]. The strong attractive behaviour, in this case, is demonstrated by the associative phase separation tendency in many of these complex systems at the equimolar mixing ratio. The complexes' solubility is increased with the increase of charge of the total system, either in surfactant or polyelectrolyte excess. This fact is shown in the phase diagram of the concentration as a function of the mixing ratios of polyelectrolyte and surfactant (Z), represented in Fig. 5.1. At $Z < 1$, in excess of surfactant, the polyelectrolyte is stabilized by the micellar structures and a single phase is observed. At $Z > 1$, a polyelectrolyte-rich phase is obtained, and depending on the concentration, monomers or micelles decorate the polymer structure [148]. The phase separation can be interesting for some specific applications, such as layer deposition or the formation of polymer gels, for example. In many other cases, it is frequently undesirable in formulations as it may cause modifications in the sensorial properties and results in the incertitude of the phases' composition [146].

In all cases, the assembly is strongly dependent on the variation of the surfactant molecular architecture and polyelectrolyte features, such as molecular weight, charge density distribution, functional groups, solvent, pH, the polymer-surfactants ratio, and also the surfactant's hydrophobic/hydrophilic balance. These parameters can be used to modulate their assembly. It is worth recalling the importance of the counter ion since the thermodynamics of complex formation also relies on their entropic contribution [149, 150].

A variety of structures can be found in polyelectrolyte-surfactant systems. Their rich behaviour depends largely on their molecular parameters. As for the surfactants assemblies, the surfactant's packing parameter also directs the type of aggregate preferentially formed. The formation of complexes containing densely packed micelles has often been observed in a core-shell shape, in a cylindrical matrix embedded with micelles, structured in a pearl-necklace of core-shell ellipsoids and the

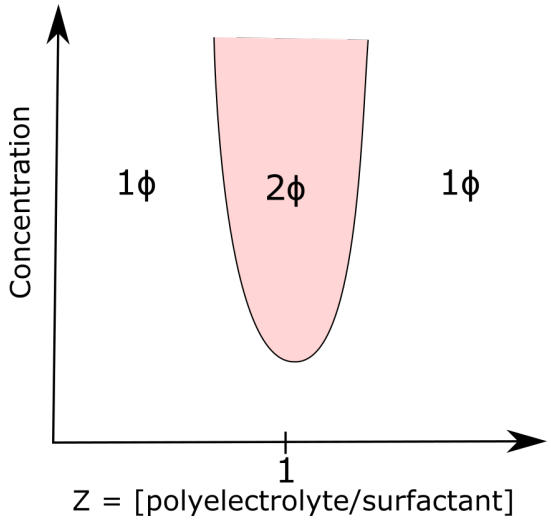

FIGURE 5.1: Schematic phase diagram of oppositely charged polyelectrolyte-surfactant systems as a function of concentration and the mixture ratio.

hexagonal packing of micelles [151]. Multilayered vesicles and gels have been reported to polyelectrolytes-surfactant systems in surfactant concentrations lower than the *cmc*. They have attracted attention due to the encapsulation properties suitable to applications in drug delivery, water purification and cosmetic technologies [152].

Adding another molecule to the system results in different directive interactions that can modify the properties of the system. The addition of a long-chain alcohol or a nonionic surfactant is able to affect the assembly process and the complexes' properties. The systematic addition of the nonionic species, in particular olygo(ethylene oxide) surfactants, generally enhances the solubility of the aggregates as a result of the changes in the micellar charge density. A minimum charge density is necessary for the strong polyelectrolyte interaction to take place and to form insoluble precipitates [151, 153]. Exceptions have been observed in cases where the cosurfactant mixing would induce the formation of immiscible aggregates (in the case of cononsurfactancy) but establishing phase diagrams is useful to identify the regions of such extended phases [150, 154]. The cononsurfactancy case can be exemplified by the addition of sodium dodecyl sulfate and poly(diallyldimethylammonium chloride) complexes at surfactant concentration below the surfactant's *cmc* and in polyelectrolyte excess using dodecyl maltoside [155] and by the addition of nonaoxyethylene oleylether to the nonaoxyethylene oleylether carboxylic acid-chitosan complex system. In the latter, the mixing ratio between nonionic and ionic surfactants and pH were able to modulate the interactions leading to the obtention of elongated micellar, core-shell and long rods structures were found [156].

Among countless combinations, the polyanion and cationic surfactants represent the majority of the systems investigated. Polyacrylates [157], polymethacrylate [158]

and polystyrene sulfonate [159] or their copolymers [160] are common anionic polyelectrolytes in such systems, usually in combination with alkyl ammonium surfactants. However, mixtures of polycations and anionic surfactants present an attractive possibility considering the toxicity of cationic surfactants, which characteristic may restrict the application of polyelectrolyte-surfactant systems in certain fields [161].

The rising interest in biocompatible, nontoxic and sustainable compounds drives attention to the class of polysaccharides, which consists of biopolymers or their chemically modified derivatives. Naturally occurring ionic polysaccharides are mostly negatively charged, and a scarce variety of cationic biopolymers is available. In turn, great sources of their precursors are available. Cellulose and chitin are the most abundant natural polymer on earth, and by simple chemical reactions, cationic derivatives of cellulose and chitosan - a cationic derivative of chitin - can be obtained.

Here, the distinct biocompatibility, biodegradability, abundance, easy obtention through renewable sources, and the anti-bacterial features of chitosan, described in the next section, motivate its investigation as well as the investigation of its complexes.

5.2 Chitosan

Chitosan is the random copolymer of glucosamine and N-acetylglucosamine linked by β-(1-4)-glycosidic bonds obtained from the deacetylation of chitin. Chitin is the main component of the exoskeleton of crustaceans, such as crabs, shrimps, and lobsters, which are copious waste products generated by the food and beverage industries [162, 163]. After cellulose, chitin is the second most abundant polymer on Earth. Their renewable potential, abundance and the need for substitution of petroleum-based polymers make chitin, its derivatives and other natural polymers very attractive from an economical and sustainable perspective.

The process of chitin deacetylation starts with the treatment of the exoskeleton shells with hydrochloric acid to remove proteins and minerals. The resulting chitin is then treated with an alkaline solution to cleave the acetyl groups to obtain amino groups. The N-acetyl-glucosamine units in the molecule determine the degree of acetylation, and the deacetylated units configure the charge density along the polymer backbone. The degree of deacetylation can vary depending on the process conditions but typically ranges from 70% to 95%, and the molecular weight varies between 100 and 1000 kDa [151]. The resulting chitosan can then be purified, dried, and ground into a fine powder for use in various applications.

Chitosan and chitin structures are shown in Fig. 5.2. Differently from chitin, chitosan is soluble in acidic solutions below pH 6, as a result of the protonation of

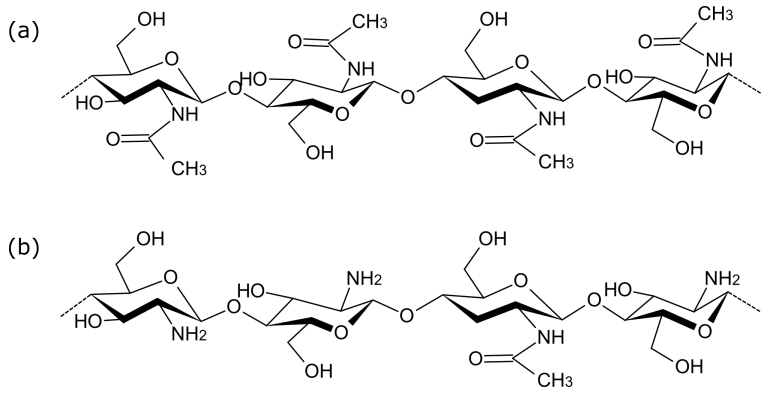

FIGURE 5.2: Chitin (a) and chitosan (b) chemical structures.

the amine groups in the glucosamine units, and below $\approx$ 3 %wt. The degree of deacetylation and molecular weight extensively affect the physicochemical properties of chitosan, such as solubility and viscosity. In terms of molecular architecture, the persistence length varying from approximately $\sim$ 5 to 30 nm and the $\sim$ 0.5 nm distance between charges highlights the relative rigidity configured by the polysaccharide backbone [164, 165]. The combination of these unique features in addition to its positive charge, high biodegradability and biocompatibility, availability and antibacterial properties widen their applicability in materials sciences. Another aspect that broadens the interest in the biopolymer is the possibility of modification offered by the hydroxyl, amino and acetyl groups in its structures [166].

Chitosan is widely applied from pharmaceutics to food industrial fields. The hair and skin's successful interactions with chitosan resulted in an increasing number of cosmetic and pharmaceutical formulations containing the biopolymer [167]. In the medical field, its use as cells stimulating materials in plants and, especially, in animals has been proven to be efficient in covering wounds and assisting in the healing process [168–171]. Drug delivery and controlled drug-release chitosan-based structures with other polysaccharides, lipids and nanoparticles have broaden the survey of pharmaceutical applications [172, 173]. The removal of metal ions and dyes from wastewater and the use of chitosan as bioflocculators are a relevant application of the polymer, presenting a sustainable alternative to the conventional methods currently applied [174–176]. In food technology, the film-forming properties of chitosan have been explored in packaging development, as an emulsifier in the stabilization of oil-in-water systems or as a carrier in the encapsulation of functional food products [177, 178].

The numerous advantages of chitosan and its possible combination with many other systems demonstrate the great potential of this biopolymer in the face of the global and necessary search for biocompatible and sustainable materials.

5.3 Chitosan - alkyl ether carboxylic acids complexes

Chitosan-surfactant complexes have received attention in the last years, particularly in the pharmaceutical, medical, food and detergent industries, as previously mentioned. The synergistic complex cooperatively formed between the electrostatic interactions of the positively charged amino groups of the biopolymer and the anionic surfactants allows many structural possibilities tuned by the pH, temperature and concentration, as well as by the other molecular architectural aspect mentioned for the polyelectrolytes-surfactant complexes in general.

Chitosan complexes with strong anionic surfactants are often employed, but they present a tendency for phase separation. This characteristic can be very valuable for a few applications. A good example in which is desired is the case of the microencapsulation properties of chitosan-sodium dodecyl sulfate complexes are extensively described in the literature in wide ranges of concentrations and mixing ratios [179–182].

Given the electrostatic nature of the interaction, the use of pH-dependent surfactants provides a promising approach to modulate the complexation. The stable aggregates of fatty acids have been commonly used in these systems owing to their biocompatibility. However, the limited solubility of these compounds restricts their use. At low pH, for example, the chitosan is soluble and the fatty acids, in their neutral molecular form, are mostly insoluble. At high pH, the opposite is found with the chitosan in its neutral form, uncharged, and the fatty acids mostly ionized. In the investigation of emulsions of different chain lengths, such pH behaviour also had proven to change the interaction's nature of the binding.

To address this issue, several ethylene oxide units can be intercalated between the aliphatic chain and the carboxylic terminal unit, producing alkyl ether carboxylates that exhibit increased solubility while maintaining the pH-responsive behaviour. Notably, the properties of these surfactants can be manipulated not only by pH but also by varying the alkyl chain length and the number of ethylene oxide units [5, 51]. The hydrophilic-hydrophobic balance in the surfactant molecule plays an essential role in determining the curvature, solubilization, and morphology of the surfactant aggregates and their complexes, making them useful for a range of applications [48].

Chitosan-alkyl ether carboxylic acids are well-described in the literature [5, 51]. The pH-dependent behaviour of these systems is similar to the alkyl carboxylates but with increased solubility. These complexes exhibit strongly responsive structures with less precipitation tendency. In addition to the pH and temperature responsiveness, the chemical architecture of the surfactant, specifically the alkyl chain and hydrophilic headgroup, the complexes can be tuned by the surfactant-to-deacetylated

glucosamine ratio. Chitosan of 100 kDa molecular weight and a degree of acetylation of 0.15 was used in the investigations conducted at pH 4.

The chitosan-alkyl oligoethylene oxide carboxylic acids complexes present a rich structural behaviour. In excess of polyelectrolyte and low pH, the chitosan network is decorated by the micelles. At intermediate ratios, two to five micelles can be found linearly ordered in a polymer cylindrical shell and, at high pH (pH $\approx$ 5) and surfactant excess, a core-corona superstructure with a packed micellar structured core stabilized by the chitosan stiff corona could be found together with multilayered vesicles [5].

The structures found in those systems have many directing forces. The overall structure relies on the compatibility between the chitosan conformation and the natural self-assembly behaviour of the surfactants. It is noteworthy that the type of aggregate formed in the pure surfactant solution is retained in the complex structure. In summary, many parameters in the complexes are found in a balance of the reduced conformation of the biopolymer, the release of counterions and the interaction of polysaccharide with the surfactant aggregates leading to an entropically favoured mechanism of complexation.

5.4 Chitosan - alkyl ether carboxylic acids - cyclodextrin complexes

Since the self-assembly behaviour of the surfactants has such an important role in the complexation, other strategies can also be used to modulate it. The alternative of adding a third component to the system is attractive and may drive the researcher to unexpected conclusions, as, for example, the mentioned induced phase separation by the addition of $C_{18:1}E_9$ to $C_{18:1}E_9CH_2COOH$-chitosan mixtures, while minor thermodynamic and structural effects are observed in their pure micellar mixtures [156]. However, it has been demonstrated in Chapters 3 and 4 that the addition of cyclodextrins is able to control the surfactants' assembly. The addition of the cyclic polysaccharide to the surfactant solution at the appropriate concentration and cyclodextrin-to-surfactant ratio leads to the formation of hierarchical aggregates. These aggregates present different forms according to the number of ethylene oxide units of the surfactant, cyclodextrin cavity size, pH and temperature. The challenge of this work was to incorporate cyclodextrin into the known polyelectrolyte-surfactant complex systems to pursue the control of the alkyl ethoxy carboxylic acids' assembly within the chitosan.

The investigations of the ternary systems were conducted with $C_{12}E_5CH_2COOH$ and $C_{12}E_5CH_2COOH$, α-cyclodextrin (αCD), β-cyclodextrin (βCD), and chitosan

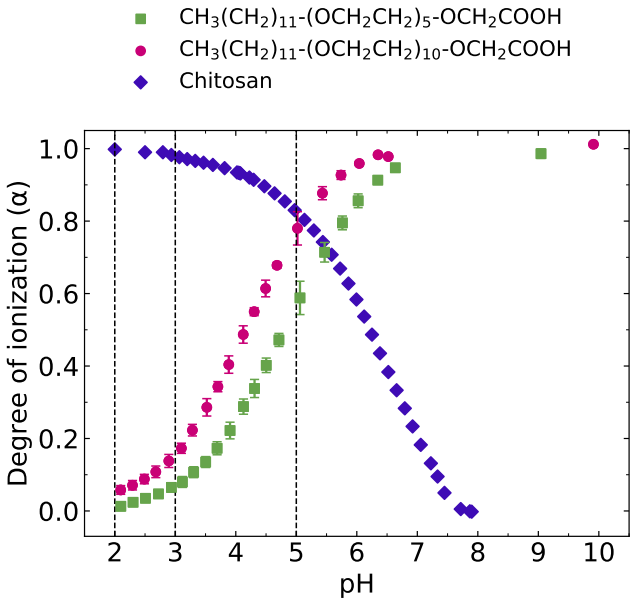

FIGURE 5.3: Titration curves of the surfactants and chitosan reported as the degree of ionization as a function of pH. The dotted lines indicate the pH evaluated.

(100 kDa, degree of acetylation: 0.15) at pH 2, 3 and 5. Hereby, it was possible to evaluate the following effects in the ternary complexes:

i) *Cyclodextrin cavity size*: It provided an insight into the influence of the inclusion complexation structural aspects and the packing parameter in the chitosan-surfactant complexes;

ii) *Ethylene oxide units*: The evaluation of the two surfactants allowed assessing the impact of the surfactant's headgroup hydrophilicity and the consequent distinct curvatures observed in their aggregates;

iii) *Charge density*: The pH adjustment allows exploring the surfactant's pH-responsiveness to control the multilevel assembly with cyclodextrin and with chitosan. As depicted in figure 5.3, the pH drives the predominance of the non-ionic or ionic molecules of the surfactants whereas the majority of glucosamine groups are protonated up to the maximum pH evaluated.

The structural characterization of the aggregates was carried out by small-angle neutron scattering and differential scanning calorimetry. The SANS measurements were conducted with D11 and D22 instruments at ILL (Grenoble, France) and the DSC with the support of the Partnership for Soft Condensed Matter (PSCM) at ILL.

The analysis is reported as a function of the molar mixing ratio of surfactant and cyclodextrin (Y=[CD]/[Surf]) and as a function of the chitosan and surfactant ratio (Z=[Chit]/[Surf]). Through an examination of the electrostatic interactions between

the polymer and the carboxylic group present in the surfactant's headgroup, the incorporation of the biopolymer chitosan into the CD/surfactant inclusion complex system presents a novel opportunity to combine the attributes of both complex systems.

The phase diagrams of the ternary systems were investigated. They are presented in Figure 5.4, the molecular weight M_w (g mol^{-1}) as a function of the chitosan and cyclodextrin to surfactant ratios are depicted.

The phase boundaries shift indicates the presence of stable aggregates and also highlights the effect of chitosan and the influence of the surfactant's headgroup. The extra EO in $C_{12}E_{10}CH_2COOH$ provides increased solubility of the complexes and aggregates with lower average molecular weight although the cyclodextrin type is observed. Aggregates of larger M_w are formed in $C_{12}E_5CH_2COOH$, and the CD type effect is marked by the assembly into larger structures in the systems containing βCD in lower Y ratios. Heating followed by slow cooling of the samples also shifts the phase boundary towards lower Y ratios in surfactant excess in αCD complexes while more soluble aggregates are observed for βCD for $C_{12}E_5CH_2COOH$. However, no clear changes were verified for $C_{12}E_{10}CH_2COOH$ samples containing the same CD.

Temperature also triggered the phase separation and obtention of a clear transparent solution and a white film deposited on the glass vial surface at high Y, mainly in αCD systems. The films were not disrupted by manual agitation of the systems.

SANS curves of the CD-to-surfactant ratio Y = 1 and CD-to-surfactant ratio Y = 2 with the intensity as a function of the scattering vector are presented in Figure 5.5.(I) and 5.5.(II), respectively. Systems presenting phase separation were not measured. The structures of the systems could not be fully resolved due to the preclusion of the Guinier region. For this reason, a qualitative analysis was conducted to extract valuable information on the measured data and verify the systems' behaviour given the previously mentioned parameters.

An important factor strongly influencing the ternary complexes is the CD/surfactant ratio. As discussed in Chapter 4, the different morphologies of inclusion complexes aggregates of ratios Y = 1 and Y = 2 are indicated in the Z = 0 curves. Hence, the complexes' supramolecular structures of the ternary system tend to be different.

In general, rich structural behaviour is obtained in the presence of the macrocycle. The surfactants' degree of ionization/pH is particularly important in this case, as it plays a role in controlling the interaction with the polymer and directing the aggregates' morphology of inclusion complexes. As discussed in Chapter 4, concentrated systems of inclusion complexes (5%wt surfactant) exhibit an increasing structural ordering with the increase of the surfactant's charge density.

The addition of the polymer to the host-guest systems promotes the collapse and

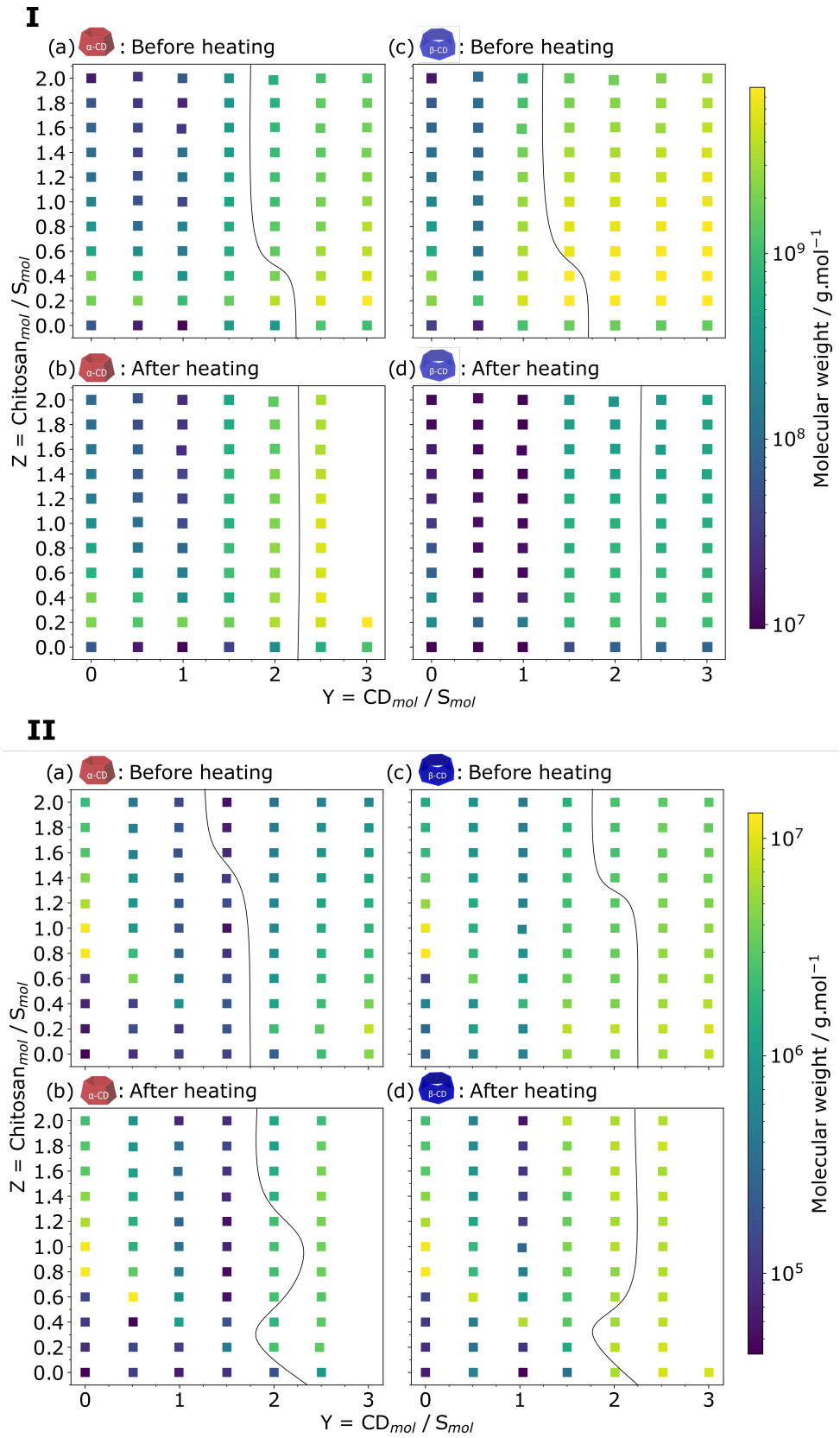

FIGURE 5.4: Phase behavior of (I) $C_{12}E_5CH_2COOH$ and (II) $C_{12}E_{10}CH_2COOH$ chitosan systems in the presence of αCD and βCD before heating (a and c) and after heating (b and d). Solid lines represent the phase boundaries in which precipitation was observed. Concentration of surfactant: 5 mM. All data were recorded at room temperature.

the reordering of the assemblies' structures remarkably verified by the disappearance of the second and third-order peaks in the $C_{12}E_{10}CH_2COOH$-αCD (Fig. 5.5.II.(b)) and the development of peaks in the curves of the systems containing chitosan. A correlation peak at ≈ 0.9 nm^{-1} is present in all pH evaluated of αCD, despite the different intensities and slight shift towards higher q, and only present in βCD systems at pH 5. It is worth recalling that such self-organization and ordering behaviour at low pH ($\alpha = 0$) was also only verified for the α-cyclodextrin/surfactant assemblies (Fig. 4.13).

The similar behaviour of the systems at pH 2 and 3 is evidenced by the rough superposition of the curves, given the small changes in the degree of ionization of the surfactant and the predominance of the nonionic surfactant molecules (Fig. 5.5). At pH 5, structural changes are observed as a function of the different structural behaviour displayed by αCD and βCD systems.

The inclusion complexes packing parameter, evidenced in the high-q region, exhibit the same pH responsiveness found in the inclusion complexes. In both CD-to-surfactant ratios evaluated, βCD complexes packing rearrangement was not triggered by pH alterations. The responsiveness of αCD systems is evidenced by the peaks at 3.45 and 5.25 nm^{-1} at low pH, progressively unfolding in one peak 4.3 nm^{-1} with higher intensity and a peak with lower intensity at 3.45 nm^{-1} at high pH. This effect is remarked in the packing of $C_{12}E_5CH_2COOH$ systems, pointing out a charge density effect, since 60% of surfactant molecules are ionized, making reasonable the consideration of a mixture of structures at pH 5. Such influence is not observed for $C_{12}E_{10}CH_2COOH$ systems where one peak is observed at 4.3 nm^{-1} at high pH.

The profiles at pH 5 are reported in Figure 5.6 as $I(q)q^2 vs.q$ representation, which helps to emphasise the characteristics of locally flat structures. This representation also emphasizes the CD/surfactant ratio effect previously mentioned. In the $C_{12}E_5CH_2COOH$ systems with Y = 1, the change in the power law of αCD systems and the progressive development of another correlation peak at 0.04 nm^{-1} upon Z increase is verified for βCD. The latter suggests a $\approx$ 160 nm distance. Unfortunately, no more conclusions can be made with respect to this feature, and further investigations are needed.

The general behaviour at pH 5 of the systems upon a chitosan content increase is the broadening of the peaks, indicating a reduction in the number of the structures in the core or their softening, irrespective of CD-to-surfactant ratio and cyclodextrin type. The peaks are also slightly shifted towards high-q, pointing to more compact microstructures. The exception is the increase in order in $C_{12}E_{10}CH_2COOH$-αCD systems. The q^{-2} power law clearly visible in the $I(q)q^2 vs.q$ representation (Fig. 5.6)

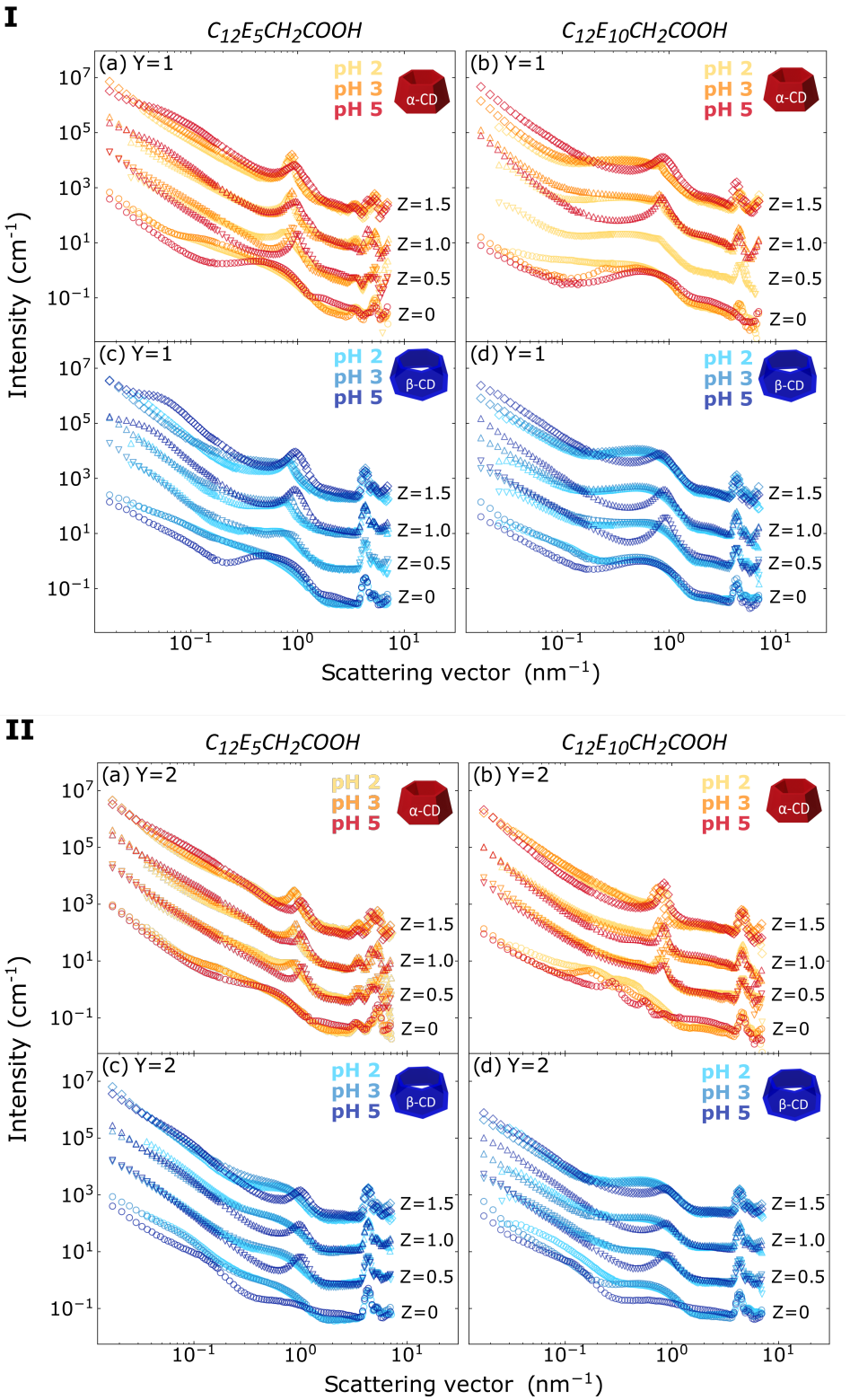

FIGURE 5.5: SANS patterns from chitosan-AEC-cyclodextrin complexes, recorded at pH 2, 3 and 5. At 2 %wt surfactant concentration, Z = 0, 0.5, 1.0 and 1.5 at (I) CD/surfactant ratio = 1 and (II) CD/surfactant ratio = 2. Chitosan systems with $C_{12}E_5CH_2COOH$ with (a) αCD and (c) βCD and $C_{12}E_{10}CH_2COOH$ with (b)αCD and (d) βCD. Successive curves are scaled by a factor of 15 for improved readability. Curves at pH 2 were recorded at D22 [119], and pH 3 and 5 were recorded at D11 (ILL, Grenoble). Curves which are not displayed were not measured due to precipitation.

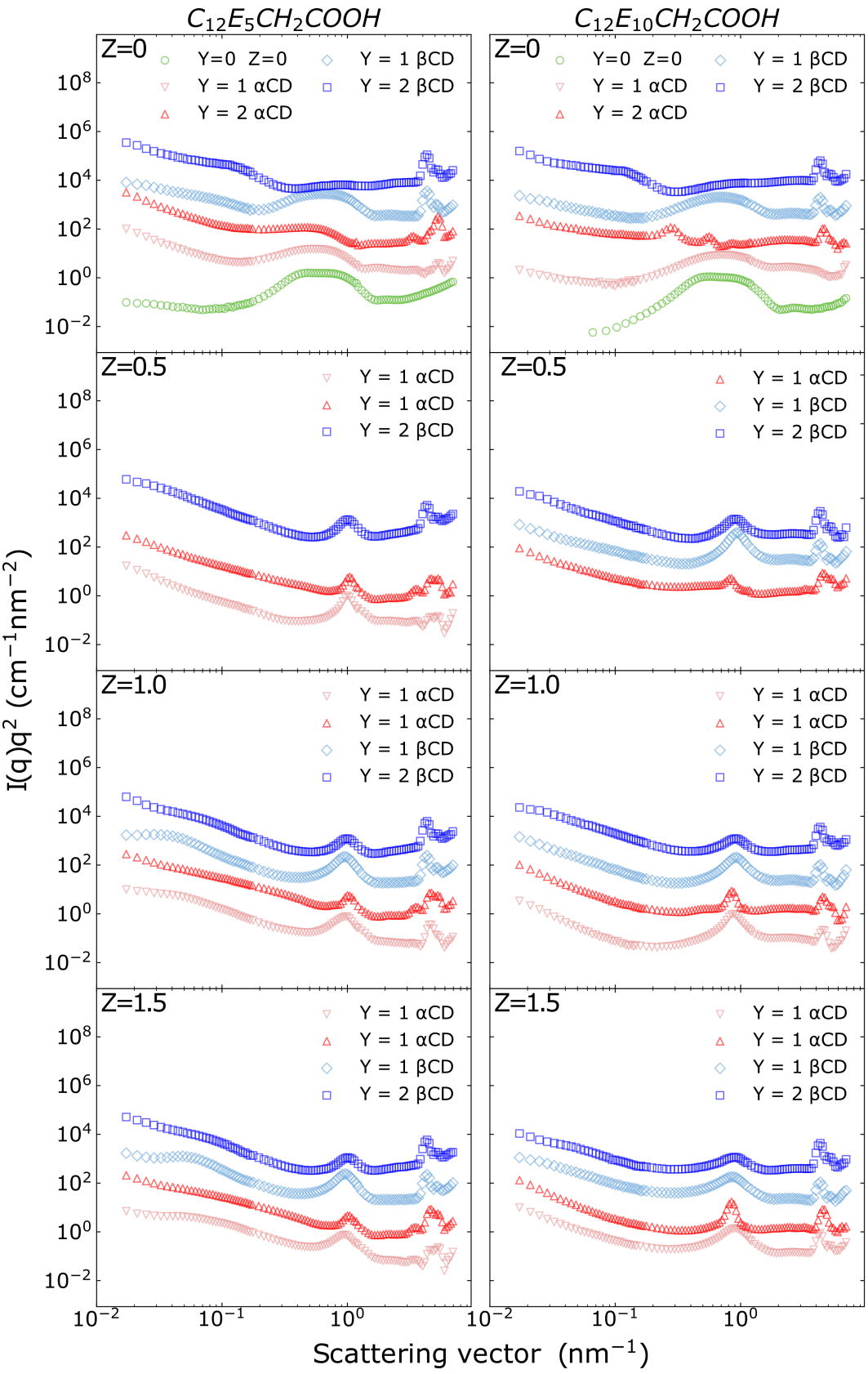

FIGURE 5.6: $I(q)q^2 vs. q$ representation of the SANS patterns from chitosan-cyclodextrin complexes with $C_{12}E_5CH_2COOH$ (left) and $C_{12}E_{10}CH_2COOH$ (right) with αCD and βCD recorded at pH 5. At 2 %wt surfactant concentration, ratios Y=1 and Y=2 and Z = 0, 0.5, 1.0 and 1.5. Successive curves are scaled by a factor of 15 for improved readability. Data recorded at D11 (ILL, Grenoble). Curves which are not displayed were not measured due to precipitation.

points to the formation of locally flat structures. It suggests that the polysaccharide-surfactant provides rigidity to the structures linking the layers of the structures which tend to compact upon increasing the chitosan content.

The peak position at q $\approx$ 1 nm^{-1} corresponds to the structures' core, and it is compatible with the surfactant double layer length in real space equal to 6.4 nm. The qualitative analysis and the complexity of the systems do not permit distinguishing the hypothesis of the purely micellar core, in which just the self-assembly of surfactant molecules is found, and the hypothesis of vesicles resulting from the inclusion complexes assembly integrates the core. Sodium dodecyl sulphate-β-cyclodextrin vesicles embedded in chitosan have been reported in the literature and support the formation of similar structures in the ionized alkyl ethoxy carboxylate systems [63].

The DSC data, however, confirmed the SANS data observations and provided insightful information on the structural stability of the aggregates containing chitosan. The thermograms obtained from the DSC experiments for the systems with CD-to-surfactant ratio Y = 2 are depicted in Fig. 5.7 and enthalpic changes in Table 5.1. As expected for these systems, systems at pH 5 presented higher stability than those at lower pH. In general, α-cyclodextrin systems exhibit stable structures upon the addition of chitosan, whereas the opposite effect is verified for β-cyclodextrin systems. At pH 3, $C_{12}E_5CH_2COOH$-βCD systems do not exhibit phase transitions (data not shown in Figure 5.7).

At pH 3, the incorporation of chitosan prevented the formation of ordered complexes evolving the inclusion complexes in the case of $C_{12}E_5CH_2COOH$-βCD systems and provided a structural collapse in $C_{12}E_{10}CH_2COOH$-βCD, indicated by the lack of transitions for Z = 0.5, 1.0 and 1.5 in the thermograms (Fig. 5.7 a and c). At pH 5, the destabilization of the structures induced by the polymer in βCD systems in spite of the surfactant headgroup is evidenced by the disappearance of inclusion complexes structures characterized by the peak melting at $\approx$ 70°C with the increase of chitosan concentration. Surprisingly, different structures with phase transition at $\approx$ 40°C arise in excess of polyelectrolyte and stable structures are obtained at Z = 1.5, mainly for $C_{12}E_{10}CH_2COOH$, as a result of the differences in the surfactants' ionization behaviour. It is noteworthy to recall that a greater surfactant's charge density effect is observed for βCD inclusion complexes and defined layers were only observed in the fully ionized systems (Fig. 4.12). For this reason, the further disassembly of host and guest and the micelle-polyelectrolyte interaction forming such structures might be the case.

The high structural stability of complexes with α-cyclodextrin despite the addition of chitosan was verified. The effect of the headgroup size is evidenced again at pH 3 and reflects the same structural behaviour of the pure inclusion complexes

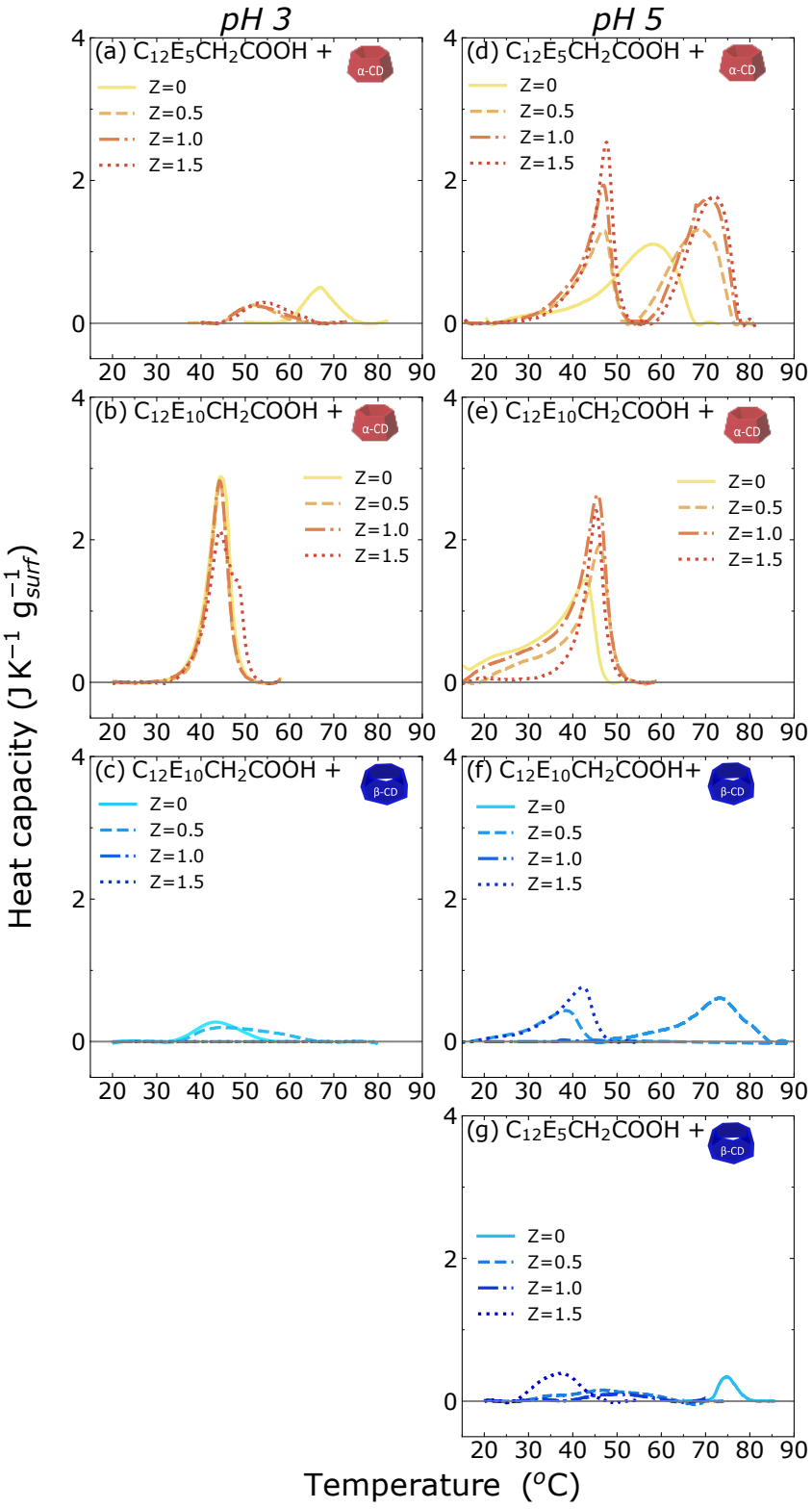

FIGURE 5.7: Thermograms of chitosan-cyclodextrin complexes with $C_{12}E_5CH_2COOH$ and $C_{12}E_{10}CH_2COOH$ at Y = 2.

TABLE 5.1: Enthalpic changes ΔH (J g^{-1}_{surf}) for the ternary systems with ratio Y = 2 at pH 3 and 5.

Systems		**ΔH (J g^{-1}_{surf})**	
		pH 3	***pH5***
$C_{12}E_5CH_2COOH$-αCD	*Z = 0*	4.13 ± 0.13	18.38 ± 0.31
	Z = 0.5	2.52 ± 0.30	1) 12.07 ± 0.15 2) 16.9 ± 0.41
	Z = 1.0	2.86 ± 0.22	1) 15.45 ± 0.16 2) 19.92 ± 0.2
	Z = 1.5	3 ± 0.08	1) 16.71 ± 0.21 2) 18.90 ± 0.9
$C_{12}E_5CH_2COOH$-βCD	*Z = 0*	-	1.7 ± 0.08
	Z = 0.5	-	2 ± 0.12
	Z = 1.0	-	1.48 ± 0.09
	Z = 1.5	-	2.1 ± 0.09
$C_{12}E_{10}CH_2COOH$-αCD	*Z = 0*	18.27 ± 0.12	18.35 ± 0.09
	Z = 0.5	15.15 ± 0.13	18.88 ± 0.16
	Z = 1.0	15.93 ± 0.1	22.30 ± 0.13
	Z = 1.5	16.90 ± 0.14	16.5 ± 0.15
$C_{12}E_{10}CH_2COOH$-βCD	*Z = 0*	3.30 ± 0.1	3.64 ± 0.11
	Z = 0.5	3.86 ± 0.4	1 ± 0.2
	Z = 1.0	-	1.1 ± 0.2
	Z = 1.5	-	4.26 ± 0.12

supramolecular aggregates. The surfactant's degree of ionization still directs the assembly, but ordered structures are evidenced by the transitions (represented in solid lines) at ≈ 65 and 45°C for systems with $C_{12}E_5CH_2COOH$ and $C_{12}E_{10}CH_2COOH$, respectively. Nonetheless, the $C_{12}E_5CH_2COOH$-αCD structures are more responsive to the chitosan addition, and the ordering is disrupted in all the Z ratios evaluated. In the case of $C_{12}E_{10}CH_2COOH$, phase transitions occurring at 45°C with similar enthalpy changes values for Z = 0, 0.5 and 1.0 and the slight changes observed at Z = 1.5 indicates that the inclusion complex structures are retained in the ternary assemblies.

The interaction of $C_{12}E_{10}CH_2COOH$-αCD and chitosan provide progressive stability with increasing chitosan concentration at pH 5. The peak definition and the slight shift of the melting towards higher temperature evidence this characteristic. The behaviour of $C_{12}E_5CH_2COOH$-αCD-chitosan systems was an unanticipated finding. The observation of a headgroup's influence in the assembly was expected to a small extent, as a shift in the phase transitions or slightly different enthalpy changes, for example, but the presence of two phase transitions was not foreseen. At Z = 0, a phase transition at ≈ 58°C characterizes the inclusion complexes aggregates. From Z=0.5 to 1.5, two peaks at 47 and 70°C with successive increasing enthalpy changes are verified.

It is possible to hypothesise that such behaviour is likely to occur in different scenarios. In the first one, with 60% of ionized molecules, it was reasonable to consider a mixture of structures arising from the non-ionized and ionized at first. However, the features in the data obtained at pH 3 dismissed the possibility. Secondly, the mixtures of aggregates could explain the presence of the peaks considering that multilayered vesicles and cylindric structures are obtained for these surfactant-chitosan binary systems [5]. The differences in the crystallization would result in the two peaks observed but would not provide a straightforward assignment of each peak to the respective structure. The third hypothesis is the occurrence of polymorphic transitions. More than one transition is likely to occur as a result of the multilevel nature of the assembly and the thermoresponsiveness reported for the inclusion complexes in **Paper III**. Further investigations need to be conducted for concise conclusions.

Chapter 6

Conclusions

"Somewhere, something incredible is waiting to be known."

Carl Sagan

This thesis presents a comprehensive characterization of the thermodynamics and structural properties of the alkyl ether carboxylic acids and cyclodextrins inclusion complexes and their ternary systems with the cationic polysaccharide chitosan. Although surfactant-cyclodextrin inclusion complexes and polyelectrolyte-surfactant complexes have been extensively studied, knowledge of some specific effects and the features arising from their combination in one singular system is still a shortfall in the literature.

The combination of isothermal titration calorimetry, differential scanning calorimetry, small-angle neutron scattering and microscopy provided a highly complementary approach to describe the thermodynamics and structural characterization of the supramolecular aggregates of the bare inclusion complexes systems and their ternary complexes with the biopolymer. The results reported in this thesis offer a comprehensive overview of the combination of long-range electrostatic interactions and short-range inclusion complexes and their role in controlling the multilevel assembly processes between alkyl ether carboxylic acids, cyclodextrin and chitosan. This final chapter summarises the main achievements and conclusions in three main research topics and perspectives.

The first part of the present work aimed to initially comprehend the complexation between weakly ethoxylated anionic surfactants and cyclodextrins. The thermodynamic investigations demonstrated that the host-guest complexes are spontaneously formed by the enthalpically driven cyclodextrin threading to the surfactant molecules in all pH 3, 4 and 5, in which the surfactant presents different degrees of ionization. The very surprising and interesting slight variation in the thermodynamic parameters with good agreement with the volumetric studies at different pH hints towards the threading in the alkyl chain rather than in the ethylene oxide units in the headgroup.

These findings were unexpected since the evaluated cyclodextrins of different sizes are reported to include two to three ethylene oxide units in the cavity.

The thermodynamic analysis allowed us to probe the strong effect of the cavity size in the energetic process, whereas the different PEG block lengths in the headgroup slightly influenced it. The opposite signals of the volume of transfer calculated from the density measurements, positive for β-cyclodextrin and negative for α-cyclodextrin, revealed distinct structural aspects of the high-energy water due to the cavity size. Their release and the hydration rearrangements occurring upon complexation dictated the overall magnitude of the volumes. Once more, the minor effect provided by the headgroup was evidenced by the similar volume of transfer obtained.

These results enhance the general understanding of the inclusion complexation process involving surfactants and bring in essential aspects concerning the charge density effect.

The spontaneous formation of ordered superstructures by cyclodextrin/alkyl ether carboxylates complexes was assessed. The aggregates' morphologies were characterized by small-angle neutron scattering at a broad length scale range. The supramolecular structures could be tuned by concentration, CD-to-surfactant mixing ratio and degree of ionization of the surfactant.

Concentration was demonstrated to be a critical parameter in the assembly process. In a CD-to-surfactant mixing ratio equal to two, highly ordered assemblies were obtained in surfactant concentrations superior to 3%wt for nonionic and ionic systems. More specifically, concentrated ionized surfactant systems presented flat multilayered structures. The charge density effect was probed by the systematic variation of the degree of ionization. It was possible to follow the development of structures from a soft to a crystalline layered microstructure upon increasing the fraction of ionized molecules disclosed the directing role of the electrostatic repulsion. These unexpected results oppose the calorimetric and densitometry findings.

The long-range ordering can be further tuned by employing macrocycles with different cavity sizes, and more compact structures are obtained for β-cyclodextrin systems. However, reorganization of the packing parameters was only observed in α-cyclodextrin aggregates. The surfactants' molecular architecture affects the interlayer repeating distances. Smaller inter-layers repeating distances are found in the surfactant with the shorter oligoethylene oxide block.

Complementing the SANS measurements, microscopy allowed the overall structural characterization of the supramolecular aggregates found in 5%wt surfactant complex systems. Micrometre-long cylindrical aggregates were formed in the ionized systems: rigid tubes in βCD systems and more flexible entangling tubes in αCD ones. In the nonionic surfactant systems at the same concentration, unilamellar

rhombic aggregates were obtained for βCD.

The thermoresponsive behaviour of the systems was investigated up to 70°C. Softening of the layered structures upon an increase in temperature was evidenced by the broadening of the peaks and the disappearance of the second-order peaks. At 70°C, the transition from multilayered structures to unilamellar structures – vesicles or disks, for example – is verified in $C_{12}E_{10}CH_2COOH$-αCD and $C_{12}E_5CH_2COOH$-βCD. Similar phase transitions, from tubular structures to vesicles were observed in sodium dodecyl sulfate and βCD [65, 80].

The main achievement reported for the alkyl ethoxy carboxylic acids is the charge density role in directing the inclusion complexes' self-assembly. The complementary thermodynamic and structural investigation further highlights the importance of assessing the tuning parameters from a short to a long interaction range when the modulation/tuning of hierarchical assemblies is envisioned.

In a double perspective of assembly control, the possibility of controlling the inclusion complexes' assembly and the polyelectrolyte-surfactant assembly involving alkyl ethoxy carboxylates was introduced. The surfactant's charge density control is essential to modulate the interaction with chitosan and direct the host-guest assembly, then it motivated the evaluation at different pH. The pH evaluation was limited to the interval between 2 and 5 for the sake of biopolymer solubility. The chitosan and the cyclodextrin content were also evaluated as a function of molar ratios to the surfactant and demonstrated to have a significant effect on the structures.

The collapse of the supramolecular aggregates found in inclusion complexes systems was induced by the increasing polymer concentration in all the pH evaluated. However, structural reordering and the formation of structures containing the surfactant assemblies with similar features to the ones found in the binary surfactant-chitosan systems were pointed by SANS at pH 5. The micellar or the multilayered vesicle nature of the core microstructure could not be resolved. The micellar core would indicate the disassembly and dethreading of cyclodextrin and the vesicles would point to the integration of the complexes in the complex superstructure and probe the co-assembly.

In the same way it impacted the inclusion complexes, the surfactant and cyclodextrin molecular architectures highly impact the structures' morphologies and stability in the ternary systems. Calorimetry experiments pointed to greater stability of αCD systems than for βCD. In addition, a remarkable effect of the number of ethylene oxide units was unveiled and indicated enriched and stable behaviour for the long polyethylene oxide headgroup.

An insight into the structural behaviour provided by interactions between the cyclodextrins and weakly anionic alkyl ethoxy carboxylates was presented, but further

investigation of the systems is necessary to extend the characterization herein presented.

Finally, a comprehensive investigation of the cyclodextrin/alkyl ethoxy carboxylic acids complexes pointed to the remarkable versatility of the systems given their multi-responsiveness. The combination of alkyl ethoxy carboxylic acids/cyclodextrin inclusion complexes with chitosan resulting in ternary systems, extended the complexity of the systems. The thermodynamics and structural results presented highlight the importance of evaluating the tuning parameters in short and long-range interactions. Although some limitations were encountered, exploring the balance of interactions in these systems and their specific arrangements may open numerous possibilities for their application in different fields.

6.1 Future perspectives

The bare inclusion complexes and the ternary polyelectrolyte-surfactant-cyclodextrin systems are far from being completely understood, especially the latter. This research aimed to raise a few conclusions about the systems allowing some predictions, such as in the size match compatibility of the guest and host, for example, but many other questions about these systems need further investigation. The charge density influence on the structural tuning dependency on the cyclodextrin type would be a topic to be investigated, considering the differences verified by SANS and calorimetry in the bilayers' development of distinct cavity sizes. It would be exciting to investigate the mixture of cyclodextrins with the same guest in the inclusion complexes as it presents great potential in selective complexation. It is supported by a successful inclusion complexation of surfactants of different ionic natures that had been performed [140].

Further assessment of the ternary systems investigated in this thesis is necessary to better comprehend the dynamics of the inclusion complexes-polyelectrolyte interactions. Exploring different components' concentrations in the ternary systems, starting with a lower surfactant concentration, would be essential to expand the phase behaviour knowledge since it was a critical parameter in the inclusion complexes systems. Other surfactants with a strong cyclodextrin binding affinity exhibiting pH responsiveness could also widen the possible systems.

In all the systems, the SANS modeling was a limitation due to the polydispersity of the surfactant. From a future perspective, the fitting of the data would provide a deep quantitative analysis of the supramolecular aggregates' structural features.

The mentioned aspects for investigations would assist the unveiling of fundamental properties and dynamics aiming for the smart control of the assemblies and their

application and open many other questions to motivate the investigation of surfactants, polyelectrolytes and cyclodextrins.

Appendix A

Paper I: Cyclodextrin/surfactant inclusion complexes: An integrated view of their thermodynamic and structural properties

Advances in Colloid and Interface Science 289 (2021) 102375

Contents lists available at ScienceDirect

Advances in Colloid and Interface Science

journal homepage: www.elsevier.com/locate/cis

Historical Perspective

Cyclodextrin/surfactant inclusion complexes: An integrated view of their thermodynamic and structural properties

Larissa dos Santos Silva Araújo [a,b], Giuseppe Lazzara [a,*], Leonardo Chiappisi [b,*]

[a] Dipartimento di Fisica e Chimica, Università degli Studi di Palermo, Viale delle Scienze pad 17, 90128 Palermo, Italy
[b] Institut Max von Laue - Paul Langevin, 71 avenue des Martyrs, 38042 Grenoble, France

ARTICLE INFO

Article history:
25 January 2021
Available online 5 February 2021

Keywords:
Surfactant
Cyclodextrin
Inclusion complexes
Thermodynamics

ABSTRACT

Cyclodextrins (CDs) play an important role in self-assembly systems of amphiphiles. The structure of CDs provides distinguished physicochemical properties, including the ability to form host-guest complexes. The complexation affects the properties of guest molecules and can produce supramolecular aggregates with desirable characteristics for fundamental and practical applications. Surfactants are particularly attractive host molecules due to their wide variety, availability, responsiveness to different stimuli, and high relevance in different fields, e.g. medical, cosmetic, pharmaceutical, and food industries. The tendency of organization in higher-order supramolecular aggregates arises the interest in applying such versatile complexes in the development of novel materials. In this review, we provide a comprehensive overview of the thermodynamics aspects of surfactants and CDs inclusion complexes formation in aqueous environment, emphasizing the assessment of the interactions, thermodynamic driving forces, and structural aspects. Also, the most common analytical techniques used to gather deep insight into the aspects of CDs complexes are discussed and the perspectives for the surfactant-cyclodextrin complexes are pointed out.

Contents

1. Introduction

Self-assembly is the phenomenon where simple molecules spontaneously organize into complex systems. The process of self-organization takes place via a number of different interaction mechanisms: unspecific electrostatic, $\pi - \pi$ interaction, dispersion, hydrophobic forces, or more specific bindings such as host-guest complexation or "lock-and-key" binding [1–3]. Among a variety of macrocyclic molecules able to establish such complexes [4], cyclodextrins are extensively studied and applied [5]. In turn, surfactants present attractive features to integrate the complexes as hosts. In this review, we focus on the spontaneous organization of cyclodextrins and surfactant into complex aggregates in aqueous environment.

Cyclodextrins (CDs) are a class of cyclic oligosaccharides, the most common ones, α, β and γ-cyclodextrins (Fig. 1), formed by six, seven and eight α-(1–4) D-glucopyranoses units, respectively. These oligosaccharides are typically cone-shaped, with the size of the internal cavity varying from 4 to 8 Å, depending on the number of sugar units forming the macrocycle. Different definitions of the two rims can be found in the literature, with the smaller one as primary rim or head, and larger one

* Corresponding authors.
E-mail addresses: giuseppe.lazzara@unipa.it (G. Lazzara), chiappisil@ill.eu (L. Chiappisi).

https://doi.org/10.1016/j.cis.2021.102375
0001-8686/

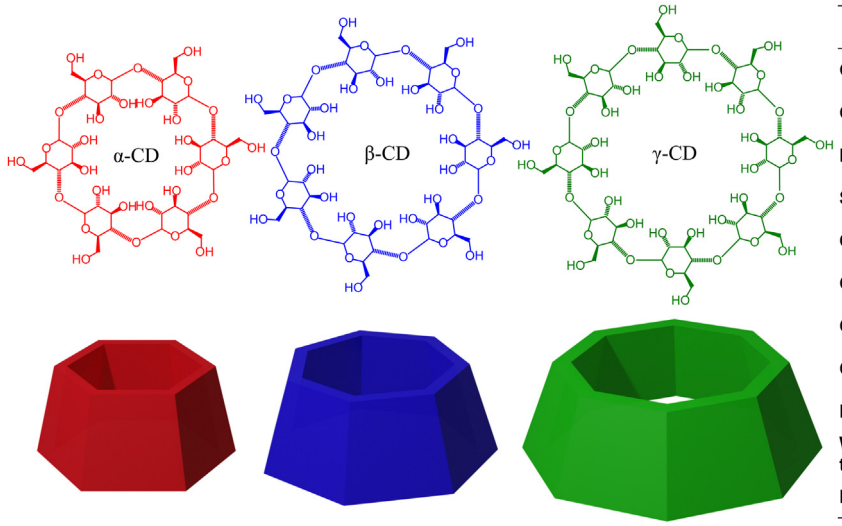

	α-CD	β-CD	γ-CD
Glucopyranose units	6	7	8
Chemical formula	$C_{36}H_{60}O_{30}$	$C_{42}H_{70}O_{35}$	$C_{48}H_{80}O_{40}$
Molar mass [g/mol]	972	1134	1296
Solubility in water [g / kg]	129.5	18.4	249.2
Outer diameter [nm]	1.52	1.66	1.77
Cavity height [nm]	0.78	0.78	0.78
Cavity diameter [nm]	0.45 – 0.53	0.6 – 0.65	0.75 – 0.83
Cavity volume [nm³]	0.174	0.262	0.427
Bound water molecules	6.4	9.6	14.2
Water molecules inside the cavity	3.6	6.3	8.9
Density [g / cm³]	1.48	1.44	1.52

Fig. 1. Chemical structure of α, β, and γ-cyclodextrins, together with a schematic representation of the toroidal structure. On the right, the most relevant physico-chemical properties of native α,β and γ cyclodextrins are given. Data are reported from Refs. [7, 8].

often defined as secondary rim or tail. In the cone structure, the C-H bonds directed inwards produce a relatively hydrophobic cavity, and the hydrophilic properties are conferred by O-H groups located in the external side of the cone. Moreover, the non-bonding electron pairs of the oxygen atoms in the glycoside bonds, pointing towards the interior of the cavity, result in high electronic density which, in turn, confers a Lewis base character to the cavity of the CD [6].

The unique structure of cyclodextrins is at the origin of their peculiar physico-chemical properties, and in particular on their ability to form host-guest complexes. The presence of hydrophilic and hydrophobic regions, the excess electron density, as well as the presence of highly structured water molecules in the cavity, drive the formation of host-guest complexes with a variety of compounds, such as drugs [4,9,10] essential oils [11], surfactants and polymers [6,12,13].

The formation of the inclusion complexes strongly affects the properties of the guest molecules. In particular, the inclusion complex causes a decrease of the chemical potential of the guest molecule, with a subsequent enhancement of solubilization [14,15], and a control of volatilization properties [16]. In addition, the low toxicity and the excellent biocompatibility of CDs make the inclusion complexes suitable for a large range of applications, like cosmetics [17,18], pharmaceutical [15], medical [19], food industries [20] and electronic technology uses [21,22].

The formation of inclusion complexes between CDs and surfactants is a very active field of research. Not only given their high relevance for the medical, food, and cosmetic industry, but also because these mixture exhibit the tendency of forming highly ordered supramolecular aggregates, resulting from the delicate balance of a variety of forces. Furthermore, the virtually endless variety of surfactants available and their responsive properties to different stimuli, make this a very fertile playground for colloidal scientists aiming at the spontaneous formation of complex materials from simple building blocks.

A further key parameter to control the supramolecular assembly of CD/surfactants inclusion complexes is adding a third component to the mixture, in particular, a different type of surfactant or polymer [23,24]. The system becomes particularly intricate as specific host-guest interactions, unspecific, long-range electrostatic and dispersion forces, interplay with directional short-range hydrogen bridge between neighbouring CD molecules.

Several review articles summarizing the literature on cyclodextrin surfactant inclusion complexes have appeared in recent years [6,25,26], focusing on the thermodynamic of binding or on the structural and stimuli-responsiveness of the inclusion complexes. Herein, we provide an updated and comprehensive overview of the thermodynamic aspects characterizing the inclusion complex formation between simple surfactant and cyclodextrins. In particular, a description of binary and ternary systems is provided, including of the thermodynamic driving forces, the structural aspects and the techniques commonly used to obtain closer insights on the CDs complexes.

2. Thermodynamic aspects of surfactant/cyclodextrin inclusion complex formation

Host-guest supramolecular complexes formation involving surfactant molecules and cyclodextrins are mainly driven by non-covalent interactions, as Van der Waals, electrostatic, charge transfer, hydrophobic interactions and hydrogen bonding [27]. The quantitative analysis of the thermodynamic parameters of the process is important to understand the complexes properties. Knowledge of the binding constant, the stoichiometry, enthalpy and entropy changes, and of the different derivatives of the Gibbs free energy of the interaction between CD and the guest molecules are essential to understand and predict its behavior.

For a better understanding of a surfactant and a CD molecule complexation, the process can be divided into stages, schematically represented in Fig. 2:

- *Dehydration of surfactant and cyclodextrin.* The water molecules hydrating the surfactant, the cyclodextrin, and those located inside the CD cavity are released (Fig. 2a). This process is entropically favored, given the strong structuring of water hydrating the exposed hydrophobic moiety of the surfactant and due to the geometrical constraints within the CD cavity. In particular, the water structure within the CD cavity is strongly affected by the cyclodextrin size, as demonstrated by the fact that the heat capacity at constant pressure, C_P, of water within the cavity of β and γCD is, approximately, 71 J K^{-1} mol^{-1}, and close to the C_P for liquid water. In contrast, a significantly lower value of 60 J K^{-1} mol^{-1} was reported for water in the αCD cavity [28]. Despite both the hydration water of the cyclodextrin and of the surfactant can be defined as high-energy water molecules, a fundamental difference between them can be drawn. Water molecules structure themselves around the hydrophobic part of the surfactant, forming a strong hydrogen-bonded network. The amount of water

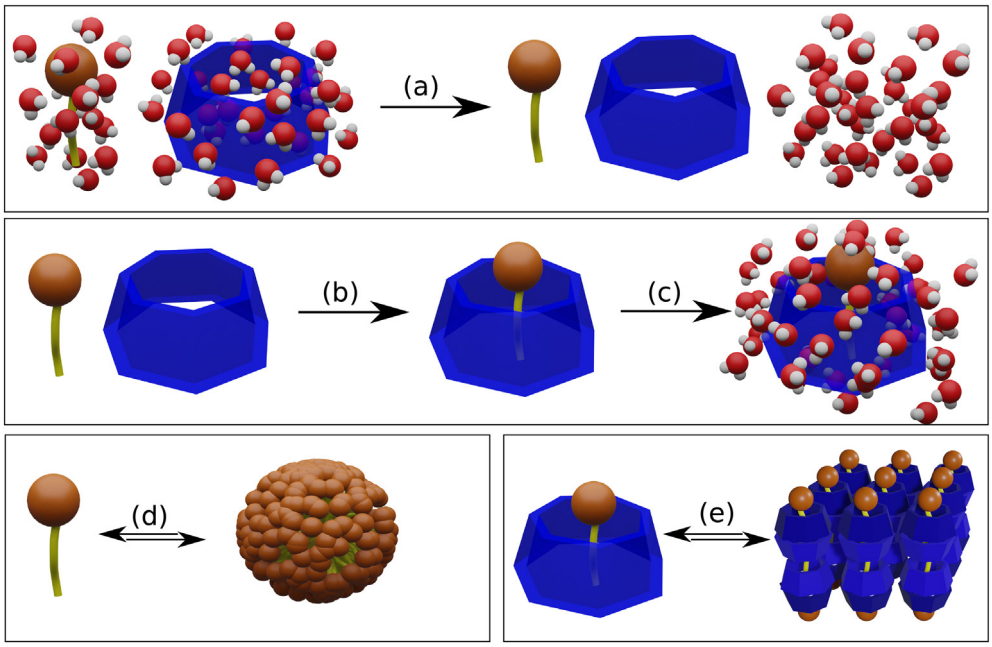

Fig. 2. Schematic representation of the steps in which the complex formation between surfactants and cyclodextrins can be divided: (a) the surfactant and the cyclodextrin are dehydrated; (b) the insertion of the surfactant molecule into the CD cavity takes place; (c) the CD/Surfactant complex is hydrated. In addition to these three fundamental steps, the equilibrium (d) between the free surfactant and the surfactant in the micelle and (e) between the inclusion complexes and the assembly of inclusion complexes has to be considered. Representation is out of scale.

molecules involved in the hydration scales linearly with the number of methylene units of the alkyl chains, thus the linear dependence on the surfactant chain length of the free energy of micellization, and similar phenomena which involve the removal of the alkyl chain from the aqueous environment. In contrast, the cyclodextrin, with its hydrogen bond donor and acceptor atoms, is embedded in the water network, partly distorting it. Similarly, the water structure within the cavity has to adapt to rigid contour conditions imposed by the cyclodextrin wall [29,30]. Both effects do not scale linearly with the cyclodextrin size, as also demonstrated by non-monotic dependence of the cyclodextrin solubility from the cavity size. It is, in fact, the release of this high energetic water, located inside the cyclodextrin cavity and hydrating the surfactant, that mainly drives the assembly of the components in aqueous environment (hydrophobic effect).

- *Inclusion of the surfactant in the CD's cavity.* The inclusion occurs effectively with the inlet of the alkyl chain of surfactant in the hydrophobic cavity, which is internally stabilized by numerous Van der Waals interactions [27,31] (Fig. 2b). A methylene group with average diameter (0.4 nm) fits tightly in the αCD cavity, while the βCD cavity (0.6–0.65 nm) allows the loose accommodation of a methylene group, increasing the number of possible conformations of the surfactant tail and the energy associated to them. If energetically favored, the accommodation of 2 methylene groups in γ-CD is expected due to its inner width (0.75–0.83 nm), leading to the 1:2 stoichiometry in a positive cooperative process. In the cases of a single alkyl chain in the cavity, the wider cavity reduces the strength of the interaction and the complex formation is not observed. Less important but still present are the interactions between the surfactant head group and the CD rim [32,33]. As an alternative to the conventional cyclodextrins, their derivatives are largely used due to the specific properties imparted by the attached group and can present extracavity effects on the stabilization of the surfactant [34,35].
- *Hydration of the inclusion complex.* Finally, the water structure of the exposed part of the guest is restored and integrates the hydration shell of the complex (Fig. 2c) [36,37].
- *Further equilibria.* Other processes take often place in concomitance to the simple inclusion complex formation. For instance, the equilibrium between the free surfactant and the surfactant associated into micelles needs to be taken into account, when the surfactant concentration is close to the critical micelle concentration (*cmc*) (Fig. 2d). This equilibrium is clearly affected by the presence of cyclodextrin, as it lowers the activity of the free surfactant involved in the micellization process. Accordingly, the micellization and the inclusion complex formation are competitive processes, and the overall speciation in the system is determined by the different equilibrium constants.
- *Supramolecular growth.* Eventually, the inclusion complexes can spontaneously organize in supramolecular structures (Fig. 2e). The assembly is mediated by hydrogen bonds of the cyclodextrin's external hydroxyl groups and occasionally leads to the precipitation of the complexes. The structural properties of the CD-surfactant complexes are further approached in Section 3.

In general terms, the process of inclusion complex formation, taking into account water displacement, can be written as:

$$hH_2O{\cdot}aCD + bG{\cdot}gH_2O \rightleftharpoons CD_a{\cdot}G_b{\cdot}(g+h-i) + iH_2O \quad (1)$$

where a and b are the stoichiometry coefficients of the cyclodextrin and the surfactant, respectively, h and g are the number of water molecules hydrating the cyclodextrin and the surfactant, and i is the net displacement of water molecules upon complexation. The key role played by water in the complex formation process is further evidences by the consequences of hydrotropes addition, such as short chain alcohols, or of inert salt to the system. A significant reduction of the CD/surfactant affinity is observed upon addition of short chain alcohols, such as ethanol, propanol, or butanol [38–40], due to the stabilization of the solvent-exposed alkyl chains. In contrast, the addition of an inert salt results in the rise of the binding constant due to the increased polarity of the solvent, which strengthens the hydrophobic interactions, and to the increased osmotic pressure which shifts the equilibrium towards less hydrated complex. Finally, the importance of the hydrophobic

interactions is further evidenced by the fact that it is the hydrophobic part of the surfactant, and not its hydrophilic head group, to be located within the CD cavity.

The formation of inclusion complexes between CDs and a wide variety of surfactants have been reported in the literature [6,37,41–43]. The size-match compatibility of host and guest is a simple concept able to anticipate possible interactions, but the exact molecular conformation and stoichiometry of a CD-surfactant complex must be evaluated case by case. Stoichiometries (CD:surfactant) of 1:1, 2:1, and 1:2 are observed for those complexes as illustrated in Fig. 3, influenced by the alkyl chain length of the surfactant and CD cavity size [44,45]. Generally, a 1:1 stoichiometry is favored for surfactants with alkyl chain length shorter than eight carbon units, being able to accommodate only one molecule of CD. The 2:1 stoichiometry complexes are most likely for surfactants with 12 or more carbon units in the alkyl chain, able to accommodate two molecules of CD. The stability of those complexes are more influenced to the interactions between the rim of CD and the surfactant head group [46,47]. In gemini surfactants, this configuration is commonly verified when each cyclodextrin interacts with one alkyl chain, and further specific 4:1 stoichiometry is reported in the interaction of two CDs with each alkyl chain [48]. The host of two entire surfactant molecules in a single molecule of CD is unlikely for the α and βCD, but may occur with unexpected stability for γ-CD due to the larger cavity of the cyclodextrin able to accommodate two alkyl chains. The 1:2 complexes occurrence can also be related to the excess of surfactant with respect to the cyclodextrin concentration [49].

As mentioned previously, the thermodynamic characterization of the inclusion complex formation is essential to understand the process from a molecular perspective. The most important parameter to be determined is the Gibbs free energy change ΔG° of complexation via the binding constant (K), followed by the enthalpy (ΔH°) and entropy change (ΔS°), and finally by the different derivatives of the free energy, namely the change in heat capacity (ΔC°) or in volume (ΔV°).

To determine the ΔG°, ΔH°, and ΔS°, two main approaches are available. In the first one, the equilibrium constant is determined at different temperatures, and, via the van't Hoff approach, the enthalpy of complex formation is obtained and, subsequently, the entropy of complex formation is calculated. In contrast, isothermal titration calorimetry (ITC) can simultaneously provide the stoichiometry of the process, the binding constant, and the enthalpy (ΔH°) change. In an ITC experiment, the results are obtained from a titration procedure. The surfactant is placed at the sample cell and the cyclodextrin is delivered by injection of several aliquots into the sample cell from a syringe coaxially inserted. The experiment can be performed also in the reversed fashion way, i.e., adding the surfactant to a cyclodextrin solution, despite this procedure is less commonly employed. After each injection, the association of host and guest molecules, in addition to other spurious processes, result in a heat exchange with the surrounding medium, which is accurately detected by the apparatus. Accordingly, after each injection, a heat pulse is observed and its integral Q corresponds to the heat exchanged upon host-guest complex formation. To extract valuable thermodynamic information from the process, such as the binding constant K and the enthalpy change of inclusion complex formation ΔH_i and stoichiometry n, the data need accurate modeling. Hereafter, we provide the procedure to derive the required equation to model the inclusion complex formation. For the sake of simplicity, we limit the description to the simplest 1:1 binding process whereby a cyclodextrin solution is injected to a sample vessel of volume V_0 filled with a surfactant solution. The approach can, however, be easily extended to more complex binding processes.

The heat exchanged after each injection, corrected for dilutions effects, is determined by the change in amount of the different species (X_i) present in the system weighted by their enthalpy H_i:

$$Q = \sum_i \Delta X_i H_i \tag{2}$$

For the case of the 1:1 binding process, the following species and enthalpy content can be defined: [S], [CD], and [CDS] being the concentrations of the free surfactant, the free cyclodextrin, and the inclusion complex, respectively, characterized by the corresponding enthalpic content of H^S, H^{CD}, and H^{CDS}. The enthalpy change of inclusion complex formation is defined as:

$$\Delta H_i = H^{CDS} - H^S - H^{CD} \tag{3}$$

substituting in Eq. (2):

$$Q = V_0\left(\Delta[S]H^S + \Delta[CD]H^{CD} + \Delta[CDS]H^{CDS}\right) \tag{4}$$

Recalling that $\Delta[S] = \Delta[CD] = -\Delta[CDS]$, Eq. (4) simplifies to:

$$Q = V_0 \Delta[CDS]\Delta H_i \tag{5}$$

Normalizing the detected heat by the amount of injected cyclodextrin ($n_{CD_{tot}} = \Delta[CD_{tot}]V_0$, Eq. (5) becomes:

$$\frac{Q}{n_{CD_{tot}}} = \frac{\Delta[CDS]}{\Delta[CD_{tot}]}\Delta H_i \tag{6}$$

in differential form:

$$\overline{Q} = \frac{\partial[CDS]}{\partial[CD_{tot}]}\Delta H_i \tag{7}$$

The speciation of the system can be determined upon combination of the mass action balances and equilibrium constant expression, resulting in the following polynomial:

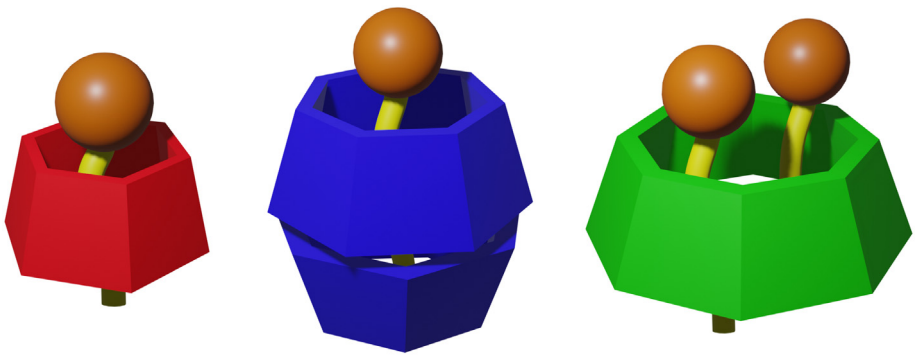

Fig. 3. Schematic representation of inclusion complexes formed with stoichiometries of, from left to right, 1:1, 2:1, 1:2. Sketches are not at scale.

$$[CDS]^2-[CDS]\left(K^{-1}+[CD_{tot}]+[S_{tot}]\right)+[CD_{tot}][S_{tot}]=0 \quad (8)$$

For the considered case of a 1:1 binding, an analytical solution to the problem is available. The quadratic expression given in Eq. (8) has only one physically meaningful root:

$$[CDS]=\frac{-b-\sqrt{b^2-4c}}{2} \quad (9)$$

with $b = -[S_{tot}]-[CD_{tot}]-K^{-1}$ and $c=[CD_{tot}][S_{tot}]$. When the last expression is differentiated with respect to $[CD_{tot}]$, the Wiseman isotherm [50] is obtained:

$$\overline{Q}=\left[\frac{1}{2}+\frac{1-(1+r)/2-X_r/2}{\sqrt{X_r^2-2X_r(1-r)+(1+r)^2}}\right]\Delta H_i \quad (10)$$

with $r=1/(K[S_{tot}])$ and $X_r=[CD_{tot}]/[S_{tot}]$. An alternative approach [51] consists in directly differentiating Eq. (8) with respect to $[CD_{tot}]$, obtaining:

$$2[CDS]\frac{\partial[CDS]}{\partial[CD_{tot}]}-\frac{\partial[CDS]}{\partial[CD_{tot}]}\left(K^{-1}+[CD_{tot}]+[S_{tot}]\right)-[CDS]+[S_{tot}]=0 \quad (11)$$

solving Eq. (11) for $\partial[CDS]/\partial[CD_{tot}]$:

$$\frac{\partial[CDS]}{\partial[CD_{tot}]}=\frac{[CDS]-[S_{tot}]}{2[CDS]-[CD_{tot}]-[S_{tot}]-K^{-1}} \quad (12)$$

and substituting the expression for $\partial[CDS]/\partial[CD_{tot}]$ in Eq. (7). The latter approach requires that $[CDS]$ is solved separately and substituted in Eq. (12). However, in contrast to the Wiseman isotherm which is applicable only to a 1:1 complex, the latter approach is applicable to all type of complex reactions, whereby resolving non-constant therms, such as $[CDS]$, likely requires the use of non-analytical solutions.

Generally, the ITC data exhibit a sigmoidal shape [31,52]. A qualitative analysis, as depicted in Fig. 4, allows to evaluate the enthalpy change of the process from the height of the curve, the stoichiometry from the abscissa of the inflection point, as well as the binding constant from the slope of the curve at the inflection point. For a more accurate, quantitative analysis, the fitting of the experimental data with the appropriate model is required. From the obtained values of K and ΔH_i, the binding free energy and entropy change can be determined according to:

$$\Delta G^{\circ}=-RT\ln K \quad (13)$$

$$\Delta S^{\circ}=\frac{\Delta H^{\circ}-\Delta G^{\circ}}{T} \quad (14)$$

Moreover, the ΔC_p can be determined from the temperature dependence of the ΔH°, if several experiments at different temperature are performed:

$$\Delta C_p^{\circ}=\frac{d\Delta H^{\circ}}{dT} \quad (15)$$

The agreement–disagreement between the enthalpy values determined by the van't Hoff approach and calorimetric measurements have been discussed in the literature, especially for supramolecular systems, and attempts to solve this issue have been debated [53,54]. The van't Hoff equation and the ITC experiments conducted for different CD-surfactant associations demonstrate the strong effect of temperature on the binding constant [31,55]. Generally, discreet variations of ΔG° were observed with temperature change and is associated to the compensation of the enthalpic fluctuations by the $T\Delta S^{\circ}$ alterations [31,55,56]. It is well known that the enthalpy and entropy changes upon transfer of non-polar moieties in water are strongly temperature-dependent, whereas the corresponding free energy change is typically mildly influenced. This provides evidence of the enthalpy-entropy compensation effect also observed in cyclodextrin and surfactants complexation. From a microscopic point of view, the compensation is related to the water molecules reorganization following the entrance of the surfactant into the CD cavity. In particular, during the inclusion phenomenon, high-energy water is expelled from the CD cavity and ice-like water surrounding the surfactant tail is released. These effects generate a large change in the thermal heat capacity (ΔC_p) and, therefore, the enthalpy-entropy compensation is observed whenever magnitude of ΔC_p is superior to ΔS [57]. It should be mentioned that enthalpy-entropy compensation effects should be analyzed with particular care as the entropy change is typically obtained as a difference between the enthalpy and standard free energy knowledge. The simple linear trend of ΔS vs ΔH plot could be misleading as it can be originated by so called "secondary" effects very well explained in terms of well-known thermodynamic equations and based on the experimental protocol [58]. For instance, from $\Delta H\text{-}T\Delta S = \Delta G$, if the standard free energy change is small (with respect to the observed ΔH values) due to experimental or intrinsic motivations, the linear correlation between entropy and enthalpy follows immediately.

As discussed earlier, studying the enthalpy and entropy changes of the inclusion complex formation and its stabilization allows distinguishing the effect of different types of non-covalent interactions between guest and the CD. The thermodynamic quantities result from the energetic contributions of all these interactions, which are

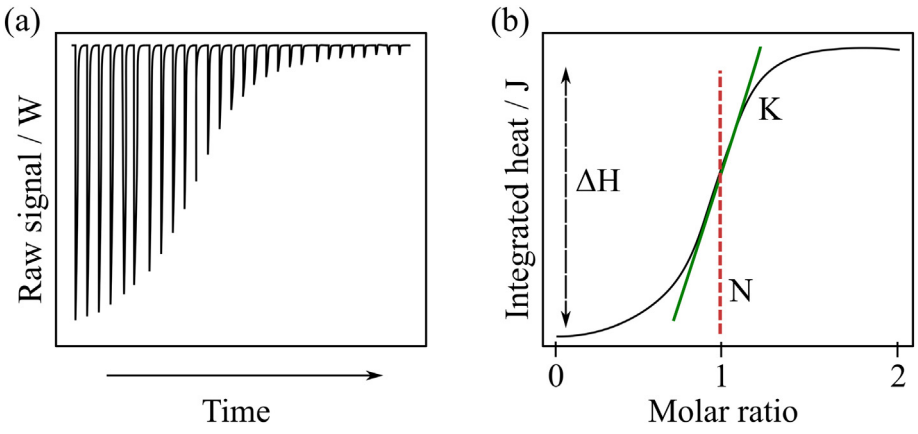

Fig. 4. Schematic representation of the graphs obtained from an ITC experiment. (a) Raw data (dq/dt) obtained after baseline correction. (b) Integrated power from which enthalpy (ΔH), binding constant (K) and stoichiometry (N) are determined.

characteristic of each host-guest pair, influenced by the ionic character and alkyl chain length of the surfactant, size of cavity of CD, and their sterical and conformational effects. For an easy qualitative prediction of the thermodynamic characteristics, the magnitude of the binding constant is used to indicate the most favorable host-guest pairs [59].

The ionic character of the surfactant head group, the alkyl chain length and the conformation of the host have determinant effect on the thermodynamic binding parameters of the CD/surfactant complexes. The series of the sodium n-alkyl sulfates and *n*-Alkyltrimethylammonium Bromide are the most reported in the investigation of the effect of surfactant ionic character in the complexes [37,60]. The studies showed small influence of the head group in 1:1 stoichiometry complexes, and slightly reduced stability of the those complexes was found when the SO_4^{2-} group is substituted for cationic groups in surfactants with homolog alkyl chain length. Nevertheless, the influence of the head group is expected for 2:1 stoichiometry complexes since the accommodation of two cyclodextrins approximate the head group to the cyclodextrin extremity. In this case, if energetically favorable, interactions for the stability and formation of the inclusion complex are established [43].

The inclusion complex formation between cyclodextrins and non-ionic surfactants has also been a matter of investigation in the past decades [61–64]. The resulting properties significantly depend on the architecture of the surfactant and the cyclodextrin size. We limit ourselves here to briefly discuss the complex formation of cyclodextrins with alcohol ethoxylate and alkylphenol ethoxylate surfactants. In both cases, the hydrophilic part of the surfactant is made by an oligo ethylene oxide chain with variable length; the hydrophobic part is composed by a mostly linear fatty alcohol chain for the former class while it is made of a bulky, often branched alkylphenol unit for the latter one. The different studies have shown that the alkylphenol unit is not complexated by αCD [62,63], which treads only the surfactant head group in a" molecular necklace" structure [65], with expected stoichiometry of two ethylene oxide units per αCD molecule [62]. For the case of alcohol ethoxylated, both the hydrophilic and hydrophobic moiety of the surfactant are included within the αCD cavity. In contrast, βCD shows a significantly higher affinity towards the bulky alkylphenol unit than for the ethoxylated head group [63,66]. The direct consequence of the preferential inclusion of the hydrophobic moiety is the increase in critical micellar concentration observed upon addition of βCD to alkylphenol based surfactants. As for ionic surfactants, γCD was also shown to be able to complexate two surfactant molecule within its large cavity [62].

The alkyl chain length effect on the thermodynamic parameters have been widely discussed in the literature [43,67–70]. The increase of the alkyl chain length and, therefore, of the stronger hydrophobic character of the guest, results in strengthen interactions evidenced by the raise of the binding constants as similarly found for the cmc [43,68]. Benko et al. also described the chain length of 6 carbons for ionic and 8 carbons for non-ionic surfactants as the critical chain length to the complexes formation [68]. It also suggests the stronger influence of the head group in shorter chain lengths. For hydrocarbon chains longer than 14 carbons, the increase is less pronounced. The Table 1 presents a general thermodynamic prediction for cationic and anionic surfactants with cyclodextrins.

As concerns ionic surfactants, the effect of the counterion has to be considered. While the ions in solutions were shown to interact with native cyclodextrins [73], the effect of counter ions on the thermodynamic parameters and binding constants of ionic surfactant complexes with CD is small compared to the magnitude of the energetic changes due to other processes [6]. However, counterion condensation was reported by potentiometric experiments [74]. Mostly, small binding constants are reported for the bromide anion to C_{12}TAB-βCD and C_{12}TAB-HPβCD and of sodium cation to the dodecyl sulfate or dodecanoate - βCD complexes [75,76].

As previously mentioned in the text, if the ITC data are correctly modelled, the method allows the simultaneous determination of both ΔH and ΔG of the binding process. However, a wide variety of other methods used to probe the thermodynamics are briefly described hereafter.

Table 1
Prediction of thermodynamic parameters of different surfactant-cyclodextrin complexes.

Ionic character	n	CD	ΔH/*kJmol*$^{-1}$	TΔS/*kJmol*$^{-1}$	ΔG/*kJmol*$^{-1}$	Reference
1:1						
$C_xSO_4^-$	8–12		- - -	–	- -	[43,71]
		αCD				
C_xTAB	8–14		- -	–	- -	[43,72]
$C_xSO_4^-$	6		–	+	–	[37,68]
	8–12		–	+	- -	
		βCD				
C_xTAB	8–16		–	+	- -	[68]
2:1						
$C_xSO_4^-$	8		- - - -	- - -	- -	24em [43,71]
	10–12		- - - -	- - -	- - -	
		αCD				
C_xTAB	16		–	+	- -	[72]

Signs correspond to the follow numeric intervals $0 \leq + \leq 15$; $16 \leq + + \leq 30$; $31 \leq + + + \leq 45$ and $46 \leq + + + + \leq 60$. The intervals are analogous for the negative values. For detailed numerical values, see the references.

- Nuclear Magnetic Resonance (NMR): NMR is a powerful technique which allows to elucidate the binding constant and biding stoichiometry of the complexation reaction. However, the technique is limited to systems where the signal from the surfactant can be clearly separated from those of the cyclodextrins [6,77]. A further approach to determine the binding constant offered by NMR diffusometry is to exploit the different diffusion coefficients of the free compounds and of the complex [46,78,79].
- Conductivity: This is a simple technique present in the routine of laboratories that provide reliable data on the thermodynamic aspects of the CD-surfactants. In the case of ionic surfactants, conductivity has been used for determination of stoichiometry [80], binding constants and thermodynamic parameters [69,70], degree of ionization of the micelles [49], critical micelle concentration and the demicellization process evidencing the formation of the complexes [81–83]
- Potentiometry: Selective ion electrodes have been also used in thermodynamic studies of CD complexation [84]. Counter ion binding to the complexes and the surfactant aggregation characteristics are determined by potentiometry with almost no pretreatment in the solutions requiring only specific electrodes for the analysis [75,84]. The use of surfactant-ion selective electrodes allows the direct determination of the surfactant binding isotherm. This technique has been mostly applied to the evaluation of systems containing trimethylalkylammonium surfactants [85,86]. The method is difficult to apply to nonionic surfactant species, due to the lack of specific electrodes.
- Spectrophotometric methods: It allows the simple and fast study the formation of host-guest complexes by the evaluation of the absorption spectrum. However, it is susceptible to interference in complex matrix and may lead to a wrong detection of the IC complex assessed [87]. Probes [88] and the decomposition in sub-bands [89] are commonly applied to obtain the binding constant and stoichiometry. Spectophotometric methods are also efficient in the verification of the encapsulation of dyes into the structures formed by the complexes. For example, Rhodamine B encapsulation in the vesicles cavity of the Tween20@2βCD complexes was verified by UV-VIS [90].
- Density and speed of sound: These measurements are usually coupled to determine apparent molar and partial volumes, the volume of transfer and adiabatic compressibilities, which are responsive to alterations in nature and degree of hydration of substances [91]. As the transfer of the surfactant molecule from water to the cavity of CD in the inclusion complex formation leads to changes of hydration in

both host and guest molecules, data regarding the effect of CD on the micellization process, nature of the complex and stoichiometry are obtained [49].

All the described techniques offer valuable advantages and suffer from specific limitations. In any case, an essential step for the extraction of thermodynamic parameters is the appropriate modeling of the data. Accordingly, the experiments need to be designed in such a way to make the data analysis as robust as possible. A problematic specific to CD/surfactant systems is the fact that often the inclusion complex formation takes simultaneously place with other process with comparable energetic parameters, most notably the demicellization process. Of course, the experimentalists have to take into account eventual side-processes when planning the experiment as well as when performing the data analysis.

3. Spontaneous organization of surfactant/cyclodextrin inclusion complexes

In the previous section, the formation of the inclusion complex from a thermodynamic perspective is presented. The complex formation generally includes a handful of components, one or two cyclodextrins, and one or two guest molecules. The investigation of the structural aspects of such mixtures was often neglected, as a general behavior of CDs was to disrupt the self-assembly properties of the amphiphilic compounds by sequestrating its hydrophobic region [92,93]. However, it has been recently shown that the inclusion complexes, depending on the sample concentration and temperature, have the tendency to organize into aggregates with ordered structure. The process of single inclusion complexes forming large structures is named *lattice self-assembly*.

The aggregates formed by the inclusion complexes are multi-scale aggregates, with the inclusion complex being the primitive building block. Typically, the inclusion complexes present the tendency to form large, planar sheets, with a bilayer-like structure [25,45,94–97], consisting of one guest molecule and two cyclodextrins, with a head-to-head arrangement [98], i.e., with the primary and secondary rims of the cyclodextrins facing each other. In contrast to the assembly of simple surfactant molecules driven by many, non-directional, weak, hydrophobic interactions, the assembly of the inclusion complexes is dictated by few, water-mediated, strong and highly directional bonds [94,98,99]. Accordingly, the inclusion complexes self-organize into highly ordered and rigid structures. The importance of direct and water-mediated hydrogen bonds between the inclusion complexes is further corroborated by the fact that this complex self-organization is generally inhibited by chemical substitutions on the CD, such as the hydroxypropylation or methylation [94,96,100,101].

Depending on the cyclodextrin type and on the guest molecule, different vertical packing types are reported in the literature, commonly named as channel, cage and brick-type packing [13,102,103]. With the term vertical packing type we refer to arrangement of the cyclodextrins along their rotational axis. A schematic representation of the different lattice types is given in Fig. 5.

- In the *cage-type* lattice structure, the cyclodextrins are arranged in a herring-bone fashion. Each side of the cavity is closed either by the face or the rim of an adjacent cyclodextrin molecule, so that each cavity is fully isolated from the other ones. Typical systems assembling into the cage structure are inclusion complexes with small, neutral guest molecules which do not protrude from the CD cavity. Typical examples are complexes between α or βCD with low molecular weight carboxylic acids [104], and pure aqueous systems of γCD [103].
- In the *brick-type* arrangement, also denominated *layer-type* packing, the inclusion complexes are arranged in layers, shifted relatively to each other by half the size of the cyclodextrin, and with an alternating sequence of head-up — tail-up of cyclodextrins. Each cavity is closed by the rim of adjecent CD molecules. This type of arrangement is found in inclusion complexes of αCD and small aromatic molecules, whose size slightly exceeds the cavity size and which cause a small distortion of the macrocycle [102].
- Finally, in the *channel-type* lattice structure, the cyclodextrins are stacked forming a channel where the guest molecule is located. The vertical packing is hold together by several inter cyclodextrin hydrogen bonds. This is the most common packing and is found in many cyclodextrin surfactant complexes, with typically two surfactant molecules and four cyclodextrins, as well as in polymer-CD rotaxanes, where one polymer chain is threaded by countless oligosaccharides [105]. A very illustrative example is the rigid, 1-dimensional tubular rotaxanes formed by polyethylene glycol and αCD [65]. For α and βCDs, the cyclodextrins alternate with typically a head-to-head and tail-to-tail arrangement. In contrast, no ordered sequence is found in γCD columns, due to the larger size and lower rigidity of the macrocycle [103]. Moreover, these columnar arrangement of cyclodextrin is also found in native, aqueous solutions of α and γ-cyclodextrins [106,107].

For the case of CD/surfactant inclusion complexes, only channel type arrangement of cyclodextrins were reported, regardless of the cavity size of the CD. Despite α, β, and γCD inclusion complexes present the same vertical lattice type (although γCDs do not regularly alternate with primary-to-primary and secondary-to-secondary rim arrangements), they strongly differ in their lateral arrangement due to the different symmetries of the cyclodextrins. A schematic representation of the three typical lateral crystal structures is given in Fig. 6.

- The αCD, with its sixfold rotational symmetry, was shown to form crystalline structures with an hexagonal arrangement of channel-type complexes with $a = b = 2.7 \sim 2.8$ nm and $\gamma = 120^{\circ}$ [60,108,109].
- Inclusion complexes formed with βCDs were shown to crystallize with a rhomboid unit cell with $a = b = 1.52$ nm and $\gamma \approx 104^{\circ}$

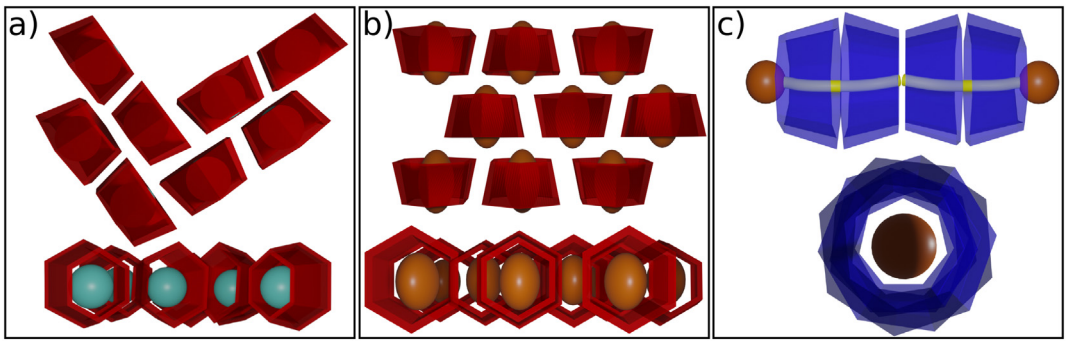

Fig. 5. Schematic representation of the three main vertical lattice types formed by cyclodextrin-inclusion complexes: (a) represents the cage-type; (b) represents the brick, or layer, type; and (c) the tubular, or columnar, type. For each case, the view perpendicular and parallel to the cyclodextrin rotational axis is provided. Sketches are not at scale.

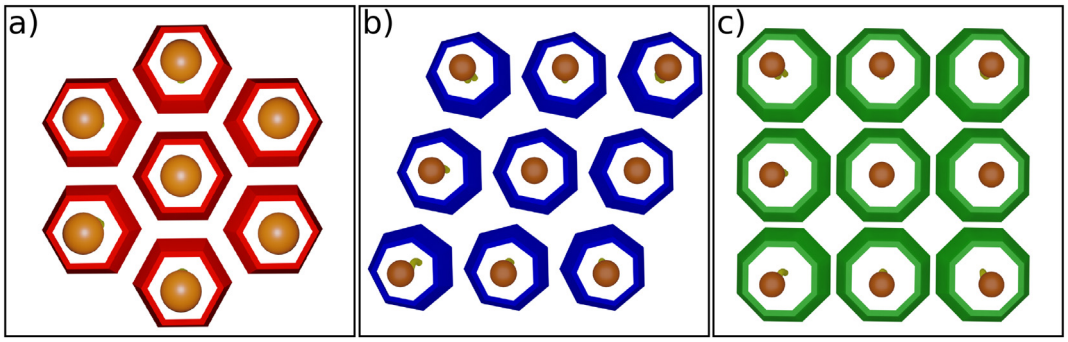

Fig. 6. Schematic representation of the typical lateral assembly found by columnar inclusion complexes formed by (a) αCDs with an hexagonal packing, (b) βCDs with a rhombic packing, and (c) γ-CDs with a square packing. Sketches are not at scale.

[94,96,98,99]. It is argued that this exotic value for γ derives from the seven-fold symmetry of the βCD.

- Finally, reports on crystal structures of γCDs/surfactant inclusion complexes are rare. However, due to the square symmetry of γCDs and due to the fact that γCD crystallize with small guests or alone in a square lattice with a = b = 2.4 nm and γ = 90° [110], supports the hypothesis that, when formed, crystal structures of γCDs/surfactant inclusion complexes exhibit a similar crystal unit cell.

After having reviewed the possible lattice structures in which surfactant and cyclodextrin inclusion complexes assemble, we focus on the ability of these systems to form colloidally stable suspensions presenting a crystalline substructure. The most studied systems are inclusion complexes formed with βCDs. In particular, the complex sodium dodecyl sulfate and βCD, with a 2:1 stoichiometry (SDS@2βCD), is the most extensive studied one [95,96,111–114]. The basic unit cell of the complex is made of two inclusion complexes, with the CDs in a tubular arrangement packed in a rhombic unit cell forming a bilayer. Depending on the sample concentration and temperature, these bilayers were shown to assemble in the uni- and multilamellar vesicles, multilayered coaxial cylinders, or regular polyhedra [95,96,112], as depicted in Fig. 7. Temperature is a particularly relevant parameter, as it weakens the CD-CD hydrogen bonds and strongly affect the structural phase behavior of SDS@2βCD [95,112]. A similar behavior is found in inclusion complexes between Tween 20, a polysorbate-type nonionic surfactant, and βCD (Tween20@2βCD), which similarly forms a 2:1 inclusion complex [90]. Such inclusion complex assembles into a bi-dimensional lattice, which, in dilute solutions (0.03–20 mM) organizes into vesicles and, in concentrated solutions (20–100 mM), into multi-lamellar flakes. A similar behavior was also reported for the inclusion complexes of βCDs with the nonionic poly (oxyethylene)nonylphenyl ether surfactant [115], cationic palmitoil triphenylphosphonium bromide or 1-[11-((Adamantane-1-carbonyl)oxy)undecyl]pyridinium bromide [97,116], as well as by the 1:1 complex of αCD and perfluorononanoic acid [117].

These results suggest that the lattice assembly is driven by three main factors, which are independent from the guest molecule: the high bending rigidity of the membranes, originating from the intramolecular interactions between adjacent cyclodextrins, the repulsion between the faces, either of steric or electrostatic nature and provided by the surfactant molecule, and the surface tension at the edges of the membrane, pushing towards the formation of closed structures [113].

A clear similarity between the colloidal assembly of the cyclodextrin/surfactant inclusion complexes with the self-assembly of proteins, e.g., in filaments or microtubes, or in viral capsids can be drawn [118]. For instance, the capsid elements are hold together by specific, directional interactions between the different protein units and with unspecific, mostly electrostatic interactions with the genetic material they carry [119].

The supramolecular assemblies of cyclodextrins and surfactants feature characteristic sizes which range from few Angstrom, the size of a single CD building block, to several μm. Accordingly, for a comprehensive characterization, a broad suite of instruments is required. Typical techniques are small-angle neutron and X-ray scattering [63,92,95,96,120,121], X-ray diffraction [95,98], Nuclear magnetic resonance [97,110], and imagining techniques such as transmission electron microscopy [96], optical microscopy [113], and atomic force microscopy [97,122].

Neutron and X-ray scattering are very powerful techniques to probe the structure of the CD complexes over a broad range of length scales. The techniques provide precise information about the size, volume, molecular weight and shape of single molecules, but also of multi-component macromolecular complexes. Both small-angle neutron and x-ray scattering are applied to the characterization of amphiphiles, CDs, and their complexes [95,120]. X-ray scattering offers the advantage of high resolution and high brilliance, essential for time-resolved and high-resolution experiments [98,113]. In contrast, neutrons offer an excellent sensitivity towards hydrogen atoms in addition to the possibility of isotopic labelling certain elements of the complex [123].

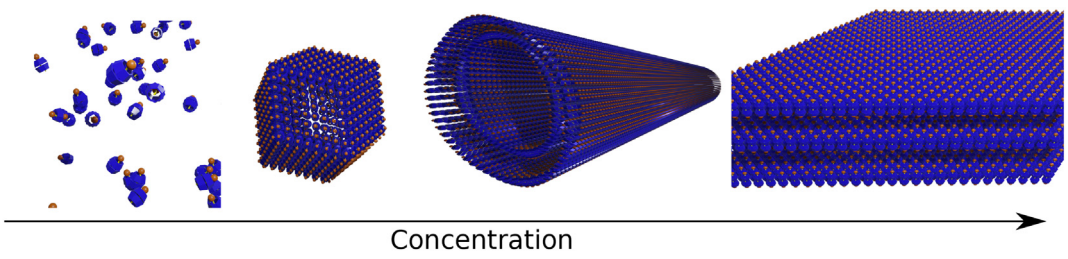

Fig. 7. Lattice supramolecular assemblies formed by 2:1 complexes of different surfactant and β-CD, schematically drawn as a function of concentration: in the dilute regime, no supramolecular assembly takes place; in semi-dilute regions, the formation of regular polyhedra or vesicles is observed; at high concentrations the inclusion complexes form concentric long cylinders; and at very high concentration the stack of bilayers has been reported. Sketches are not at scale.

Imaging techniques, such as cryo-transmision electron microscopy (Cryo-TEM), or scanning electron microscopy (SEM) offers a direct image of the supramolecular structure [90,115], highlighting small details, such as the presence of pores at the vertices of rhombic dodecahedra in the SDS@2βCD systems [96].

Nuclear magnetic resonance is also a valuable tool for the structural characterization of these complex inclusion complexes, as 2D NMR spectra can provide information on the spacial vicinity of the different functional groups, allowing to precisely resolve the relative position of host and guest molecules [90,97,124].

In addition of being highly interesting from a fundamental science perspective, colloidal assemblies formed by surfactants and cyclodextrins bear a high applicative value, for instance in the fields of drug delivery, food industry and cultural heritage [125]. The interest mostly arises from the responsive properties and the high biodegradability and low toxicity of the components, as well as the reversible stimuli responsive behavior. The spontaneously formed aggregates can in fact be used to confine and deliver specific cargos. For instance, SDS and βCD microtubes can be loaded with colloidal spheres, offering a simple approach for confining and releasing 100 nm-sized particles [111]. Similarly, light-responsive complexes can be used to release drug molecules upon irradiation [126]. The stimuli-responsive assembly behavior was further exploited to formulate responsive hydrogels [48,97,127].

4. Conclusions and perspectives

In this brief review, the importance of understanding the CD/surfactant threading process as well as the lattice assembly of the inclusion complexes have been stressed. The characteristics and dimensional compatibility of host and guest molecules anticipate the thermodynamics of the inclusion complexation processes. The size and the structured water of the cyclodextrin's cavity, the surfactants's alkyl chain length and head group strongly influence the energy quantities of complexes formation and their stability. Moreover, the spontaneous aggregation behavior of the inclusion complexes was described with a multiscale approach: starting from the lateral and vertical arrangement of the inclusion complexes, an overview of the large scale colloidal assembly into tubular, vesicular, or layered structures is provided.

Despite the fact that mixtures of surfactants and cyclodextrins have been under investigation for over sixty years [128], the topic is exhibiting a renaissance in the last years. This renewed interest is in part due to the discovery that surfactant/cyclodextrin inclusion complexes can spontaneously assembly in highly hierarchical structures, resulting from the interplay of numerous, short and long-range, specific and non-specific, as well as highly directional and non-directional forces. Significant efforts have been made to shade light on the mechanism underlying the formation of μm-sized tubes, vesicles, or polyhedra [113], but the overall details governing the lattice assembly remain still elusive. Clearly, further efforts are needed to improve our understanding and control of the lattice assembly of surfactant/CD inclusion complexes. The understanding of this process, in addition to satisfying the mere scientific curiosity, is essential for the design of mechanically robust capsules and carries, with remarkable analogies to viral proteic capsids, for a different purposes, e.g., drug delivery, nanoreactors, etc.

The studies made so far, where mostly focused on the characterization of self-assembled systems of surfactant and CDs, and their responsive to temperature has been probed. A certain degree of stimuli-responsive behavior was studied upon addition to the system of α-amylase, which opens the CD ring destroying the inclusion complex [129,130], by illuminating surfactant inclusion complexes bearing a light responsive group [97,131] or by changing the electrochemical potential of solutions contaning redox-responsive surfactants [122]. Extending the studies to inclusion complexes with stimuli responsive surfactants, i.e., towards pH, light, or specific chemical compounds, would allow for a facile control the properties of the supramolecular assemblies in a reversible fashion.

Admixing to the supramolecular assemblies of surfactant/CD inclusion complexes a macromolecule, with tunable interaction with the surfactant, would further allow for extending the range of hierarchical structures in the systems. Keeping in mind that the reversibility and responsiveness arises in the system when the different interaction forces involved are close to thermal energy and similar between each other.

Declaration of Competing Interest

The authors declare that they have no known competing financial interests or personal relationships that could have appeared to influence the work reported in this paper.

Acknowledgements

L.S.S.A. is grateful to the ILL and the University of Palermo for a doctoral fellowship through the ILL Ph.D. programme.

References

[1] Grzelczak M, Liz-Marzán LM, Klajn R. Stimuli-responsive self-assembly of nanoparticles. Chem Soc Rev. 2019;48:1342–61.
[2] Seeman NC, Sleiman HF. DNA nanotechnology. Nat Rev Mater. 2018;3:17068.
[3] Whitesides GM, Grzybowski B. Self-assembly at all scales. Science (80-). 2002;295:2418–21.
[4] Geng WC, Sessler JL, Guo DS. Supramolecular prodrugs based on host-guest interactions. Chem Soc Rev. 2020;49:2303–15.
[5] Szejtli J. Past, present, and future of cyclodextrin research. Pure Appl Chem. 2004;76:1825–45.
[6] Valente AJ, Söderman O. The formation of host-guest complexes between surfactants and cyclodextrins. Adv Colloid Interface Sci. 2014;205:156–76.
[7] Sabadini E, Cosgrove T, Egídio FDC. Solubility of cyclomaltooligosaccharides (cyclodextrins) in H2O and D2O: a comparative study. Carbohydr Res. 2006;341:270–4.
[8] Raffaini G, Ganazzoli F. Hydration and flexibility of α-, β-, γ- and δ-cyclodextrin: a molecular dynamics study. Chem Phys. 2007;333:128–34.
[9] Jacob S, Nair AB. Cyclodextrin complexes: perspective from drug delivery and formulation. Drug Dev Res. 2018;79:201–17.
[10] Davis ME, Brewster ME. Cyclodextrin-based pharmaceutics: past, present and future. Nat Rev Drug Discov. 2004;3:1023–35.
[11] Kfoury M, Auezova L, Greige-Gerges H, Fourmentin S. Cyclodextrins for essential oils applications. Cyclodext. Appl. Med. Food, Environ. Liq. Cryst. Springer International Publishing; 2018. p. 81–123.
[12] Lazzara G, Milioto S. Copolymer-cyclodextrin inclusion complexes in water and in the solid state. A physico-chemical study. J Phys Chem B. 2008;112:11887–95.
[13] Tonelli AE. Nanostructuring and functionalizing polymers with cyclodextrins. Polymer (Guildf). 2008;49:1725–36.
[14] Murtaza G. Solubility enhancement of simvastatin: a review. Acta Pol Pharm Drug Res. 2012;69:581–90.
[15] Singh A, Worku ZA, Van Den Mooter G. Oral formulation strategies to improve solubility of poorly water-soluble drugs. Expert Opin Drug Deliv. 2011;8:1361–78.
[16] Loftsson T, Brewster ME. Cyclodextrins as functional excipients: methods to enhance complexation efficiency. J Pharm Sci. 2012;101:3019–32.
[17] Buschmann HJ, Schollmeyer E. Applications of cyclodextrins in cosmetic products: a review. J Cosmet Sci. 2002;53:185–91.
[18] Santos AC, Morais F, Simões A, Pereira I, Sequeira JA, Pereira-Silva M, et al. Nanotechnology for the development of new cosmetic formulations. Expert Opin Drug Deliv. 2019;16:313–30.
[19] Wang J, Liu L, Chen J, Deng M, Feng X, Chen L. Supramolecular nanoplatforms via cyclodextrin host-guest recognition for synergistic gene-photodynamic therapy. Eur Polym J. 2019;118:222–30.
[20] Astray G, Mejuto JC, Morales J, Rial-Otero R, Simal-Gándara J. Factors controlling flavors binding constants to cyclodextrins and their applications in foods. Food Res Int. 2010;43:1212–8.
[21] Chen J, Huo Y, Li S, Huang Y, Lv S. Host-guest complexes of β-cyclodextrin with methyl orange/methylene blue-derived multi-heteroatom doped carbon materials for supercapacitors. Compos Commun. 2019;16:117–23.
[22] Wang Y, Ning G, Wu Y, Wu S, Zeng B, Liu G, et al. Facile combination of beta-cyclodextrin host-guest recognition with exonuclease-assistant signal amplification for sensitive electrochemical assay of ochratoxin a, Biosens. Bioelectron. 2019;124-125:82–8.
[23] Amiel C, Galant C, Auvray L. Ternary complexes involving a β-cyclodextrin polymer, a cationic surfactant and an anionic polymer. Prog Colloid Polym Sci. 2004;126:44–6.
[24] Galant C, Amiel C, Auvray L. Ternary complex formation in aqueous solution between a β-cyclodextrin polymer, a cationic surfactant and DNA. Macromol Biosci. 2005;5:1057–65.

[25] Liu K, Ma C, Wu T, Qi W, Yan Y, Huang J. Recent advances in assemblies of cyclodextrins and amphiphiles: construction and regulation. Curr Opin Colloid Interface Sci. 2020;45:44–56.
[26] Zhu H, Shangguan L, Shi B, Yu G, Huang F. Recent progress in macrocyclic amphiphiles and macrocyclic host-based supra-amphiphiles. Mater Chem Front. 2018; 2:2152–74.
[27] Liu L, Guo QX. The driving forces in the inclusion complexation of cyclodextrins. J Incl Phenom. 2002;42:1–14.
[28] Briggner LE, Wadsö I. Heat capacities of maltose, maltotriose, maltotetrose and α-, β-, and γ-cyclodextrin in the solid state and in dilute aqueous solution. J Chem Thermodyn. 1990;22:1067–74.
[29] Pereva S, Nikolova V, Angelova S, Spassov T, Dudev T. Water inside β-cyclodextrin cavity: amount, stability and mechanism of binding, Beilstein. J Org Chem. 2019; 15:1592–600.
[30] Sandilya AA, Natarajan U, Priya MH. Molecular view into the Cyclodextrin cavity: structure and hydration. ACS Omega. 2020;5:25655–67.
[31] Bouchemal K, Mazzaferro S. How to conduct and interpret ITC experiments accurately for cyclodextrin-guest interactions. Drug Discov Today. 2012;17:623–9.
[32] Iza N, Guerrero-Martínez A, Tardajos G, Ortiz MJ, Palao E, Montoro T, et al. Using inclusion complexes with cyclodextrins to explore the aggregation behavior of a ruthenium metallosurfactant. Langmuir. 2015;31:2677–88.
[33] Nagaraj K, Arunachalam S. Synthesis, CMC determination and influence of the micelles, β-cyclodextrin, ionic liquids and liposome(dipalmitoylphosphatidylcholine) vesicles on the kinetics of an outer-sphere electron transfer reaction. J Incl Phenom Macrocycl Chem. 2014;79:425–35.
[34] García-Río L, Méndez M, Paleo MR, Sardina FJ. New insights in cyclodextrin: surfactant mixed systems from the use of neutral and anionic cyclodextrin derivatives. J Phys Chem B. 2007;111:12756–64.
[35] Vargas C, Schönbeck C, Heimann I, Keller S. Extracavity effect in Cyclodextrin/surfactant complexation. Langmuir. 2018;34:5781–7.
[36] Dodziuk H. Cyclodextrins and Their Complexes: Chemistry, Analytical Methods, Applications. Wiley Online Library; 2006.
[37] Benko M, Király Z. Thermodynamics of inclusion complex formation of β-cyclodextrin with a variety of surfactants differing in the nature of headgroup. J Chem Thermodyn. 2012;54:211–6.
[38] Martin JV, Turmine M, Letellier P, Hemery P. Study of β-Cyclodextrin / Dodecyltrimethylammonium bromide complex into water-isopropanol mixtures. Electrochim Acta. 1995;40:2749–53.
[39] Okubo T, Kitano H, Ise N. Conductometric studies on association of cyclodextrin with colloidal electrolytes. J Phys Chem. 1976;80:2661–4.
[40] Rafati AA, Safatian F. Thermodynamic studies of inclusion complex between cetyltrimethylammonium bromide (CTAB) and β-cyclodextrin (β-CD) in water/ n-butanol mixture, using potentiometric technique. Phys Chem Liq. 2008;46: 587–98.
[41] Martín VI, López-Cornejo P, López-López M, Blanco-Arévalo D, Moreno-Vargas AJ, Angulo M, et al. Influence of the surfactant degree of oligomerization on the formation of cyclodextrin: surfactant inclusion complexes, Arab. J Chem. 2020;13: 2318–30.
[42] Nilsson M, Valente AJ, Olofsson G, Söderman O, Bonini M. Thermodynamic and kinetic characterization of host-guest association between bolaform surfactants and α- and β-cyclodextrins. J Phys Chem B. 2008;112:11310–6.
[43] Ondo D, Costas M. Complexation thermodynamics of α-cyclodextrin with ionic surfactants in water. J Colloid Interface Sci. 2017;505:445–53.
[44] Rekharsky MV, Inoue Y. Complexation thermodynamics of cyclodextrins. Chem Rev. 1998;98:1875–917.
[45] Jiang L, Yan Y, Huang J. Versatility of cyclodextrins in self-assembly systems of amphiphiles. Adv Colloid Interface Sci. 2011;169:13–25.
[46] Funasaki N, Ishikawa S, Neya S. Proton NMR study of α-cyclodextrin inclusion of short-chain surfactants. J Phys Chem B. 2003;107:10094–9.
[47] Funasaki N, Ishikawa S, Neya S. 1:1 and 1:2 complexes between long-chain surfactant and a-cyclodextrin studied by NMR. J Phys Chem B. 2004;108:9593–8.
[48] Shen J, Song L, Xin X, Wu D, Wang S, Chen R, et al. Self-assembled supramolecular hydrogel induced by β-cyclodextrin and ionic liquid-type imidazolium gemini surfactant. Colloids Surfaces A Physicochem Eng Asp. 2016;509:512–20.
[49] De Lisi R, Lazzara G, Milioto S, Muratore N. Characterization of the Cyclodextrin-surfactant interactions by volume and enthalpy. J Phys Chem B. 2003;107: 13150–7.
[50] Wiseman T, Williston S, Brandts JF, Lin LN. Rapid measurement of binding constants and heats of binding using a new titration calorimeter. Anal Biochem. 1989;179:131–7.
[51] Poon GMK. Probing solution thermodynamics by microcalorimetry. In: Pirajᾶn JCM, editor. Thermodyn. - interact. Stud. - solids, Liq. Gases. InTech; 2011. p. 871–90.
[52] Loh W, Brinatti C, Tam KC. Use of isothermal titration calorimetry to study surfactant aggregation in colloidal systems. Biochim Biophys Acta - Gen Subj. 2016;1860: 999–1016.
[53] Moulik SP, Mitra D. Amphiphile self-aggregation: An attempt to reconcile the agreement-disagreement between the enthalpies of micellization determined by the van't Hoff and calorimetry methods. J Colloid Interface Sci. 2009;337:569–78.
[54] Tellinghuisen J. Van't Hoff analysis of K (T): How good...or bad? Biophys Chem. 2006;120:114–20.
[55] Schmidtchen FP. Isothermal titration calorimetry in supramolecular chemistry. In: Schalley CA, editor. Anal. Methods Supramol. Chem. 2nd ed. Wiley; 2007. p. 55–78. https://doi.org/10.1002/9783527610273.ch3.
[56] Bouchemal K, Couvreur P, Daoud-Mahammed S, Poupaert J, Gref R. A comprehensive study on the inclusion mechanism of benzophenone into supramolecular nanoassemblies prepared using two water-soluble associative polymers. J Therm Anal Calorim. 2009;98:57–64.
[57] Lee B. Enthalpy-entropy compensation in the thermodynamics of hydrophobicity. Biophys Chem. 1994;51:271–8.
[58] Sharp K. Entropy – enthalpy compensation : fact or artifact ? Protein Sci. 2001;10: 661–7.
[59] Cooper A, Johnson CM, Lakey JH, Nöllmann M. Heat does not come in different colours: entropy-enthalpy compensation, free energy windows, quantum confinement, pressure perturbation calorimetry, solvation and the multiple causes of heat capacity effects in biomolecular interactions. Biophys Chem. 2001;93:215–30.
[60] Brocos P, Díaz-Vergara N, Banquy X, Pérez-Casas S, Costas M, Piñeiro Á. Similarities and differences between cyclodextrin-sodium dodecyl sulfate host-guest complexes of different stoichiometries: molecular dynamics simulations at several temperatures. J Phys Chem B. 2010;114:12455–67.
[61] Topchieva I, Karezin K. Self-assembled supramolecular micellar structures based on non-ionic surfactants and cyclodextrins. J Colloid Interface Sci. 1999;213:29–35.
[62] Popova EI, Topchieva IN. Complex formation between polyethylene oxide-containing nonionic surfactants and α-and β-cyclodextrins. Russ Chem Bull. 2001;50:620–5.
[63] Saito Y, Ueda H, Abe M, Sato T, Christian SD. Inclusion complexation of triton X-100 with α-,β- and γ- cyclodextrins. Colloids Surfaces A Physicochem Eng Asp. 1998; 135:103–8.
[64] Turco Liveri V, Cavallaro G, Giammona G, Pitarresi G, Puglisi G, Ventura C. Calorimetric investigation of the complex formation between surfactants and α-, β- and γ-cyclodextrins. Thermochim Acta. 1992;199:125–32.
[65] Harada A, Li J, Kamachi M. The molecular necklace: a rotaxane containing many threaded α-cyclodextrins. Nature. 1992;356:325–7.
[66] Mahata A, Bose D, Ghosh D, Jana B, Bhattacharya B, Sarkar D, et al. Studies of triton X-165-β-cyclodextrin interactions using both extrinsic and intrinsic fluorescence. J Colloid Interface Sci. 2010;347:252–9.
[67] Wilson LD, Verrall RE. A volumetric study of β-cyclodextrin/hydrocarbon and β-cyclodextrin/fluorocarbon surfactant inclusion complexes in aqueous solutions. J Phys Chem B. 1997;101:9270–9.
[68] BenkÅ M, Tabajdi R, Király Z. Thermodynamics of formation of β-cyclodextrin inclusion complexes with four series of surfactant homologs. J Therm Anal Calorim. 2013;112:969–76.
[69] Petek A, Krajnc M, Petek A. Study of host–guest interaction between ß-cyclodextrin and alkyltrimethylammonium bromides in water. J Incl Phenom Macrocycl Chem. 2016;86:221–9.
[70] Rafati AA, Bagheri A, Iloukhani H, Zarinehzad M. Study of inclusion complex formation between a homologous series of n-alkyltrimethylammonium bromides and β-cyclodextrin, using conductometric technique. J Mol Liq. 2005;116:37–41.
[71] Luviano AS, Hernández-Pascacio J, Ondo D, Campbell RA, Piñeiro Á, Campos-Terán J, et al. Highly viscoelastic films at the water/air interface: α-Cyclodextrin with anionic surfactants. J Colloid Interface Sci. 2020;565:601–13.
[72] Gharibi H, Jalili S, Rajabi T. Electrochemical studies of interaction between ceyltrimethylammonium bromide and α-, β-cyclodextrins at various temperature. Colloids Surfaces A Physicochem Eng Asp. 2000;175:361–9.
[73] Prochowicz D, Kornowicz A, Lewiński J. Interactions of native Cyclodextrins with metal ions and inorganic nanoparticles: fertile landscape for chemistry and materials science. Chem Rev. 2017;117:13461–501.
[74] Sammalkorpi M, Karttunen M, Haataja M. Structural properties of ionic detergent aggregates: a large-scale molecular dynamics study of sodium dodecyl sulfate. J Phys Chem B. 2007;111:11722–33.
[75] Machperson Y, Palepu R, Reinsborough V. Counterion binding by surfactant /β-Cyclodextrin inclusion complexes. J Incl Phenom Mol Recognit Chem. 1990;9: 137–43.
[76] Junquera E, Peña L, Aicart E. A Conductimetric study of the interaction of β-Cyclodextrin or Hydroxypropyl-β-cyclodextrin with Dodecyltrimethylammonium bromide in water solution. Langmuir. 1995;11:4685–90.
[77] Guerrero-Martínez A, González-Gaitano G, Viñas MH, Tardajos G. Inclusion complexes between β-cyclodextrin and a gemini surfactant in aqueous solution: An NMR study. J Phys Chem B. 2006;110:13819–28.
[78] Cabaleiro-Lago C, Nilsson M, Söderman O. Self-diffusion NMR studies of the host-guest interaction between β-cyclodextrin and alkyltrimethylammonium bromide surfactants. Langmuir. 2005;21:11637–44.
[79] Wimmer R, Aachmann FL, Larsen KL, Petersen SB. NMR diffusion as a novel tool for measuring the association constant between cyclodextrin and guest molecules. Carbohydr Res. 2002;337:841–9.
[80] Palepu R, Richardson JE, Reinsborough C. Binding constants of β-Cyclodextrin/ surfactant inclusion by conductivity measurements. Langmuir. 1989;5:218–21.
[81] Palepu R, Reinsborough C. Surfactant-cyclodextrin interactions by conductance measurements. Can J Chem. 1988;66:325–8.
[82] de Miranda TM, de Oliveira AR, Pereira JR, da Silva JG, Lula IS, Nascimento CS, et al. Inclusion vs. micellization in the cethylpyridine chloride / β-cyclodextrin system: a structural and thermodynamic approach. J Mol Struct. 2019;1184:289–97.
[83] Martín VI, Ostos FJ, Angulo M, Márquez AM, López-Cornejo P, López-López M, et al. Host-guest interactions between cyclodextrins and surfactants with functional groups at the end of the hydrophobic tail. J Colloid Interface Sci. 2017;491:336–48.
[84] Li G, Ma H, Hao J. Surfactant ion-selective electrodes: a promising approach to the study of the aggregation of ionic surfactants in solution. Soft Matter. 2012;8: 896–909.
[85] Patil SR, Turmine M, Peyre V, Durand G, Pucci B. Study of β-cyclodextrin/ fluorinated trimethyl ammonium bromide surfactant inclusion complex by fluorinated surfactant ion selective electrode. Talanta. 2007;74:72–7.

[86] Funasaki N, Nagaoka M, Hirota S. Competitive potentiometric determination of binding constants between α-cyclodextrin and 1-alkanols. Anal Chim Acta. 2005; 531:147–51.
[87] Mura P. Analytical techniques for characterization of cyclodextrin complexes in aqueous solution: a review. J Pharm Biomed Anal. 2014;101:238–50.
[88] He Y, Shen X, Gao H, He Y. Spectral and photophysical studies on the inclusion complexation between triton X-100 and β-cyclodextrin: a competitive method using a substituted 3H-indole probe. J Photochem Photobiol A Chem. 2008;193: 178–86.
[89] García-Río L, Godoy A. Use of spectra resolution methodology to investigate surfactant/β- cyclodextrin mixed systems. J Phys Chem B. 2007;111:6400–9.
[90] Zhou C, Cheng X, Zhao Q, Yan Y, Wang J, Huang J. Self-assembly of nonionic surfactant tween 20@2β-CD inclusion complexes in dilute solution. Langmuir. 2013;29: 13175–82.
[91] González-Gaitano G, Crespo A, Tardajos G. Thermodynamic investigation (volume and compressibility) of the systems β-Cyclodextrin + n-Alkyltrimethylammonium bromides + water. J Phys Chem B. 2000;104:1869–79.
[92] Lazzara G, Prevost S, Gradzielski M. Selectivity of cyclodextrins as a parameter to tune the formation of pseudorotaxanes and micelles supramolecular assemblies. A systematic SANS study. Soft Matter. 2011;7:6082–91.
[93] Xing H, Lin SS, Yan P, Xiao JX. Demicellization of a mixture of cationic-anionic hydrogenated/fluorinated surfactants through selective inclusion by α- and β-cyclodextrin. Langmuir. 2008;24:10654–64.
[94] Wu C, Xie Q, Xu W, Tu M, Jiang L. Lattice self-assembly of cyclodextrin complexes and beyond. Curr Opin Colloid Interface Sci. 2019;39:76–85.
[95] Ouhajji S, Landman J, Prévost S, Jiang L, Philipse AP, Petukhov AV. In situ observation of self-assembly of sugars and surfactants from nanometres to microns. Soft Matter. 2017;13:2421–5.
[96] Yang S, Yan Y, Huang J, Petukhov AV, Kroon-Batenburg LM, Drechsler M, et al. Giant capsids from lattice self-assembly of cyclodextrin complexes. Nat Commun. 2017; 8:1–7.
[97] Wang J, Yao M, Li Q, Yi S, Chen X. β-Cyclodextrin induced hierarchical self-assembly of a cationic surfactant bearing an adamantane end group in aqueous solution. Soft Matter. 2016;12:9641–8.
[98] Makedonopoulou S, Mavridis IM. Structure of the inclusion complex of β-cyclodextrin with 1,12-dodecanedioic acid using synchrotron radiation data; a detailed dimeric β-cyclodextrin structure. Acta Crystallogr Sect B Struct Sci. 2000;56: 322–31.
[99] Jiang L, Peng Y, Yan Y, Deng M, Wang Y, Huang J. "Annular ring" microtubes formed by SDS@2β-CD complexes in aqueous solution. Soft Matter. 2010;6:1731–6.
[100] Fajalia AI, Antoniou E, Alexandridis P, Tsianou M. Self-assembly of sodium bis(2-ethylhexyl) sulfosuccinate in aqueous solutions: modulation of micelle structure and interactions by cyclodextrins investigated by small-angle neutron scattering. J Mol Liq. 2015;210:125–35.
[101] Carlstedt J, Bilalov A, Krivtsova E, Olsson U, Lindman B. Cyclodextrin-surfactant coassembly depends on the cyclodextrin ability to crystallize. Langmuir. 2012;28: 2387–94.
[102] Saenger W. Crystal packing patterns of cyclodextrin inclusion complexes. J Incl Phenom. 1984;2:445–54.
[103] Saenger W, Steiner T. Cyclodextrin inclusion complexes: host-guest interactions and hydrogen-bonding networks. Acta Crystallogr Sect A Found Crystallogr. 1998;A54:798–805.
[104] Aree T, Schulz B, Reck G. Crystal structures of β-cyclodextrin complexes with formic acid and acetic acid. J Incl Phenom. 2003;47:39–45.
[105] Wenz G, Han BH, Müller A. Cyclodextrin rotaxanes and polyrotaxanes. Chem Rev. 2006;106:782–817.
[106] Hunt MA, Rusa CC, Tonelli AE, Balik CM. Structure and stability of columnar cyclomaltohexaose (α- cyclodextrin) hydrate. Carbohydr Res. 2004;339:2805–10.
[107] Hunt MA, Rusa CC, Tonelli AE, Balik CM. Structure and stability of columnar cyclomaltooctaose (γ- cyclodextrin) hydrate. Carbohydr Res. 2005;340:1631–7.
[108] Rodríquez-Llamazares S, Yutronic N, Jara P, Englert U, Noyong M, Simon U. The structure of the first supramolecular α-cyclodextrin complex with an aliphatic monofunctional carboxylic acid, European. J Org Chem. 2007:4298–300.
[109] Takeo K, Kuge T. Complexes of starchy materials with organic compounds. Agric Biol Chem. 1970;34:1787–94.
[110] Lindner K, Saenger W. Crystal structure of the γ-cyclodextrin n-propanol inclusion complex: correlation of α-, β-, γ-cyclodextrin geometries. Biochem Biophys Res Commun. 1980;92:933–8.
[111] Jiang L, De Folter JW, Huang J, Philipse AP, Kegel WK, Petukhov AV. Helical colloidal sphere structures through thermo-reversible co-assembly with molecular microtubes. Angew Chem Int Ed. 2013;52:3364–8.
[112] Zhou C, Cheng X, Yan Y, Wang J, Huang J. Reversible transition between SDS@2β-CD microtubes and vesicles triggered by temperature. Langmuir. 2014;30:3381–6.
[113] Landman J, Ouhajji S, Prévost S, Narayanan T, Groenewold J, Philipse AP, et al. Inward growth by nucleation: multiscale self-assembly of ordered membranes. Sci Adv. 2018;4:1–8.
[114] Wang H, Chen W, Wagner JC, Xiong W. Local ordering of lattice self-assembled SDS@2β-CD materials and adsorbed water revealed by vibrational sum frequency generation microscope. J Phys Chem B. 2019;123:6212–21.
[115] Guerrero-Martínez A, Ávila D, Martínez-Casado FJ, Ripmeester JA, Enright GD, Cola LD, et al. Solid crystal network of self-assembled Cyclodextrin and nonionic surfactant Pseudorotaxanes. J Phys Chem B. 2010;114:11489–95.
[116] Li S, Xing P, Hou Y, Yang J, Yang X, Wang B, et al. Formation of a sheet-like hydrogel from vesicles via precipitates based on an ionic liquid-based surfactant and β-cyclodextrin. J Mol Liq. 2013;188:74–80.
[117] Zhang J, Yang Z, Zhang H, Hua Z, Hu X, Liu C, et al. Hydrogels consisting of vesicles constructed via the self-assembly of a supermolecular complex formed from α-Cyclodextrin and Perfluorononanoic acid. Langmuir. 2019;35:16893–9.
[118] Yang L, Liu A, Cao S, Putri RM, Jonkheijm P, Cornelissen JJ. Self-assembly of proteins: towards supramolecular materials. Chem - A Eur J. 2016;22:15570–82.
[119] Zandi R, Reguera D. Mechanical properties of viral capsids. Phys Rev E - Stat Nonlinear Soft Matter Phys. 2005;72:21917.
[120] Tsianou M, Fajalia AI. Cyclodextrins and surfactants in aqueous solution above the critical micelle concentration: where are the cyclodextrins located? Langmuir. 2014;30:13754–64.
[121] Alami E, Abrahmsén-Alami S, Eastoe J, Grillo I, Heenan RK. Interactions between a nonionic gemini surfactant and cyclodextrins investigated by small-angle neutron scattering. J Colloid Interface Sci. 2002;255:403–9.
[122] Zhang H, An W, Liu Z, Hao A, Hao J, Shen J, et al. Redox-responsive vesicles prepared from supramolecular cyclodextrin amphiphiles. Carbohydr Res. 2010;345:87–96.
[123] Krueger S. SANS provides unique information on the structure and function of biological macromolecules in solution. Phys B Condens Matter. 1998;241-243:1131–7.
[124] Narayanan G, Boy R, Gupta BS, Tonelli AE. Analytical techniques for characterizing cyclodextrins and their inclusion complexes with large and small molecular weight guest molecules. Polym Test. 2017;62:402–39.
[125] Dan Z, Cao H, He X, Zeng L, Zou L, Shen Q, et al. Biological stimuli-responsive cyclodextrin-based host-guest nanosystems for cancer therapy. Int J Pharm. 2015;483:63–8.
[126] Zhao Q, Wang Y, Yan Y, Huang J. Smart nanocarrier: self-assembly of bacteria-like vesicles with photoswitchable cilia. ACS Nano. 2014;8:11341–9.
[127] Zhang J, Shen X. Temperature-induced reversible transition between vesicle and supramolecular hydrogel in the aqueous ionic liquid-β-cyclodextrin system. J Phys Chem B. 2013;117:1451–7.
[128] Schlenk H, Sand DM. The association of α- and β-Cyclodextrins with organic acids. J Am Chem Soc. 1961;83:2312–20.
[129] Jiang L, Yan Y, Drechsler M, Huang J. Enzyme-triggered model self-assembly in surfactant-cyclodextrin systems. Chem Commun. 2012;48:7347–9.
[130] Kang Y, Cai Z, Tang X, Liu K, Wang G, Zhang X. An amylase-responsive Bolaform supra-Amphiphile. ACS Appl Mater Interfaces. 2016;8:4927–33.
[131] Wang Y, Ma N, Wang Z, Zhang X. Photocontrolled reversible supramolecular assemblies of an azobenzene-containing surfactant with α-cyclodextrin. Angew Chem Int Ed. 2007;46:2823–6.

Appendix B

Paper II: Hierarchical assembly of pH-responsive surfactant-cyclodextrin complexes

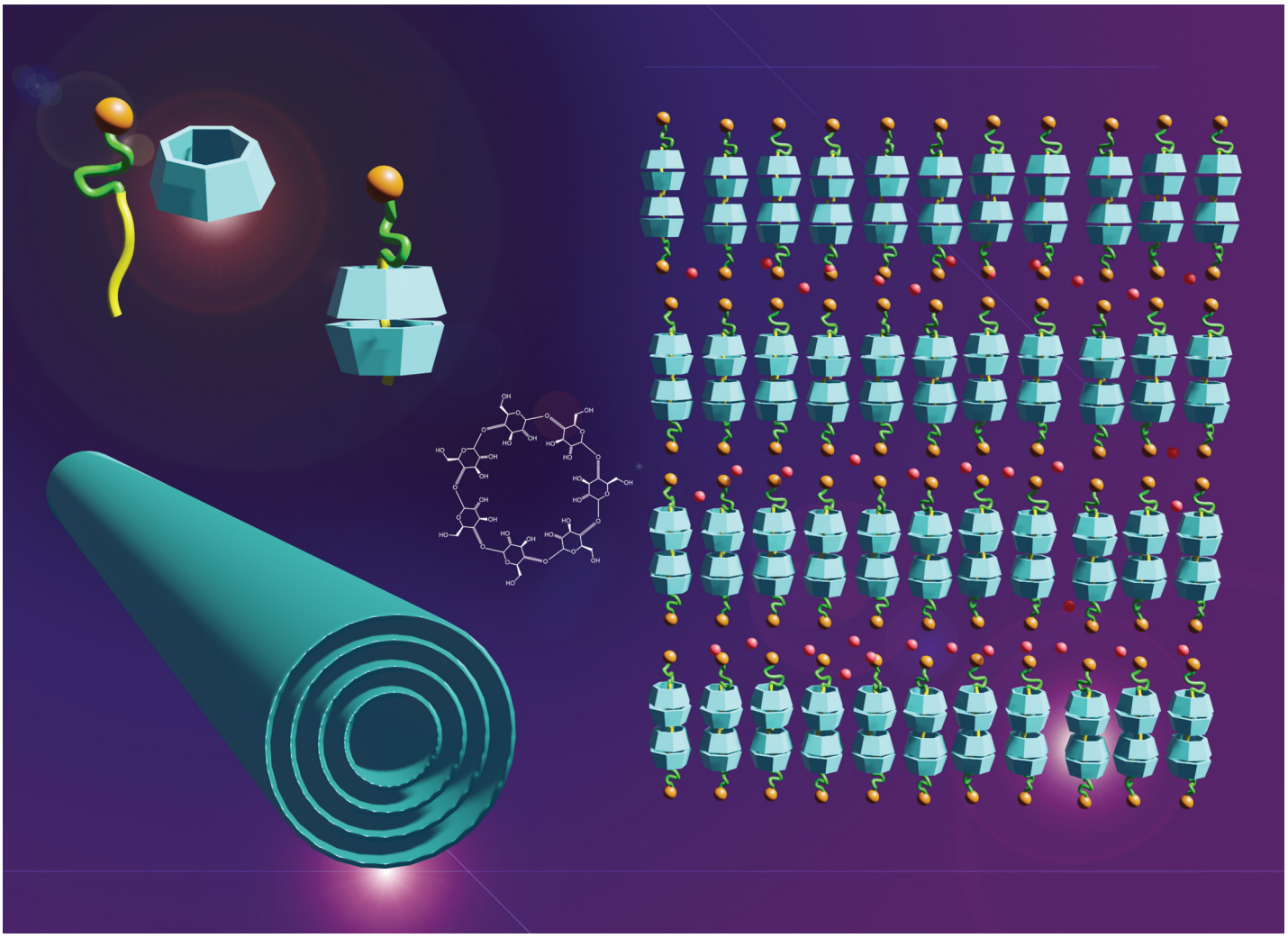

Highlighting research from the group of Dr Leonardo Chiappisi of the Partnership for Soft Condensed Matter at the Institut Laue–Langevin in Grenoble in collaboration with the University of Palermo.

Hierarchical assembly of pH-responsive surfactant–cyclodextrin complexes

We present the hierarchical assembly of cyclodextrins with pH-responsive surfactant into highly structured supramolecular assemblies, with typical length scales spanning several orders of magnitude. The spontaneously formed inclusion complexes crystallize in ordered lattices, which further organize into multilayered cylinders of several micrometers length.

As featured in:

See Leonardo Chiappisi *et al.*, *Soft Matter*, 2022, **18**, 6529.

ROYAL SOCIETY OF CHEMISTRY

rsc.li/soft-matter-journal

Registered charity number: 207890

Soft Matter

PAPER

View Article Online
View Journal | View Issue

Cite this: *Soft Matter*, 2022, **18**, 6529

Hierarchical assembly of pH-responsive surfactant–cyclodextrin complexes†

Larissa dos Santos Silva Araújo,[ab] Leah Watson,[b] Daouda A. K. Traore,[bc] Giuseppe Lazzara[a] and Leonardo Chiappisi*[b]

Received 17th June 2022,
Accepted 16th July 2022

DOI: 10.1039/d2sm00807f

rsc.li/soft-matter-journal

In this work, the inclusion complexes of alkyl ethoxy carboxylates with α-cyclodextrin (αCD) and β-cyclodextrin (βCD) were investigated. The thermodynamics of the complexation process was probed by isothermal titration calorimetry (ITC) and volumetry as a function of the degree of ionization of the surfactant. The complexation process was shown to be an enthalpically driven pH-independent process. For both types of cyclodextrins, the complexes were found to spontaneously self-assemble into highly-ordered supramolecular aggregates probed by small-angle neutron scattering and electron and optical microscopy. Herein, we report the formation of thin platelets for nonionized surfactant systems and equally spaced multilayered hollow cylinders for ionized systems in a hierarchical self-assembly process. In addition, the analysis allowed unveiling the effect of the number of ethylene oxides in the surfactants and the CD cavity size on the morphology of the aggregates. Finally, this study also highlights the importance of examining the tuning parameters' influence on the short and long-range interactions involved in the control of the assembly process.

1 Introduction

Cyclodextrins (CD) are a class of cyclic oligosaccharides formed through α(1–4) ether linkage glucopyranose units. The most common ones, α, β, and γCD are respectively formed by six, seven, and eight glucopyranose units. The truncated cone shape structure with a hydrophilic outer surface and a hydrophobic cavity, ranging from 5 to 8 Å, provide unique physicochemical properties to CDs, particularly the ability to form host–guest complexes.[1] The hydrophobic cavity, hydrophilic rims, the electron density, and the presence of the high-energy water in the cavity drive the assembly with a large range of different molecules, such as drugs,[2] polymers,[3–5] and surfactants,[6,7] affecting their properties.[8]

In turn, surfactant molecules and amphiphilic polymers self-assemble in aqueous solutions above a defined concentration. Admixing cyclodextrins to self-assembled copolymer aggregates generally leads to the disruption of the micelles when the hydrophobic moieties are complexed or to the formation of decorated micelles, when the hydrophilic part of the polymer is threaded.[9–11]

In contrast to the CD-induced disassembly of copolymer aggregates, highly ordered supramolecular complexes are found in mixtures with low molecular weight surfactants, such as sodium dodecyl sulfate,[12] polyoxyethylene sorbitol esters[13] and dodecyltrimethylammonium bromide.[14] In these mixtures, vesicles,[12,13] hydrogels,[15] fibers,[16] tubular and lamellar[17] structures have been reported, depending on the concentration, temperature, and mixing ratio. Such hierarchical assembly process is mainly governed by the intermolecular interactions between the cyclodextrins and the repulsive forces provided by the guest molecules. In addition, the importance of the water-mediated hydrogen-bonding network in the inclusion complexes' self-organization into ordered structures has been proven.[14,18,19] Up to now, however, systematic structural studies have been performed with either ionic or non-ionic surfactant complexes.

In contrast, this work deals with the investigation of inclusion complexes between α and βCD with the weakly anionic alkyl ethylene oxide carboxylic acids (AECs), whose carboxylic headgroup exhibits a pK_a of approx. 4.[20] The presence of terminal carboxylic group and ethylene oxide units (EO) in their molecules provide them pH and temperature responsiveness, respectively.[20]

Previous studies have shown that the nature of the surfactant has remarkably little impact on the supramolecular assembly of the inclusion complexes into bilayered structures, which is mainly governed by CD–CD interactions. In contrast, electrostatic

[a] *Dipartimento di Fisica e Chimica, Università degli Studi di Palermo, Viale delle Scienze pad 17, 90128, Palermo, Italy*
[b] *Institut Max von Laue – Paul Langevin, 71 Avenue des Martyrs, 38042, Grenoble, France. E-mail: chiappisil@ill.eu*
[c] *School of Life Sciences, Keele University, Staffordshire ST5 5BG, UK*

† Electronic supplementary information (ESI) available: Thermogravimetric analysis of CDs, additional phase diagrams, thermodynamic paramterers obtained from volumetric studies, additional small-angle neutron scattering data, additional microscopy data. See DOI: https://doi.org/10.1039/d2sm00807f

interactions determine the spacing and the ordering in multilayered aggregates.[21] The aim of this work is to systematically investigate the effect of the surfactant charge on the inclusion complex formation and self-assembly properties.

The use of a pH-responsive surfactant allows us, on the one hand, to systematically investigate the effect of the charge density on the supramolecular assembly of the complexes, and on the other hand, is expected to provide pH sensitivity to mixtures for applications in the field of cosmetics, drug delivery, and food science.[8]

In detail, we investigated the thermodynamics of the inclusion complexes formation between two alkyl ether carboxylic acids: the pentaoxyethylene dodecyl carboxylic acid ($C_{12}E_5Ac$) and the decacyloxyethylene dodecyl carboxylic acid ($C_{12}E_{10}Ac$), with αCD and βCD by isothermal titration calorimetry (ITC) and densitometry. The structural characterization of the supramolecular aggregates arising from their assembly was conducted by small-angle neutron scattering (SANS) and optical and electron microscopy. We probed the effect of the chemical architechture of surfactant and CD, as well as the mixing ratio of the components (Y = [CD]/[S]), total concentration, surfactant degree of ionization – defined as the sodium hydroxide and surfactant molar ratio (α = [NaOH]/[S_{tot}]) – on the formation of the inclusion complexes and the morphology of the structures arising from their assembly.

To the best of our knowledge, this study provides the first evidence of the pH-modulated assembly of the surfactant-CD inclusion complexes in different length scales, from the complexation to the assembly in higher magnitude supramolecular aggregates. Herein, the results presented open many possibilities for investigating the role of electrostatic interactions in the self-assembly process into supramolecular aggregates.

2 Experimental section

2.1 Materials

Pentaoxyethylene dodecyl carboxylic acid ($C_{12}E_5Ac$) and decacyloxyethylene dodecyl carboxylic acid ($C_{12}E_{10}Ac$) are technical surfactants provided by KAO chemicals under the trade names AKYPO RLM45CA (444 g mol^{-1}, 92% purity) and AKYPO RLM100 (686 g mol^{-1}, 90% purity), with 7.3 and 9.8 wt% water content, respectively, according to the producer. According to previous studies,[20,22] the hydrophobic part of the surfactants is a mixture (C_{12}, C_{14}, C_{16}) in approx. ratio 2 : 1 : 0.25. The ethylene oxide units (EO) are Gaussian distributed over a mean of 5 and 9 averaged distributions for AKYPO RLM45CA and AKYPO RLM100. αCD and βCD were purchased from TCI Europe. The water content of the cyclodextrins was determined from thermogravimetry, and it is 10.1 and 11.5 wt% for α and βCD, respectively. Sodium hydroxide (Fluka, puriss) was used to adjust the pH of the solutions. The water content in the reagents was considered for sample preparation. All chemicals mentioned were used as received. Solutions were prepared using Milli-Q water. Heavy water (D content > 99.8%) from Eurisotop (Gif-sur-Yvette, France) was used for the small-angle neutron scattering experiments.

2.2 Sample preparation

The samples were prepared by adding the cyclodextrin solution to the surfactant solution to obtain the desired concentrations in the samples at ambient conditions. Samples were allowed to stabilize for 24 hours.

2.3 Molecular weight determination

The molecular weight of the aggregates (M_w) was calculated using eqn (1) using the determined transmission values T recorded at wavelength λ = 633 nm on a Varian Cary 50 UV-vis spectrometer (PSCM, Grenoble, France). After the measurement, the samples were heated for one hour at 70 °C and let to cool down overnight before another set of measurements. The measurements were repeated after seven days.

$$M_w = -\frac{\ln T}{c \cdot l \cdot H_0} \quad (1)$$

with, T being the transmittance of the sample, l is the thickness of the cuvette, c, the total concentration of surfactant and cyclodextrin and, $H^0 = 32\pi^3 n_0^2 (dn/dc)^2/(3N_A\lambda^4)$, in which n_0 = 1.33, is the refractive index of the solvent, λ is the wavelength of light used, N_A is the Avogadro constant $dn/dc \approx 0.120$ cm^3 g^{-1} and $dn/dc \approx 0.186$ cm^3 g^{-1} as refractive index increments of surfactant and CD, respectively.[23,24]

The concentration of the surfactant was kept constant at 7 × 10^{-3} mol kg^{-1} and 4 × 10^{-3} mol kg^{-1} for αCD and βCD systems, respectively.

2.4 Densitometry

The apparent molar volume of the cyclodextrin in surfactant solution was determined using an Anton Paar oscillating tube density meter DMA 5000M (PSCM, Grenoble, France).

$$V_\Phi = \frac{M_w}{\rho} - \frac{10^3(\rho - \rho_0)}{m \cdot \rho \cdot \rho_0} \quad (2)$$

where, M_w, m, ρ, and ρ_0 are the molecular weight (g mol^{-1}) and the molality of the CD (mol kg^{-1}), and the density of the CD/surfactant solution (g cm^{-3}) and the corresponding surfactant solution (g cm^{-3}), respectively.

The volume of transfer of cyclodextrin from water to the surfactant solutions (ΔV^{CD}) was calculated by the difference between the apparent molar volume of the cyclodextrin in the samples ($V^{CD}_{\Phi,sample}$) and in water ($V^{CD}_{\Phi,water}$), *i.e.*, at zero surfactant concentration by

$$\Delta V^{CD} = V^{CD}_{\Phi,sample} - V^{CD}_{\Phi,water} \quad (3)$$

2.5 Isothermal titration calorimetry

Experiments were conducted in a Microcal VP-ITC (IBS, Grenoble, France) at 25 °C. Aliquots of the cyclodextrin solution were added to the reaction cell containing the surfactant solution. Measurements were carried out at pH 3, 4, and 5 in triplicate. Averaged ITC data of triplicates were analyzed.

2.6 Small-angle neutron scattering (SANS)

SANS patterns were recorded using 1 mm path quartz cells at *D*11,[25] and *D*22[26] at the Institut Laue–Langevin (Grenoble, France). At *D*11, with the wavelength of 6 Å ($\lambda/\Delta\lambda$ = 10%), three sample-detector configurations were used 1.4, 8 and 39 m and collimation of 5.5, 8 and 40.5 m, covering a q-range from 0.01 to 6 nm^{-1}, where $q = 4\pi \sin(\theta/2)/\lambda$. At *D*22, with a two ^{3}He detector setup, one fixed detector at 1.4 m sample-to-detector distance and, the second, used in two sample-to-detectors centre distance of 5.6 and 17.6 m distance with corresponding collimation of 5.6 and 17.6 m, covering a total q-range of 0.03 to 6 nm^{-1}.

2.7 Optical microscopy

For the observation of the aggregates' morphology, the samples were directly placed over a glass plate and examined using a BX61 Olympus (PSCM, Grenoble, France), in differential interference contrast (DIC) mode, and a Zeiss standard Polarized light Microscope (Olympus BX50) equipped with a camera CMOS.

2.8 Electron microscopy

For TEM, a small drop of sample was placed onto a copper TEM grid, and the excess was removed with filter paper. The sample was not stained. TEM observations were performed in a Tecnai12 Microscope operating at 120 kV (IBS, Grenoble, France). For Cryo-EM analysis, a few microliters of samples were placed onto a copper TEM grid, and the excess was removed using filter paper. Vitrification was conducted using a Vitrobot Mark IV (Thermo-Fisher Scientific) set to 10 °C and 100% humidity by plunging into liquid ethane. Image acquisition was performed on a FEI Talos Arctica TEM (200 kV).

3 Results and discussion

3.1 Phase behaviour

The goal of this study is to probe the interaction between the CDs and alkyl ether carboxylates and to explore the assembly behaviour as a function of the charge density α of the surfactant – defined as the ratio of added sodium hydroxide and surfactant molecules – and as a function of the surfactant/CD polymer ratio *Y*. Herewith, α defines the degree of ionization of the surfactant and the mixing ratio *Y* is a key parameter which controls the stoichiometry between host and guest. Experiments are performed at surfactant concentration approx. three orders of magnitude above the cmc, thus the interaction between CDs and micellized surfactant are being probed.

The assembly of the inclusion complexes between surfactants and cyclodextrins is characterized by the increase of the turbidity followed, in some cases, by the precipitation of white solids, as observed for other nonionic and ionic surfactants.[13,17] Aiming to understand the behaviour of those systems observing the mentioned parameters, the phase behaviour of the mixtures of each surfactant with αCD and βCD was investigated before and after being heated up to 70 °C for one hour and cooled at room temperature for 24 hours.

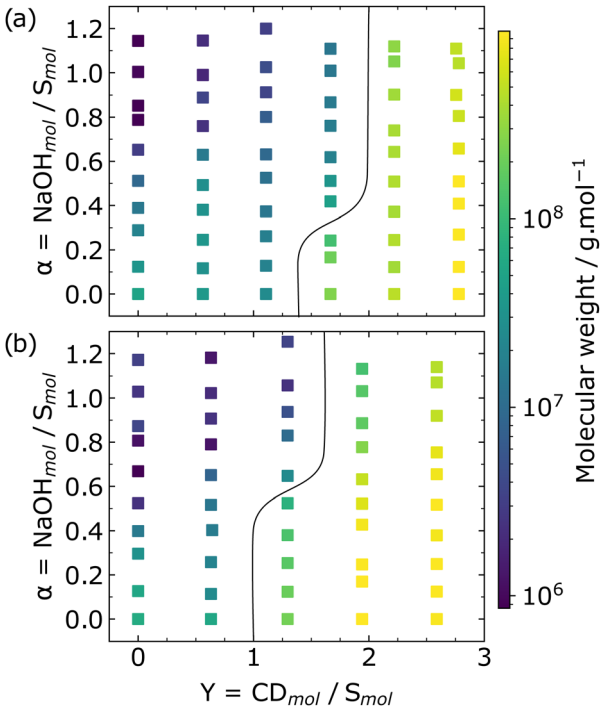

Fig. 1 Phase behaviour of $C_{12}E_5$Ac-αCD before heating (A) and after heating (B). The solid line separates the one-phase (left) and the two phase (right) regions. All data are recorded at room temperature. Phase diagrams of the $C_{12}E_5$Ac-βCD, $C_{12}E_{10}$Ac-αCD and $C_{12}E_{10}$Ac-βCD systems can be found in the ESI† (S2).

Macroscopically, we observed that all the systems examined presented increased turbidity from a particular value of *Y*, and clearer solutions were obtained with the increase of the pH, *i.e.* increasing the degree of ionization of the surfactant. The average molecular weight of each sample calculated by eqn (1) provides quantitative support to the macroscopic observations.

The phase boundaries were assigned at the phase diagrams for observations of $C_{12}E_5$Ac-αCD complexes before and after heating and cooling are presented in Fig. 1 (see ESI† for the phase diagrams of $C_{12}E_5$Ac-βCD (Fig. S2, ESI†) and $C_{12}E_{10}$Ac systems (Fig. S3, ESI†). Heating followed by slow cooling of the samples shifts the phase boundaries towards greater values of *Y* regardless the CD type. This shift indicates the presence of colloidally stable aggregates, which can be an interesting feature for systems in different areas of applications. By increasing the ionization of the surfactant, the stabilization of the aggregates due to the electrostatic repulsion results in the decrease of the M_w observed. In order to gain insights into the inclusion complexes formation, calorimetric and volumetric studies were performed to provide information about the thermodynamics of the process.

3.1.1 Isothermal titration calorimetry (ITC). ITC allows provides a direct measurement of the interaction heat between the CD and surfactant, making the determination of binding constant (K), enthalpy change (ΔH) and stoichiometry (n) possible. Titration curves of the four surfactant–CD systems at pH 3, 4 and 5 are depicted in Fig. 2.

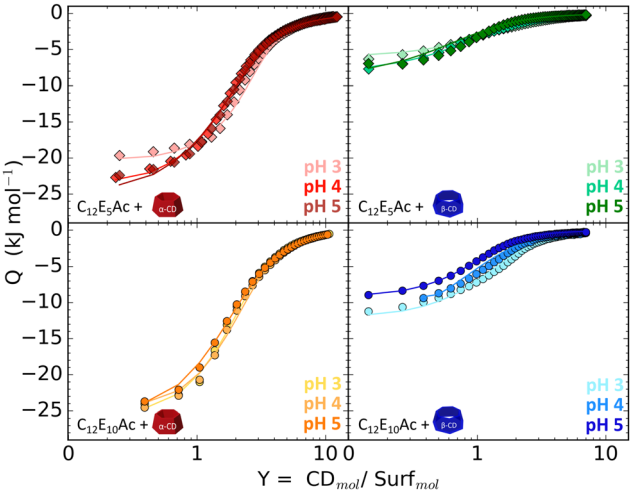

Fig. 2 Calorimetric curves for titration of $C_{12}E_5Ac$ (◊) and $C_{12}E_{10}Ac$ (○) with αCD (left) and βCD (right) at pH 3, 4 and 5, 25 °C. Solid lines are the fits by the one-to-one binding model, which data is depicted in Fig. 3.

The heat of dilution of each component was measured, and the demicellization heat of the surfactants was assessed, both confirmed to be negligible. The heats of interaction were fitted assuming the presence of n independent and equal binding sites per surfactant molecule.

From the fit, the binding constant K, the stoichiometry n, *i.e.* the number of CD per surfactant, and the enthalpy of inclusion ΔH obtained allowed the calculation of the binding free energy and entropy change using the eqn (4) and (5), using a dimensionless K for the calculations.

$$\Delta G^\circ = -RT\ln K \quad (4)$$

$$\Delta S = \frac{\Delta H - \Delta G^\circ}{T} \quad (5)$$

The obtained thermodynamic quantities, *i.e.*, ΔH, ΔG, ΔS, are calculated per mole of surfactant and are given in Fig. 3. The data indicates the spontaneous formation of the host–guest complexes ($\Delta G^\circ < 0$) for all the systems evaluated. Both ΔH and $T\Delta S$ present negative values. In all the cases, the lowest enthalpic change value provides a greater contribution to the complexation process, characterizing it as an enthalpically-driven mechanism.

The differences in the entropic contributions of α and β-cyclodextrins are mostly associated with the water structure inside the CD cavity, which is directly related to the CD size. In the cavity, the conformation of the glucopyranose units limits their hydrogen-bonding network, which provides more conformational freedom. In addition, the hydroxyl groups present at the CD rim can also be incorporated into the water network.[27] The full reestablishment of the hydrogen bonding network of those molecules is achieved with their release to the bulk, adding a contribution to the decrease in enthalpy. Oppositely to the straightforward assumption of the scaling of these effects with the increase of the cavity size, the heat capacity of the water within βCD is closer to the liquid water than the within the αCD,[28] resulting from structural differences between them. Hence, due to the different density of the water molecules inside the cavities, a greater enthalpic and unfavored entropic contribution for the inclusion complexation with αCD can be observed.

From the graphs, it is possible to notice that the main energetic features are related to the type of cyclodextrin. The most noticeable difference between the αCD and βCD systems curves is the magnitude of the enthalpy and entropy binding, whereas a small effect of the EO number is evidenced by the difference in the systems with $C_{12}E_5Ac$ and $C_{12}E_{10}Ac$ for both CD types. Minor effects of pH were observed, indicating that the terminal carboxylic group is not included in the CD cavity. Moreover, due to the very different hydration of the EO units in the ionized and non-ionized form of the surfactant, it is likely that the binding involves the hydrophobic part of the surfactant only. It is noteworthy that the experiments are carried out well above the cmc of the surfactant, and thus the interaction of the CDs with the surfactant micelles is also probed. In addition, the great affinity between host and guest is verified by the high binding constant values.

Similar thermodynamic/energetic behaviour had been reported in the literature for fatty acids and non ionic

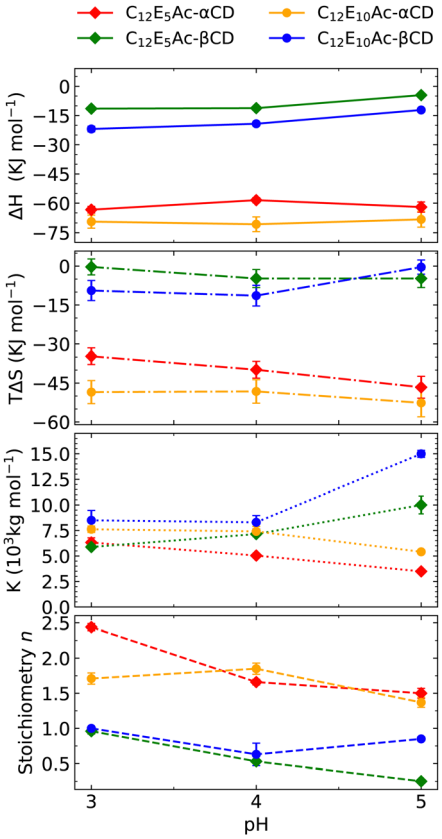

Fig. 3 Thermodynamic parameters obtained by ITC for the formation of host–guest complexes between AECs and cyclodextrins at 25 °C: ΔH (– solid line), $T\Delta S$ (·—·), binding constant 'K' (· · ·) and stoichiometry (– –). The stoichiometry n is given in CD per surfactant molecule, while ΔS and ΔH are given in Joule per mole of surfactant.

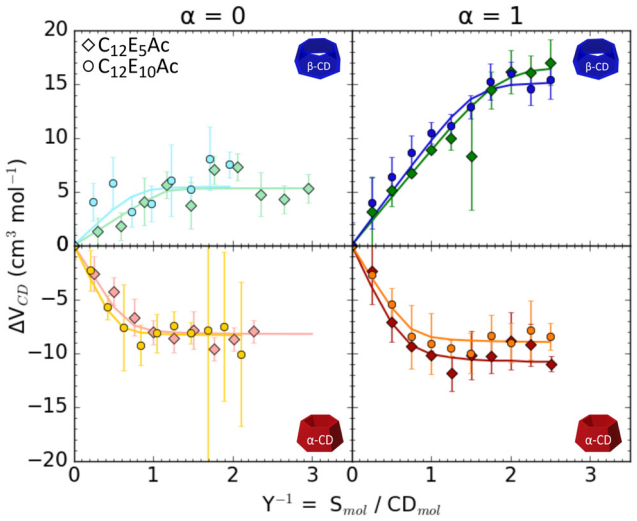

Fig. 4 Volume of transfer (ΔV^{CD}) of α-cyclodextrin and β-cyclodextrin from water to aqueous solution of $C_{12}E_5Ac$ (◊) and $C_{12}E_{10}Ac$ (○) as function of surfactant–CD ratio. Solid lines are the best fit according to eqn (6).

surfactants containing EO units. For the fatty acids containing 11 and 13 carbons in the alkyl chain, the inclusion complexation was also enthalpically driven and present $\Delta G < 0$, slightly more negative for the longer alkyl chain.[29] Inclusion complexes of βCD with Brij surfactants, also above the cmc, and Triton-100, in concentrations below the cmc, presented similar thermodynamic behaviour. However, the encapsulation of both hydrophobic and hydrophilic moieties was observed for the former, while for the latter, only the encapsulation of the hydrophobic moiety was reported.[30,31]

3.1.2 Volumetry. The inclusion complexation mechanism of a guest into the CD cavity is related to the spatial/geometric and energetic aspects *via* non-covalent interactions, such as electrostatic, van der Waals, hydrophobic, charge-transfer interactions and hydrogen bonding.[32] Thus, the volumetric study of CD complexes can provide a good insight into the solvation behaviour, and a better understanding of the phenomena and the interactions involved in the formation of such complexes.[33]

The volumes of transfer of αCD and βCD from water to the aqueous surfactant solution as a function of the S/CD molar ratio in the nonionic form (α = 0) and in the completely ionized form (α = 1) are presented in Fig. 4. The V_Φ determined for both CDs, 604.1 ± 0.1 and 706.7 ± 0.1 $cm^3\ mol^{-1}$, for αCD and βCD, respectively, are in accordance with the literature[34,35] and were used in the calculation of the volumes of transfer.

The volumes of transfers are reported in Fig. 4, and it can be seen that: (i) the number of EO units of the surfactant has no effect on the volume of transfer; (ii) the volumes of complexation are positive for βCD and negative for αCD, as a consequence of the different water density within the cavity prior to complexation;[36,37] the charge of the surfactant has no effect for the complexation with αCD. The data can also be quantitatively

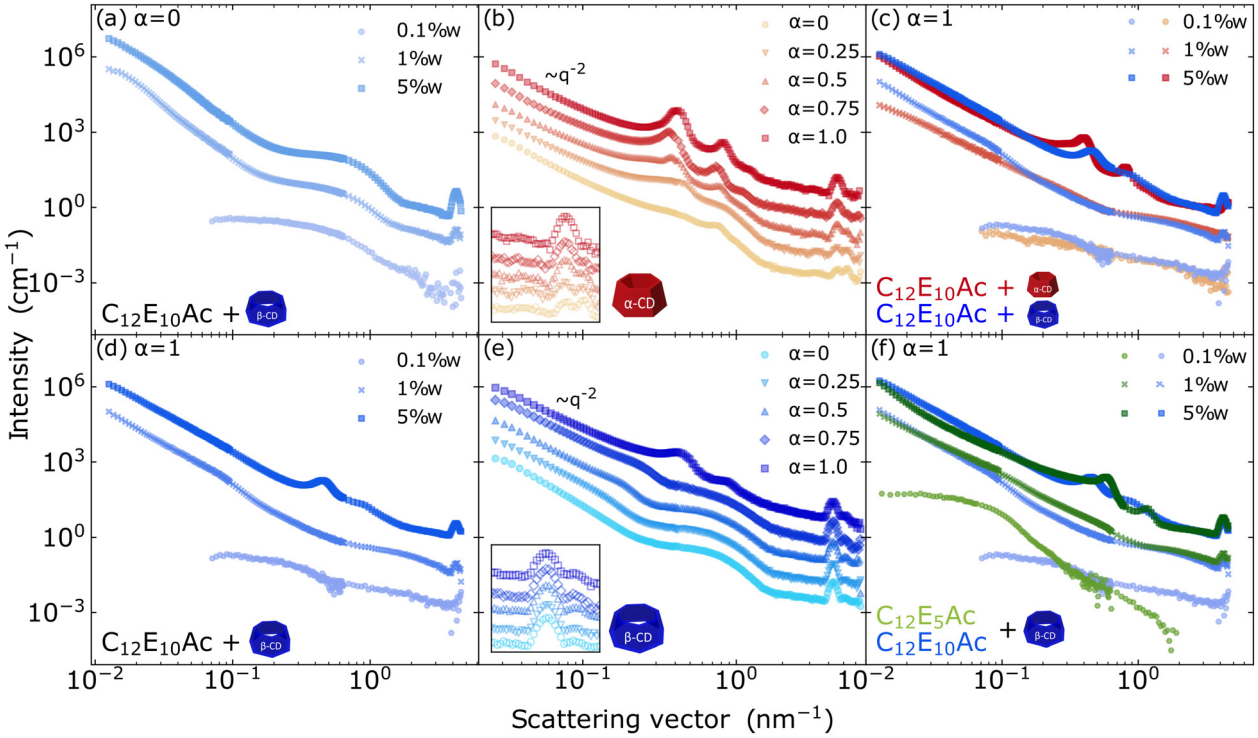

Fig. 5 At ratio CD/surfactant = 2, different concentrations of the $C_{12}E_{10}Ac$ with βCD at (a) α = 0 (nonionized), (d) α = 1 (ionized). Different degree of ionization (α) scattering profile curves of $C_{12}E_{10}Ac$ with αCD (b) and βCD (e). (c) Ionized surfactant with αCD (red) and βCD (blue). (f) Comparison of βCD with ionized $C_{12}E_5Ac$ (green) and $C_{12}E_{10}Ac$ (blue) at different surfactant concentrations. Curves are scaled by successive factors of 7 for readability. Measurements of a, c, d and f were performed on *D*11 and b and e on *D*22 at ILL.

interpreted. As performed for the ITC modelling, the one-to-one modelling approach was applied. The partial molar volume V_Φ was obtained by assuming two states for the cyclodextrin, *i.e.*, involved in the inclusion complex with a molar volume V and free in water with a molar volume V_0:

$$V_\Phi = V \cdot \frac{m_{CD-S}}{m_{CD}} + \left(1 + \frac{m_{CD-S}}{m_{CD}}\right) \cdot V_0 \quad (6)$$

with m_{CD} and m_{CD-S} being the concentration of the free CD and of the CD involved in the inclusion complexes, obtained trough the following binding constant:

$$K = \frac{m_{CD-S}}{m_{CD} \cdot (n \cdot m_S - m_{CD-S})} \quad (7)$$

where K is the binding constant, n is the stoichiometry, m_{CD} and m_S are the CD and surfactant molalities, respectively.

The fits are reported together with the data in Fig. 4, and the obtained fit parameters are given in the ESI† (S.3). The obtained stoichiometry values agree well with those obtained from the ITC experiments. Furthermore, high binding affinity was obtained for all the systems evaluated, and increased affinity was observed for βCD systems with ionized surfactants, whereas the opposite was found for the surfactant–αCD systems.

The volume of transfer dependence on the surfactant concentration also highlights the saturation of the cavity sites available, noticed by the constant values of ΔV^{CD} with the increase of the surfactant concentration, pointing out no further solvent displacement.

3.2 Structure of the supramolecular assemblies

One of the interesting characteristics of surfactant–CD inclusion complexes is their ability to assemble into ordered aggregates.[38] To probe these structures, small-angle scattering is an excellent technique which provides detailed insight into the organization of surfactants and CDs at the 1–100 nm scale.[21,39,40] Larger structures are well investigated using microscopy techniques.

In particular, the effect on the aggregate morphologies of the concentration, the molecular architecture of the surfactant and cyclodextrin type, and of the degree of ionization of surfactant were probed by small-angle neutron scattering. Data with mixing ratio [CD]/[S] = 2 are shown in Fig. 5.

For all the systems, macroscopically changes were observed as a function of the concentration. At 0.1 wt%, transparent fluids are obtained, while a white liquid fluid is obtained at 1% and gel aspect is observed over 3.5% for αCD systems and an increase in the birefringence and viscosity for βCD systems. The scattering profiles of those samples also point structural changes with the increase of the concentration. As shown in Fig. 5a and d, from the 0.1 to 5 wt% in the ionized surfactant complex for both surfactants, enriched microstructure is observed in more concentrated samples.

The effect of charge density is systematically probed in Fig. 5b and e for samples with 5 wt% surfactant content and mixing ratio $Y = 2$. At high charge density of the surfactant, the scattering pattern feature a $^{-2}$ power low at low-q, and the presence of a second-order peak at a position $q_2^* = 2q_1^2$. These features are the scattering signature of periodic lamellar structures. Similar morphologies have been identified also in SDS-βCD,[41] DTAB-βCD[14] and for αCD/phytosterol ethoxylate surfactant[15] complexes. Differently, these features are not present in the curves of the nonionized surfactant complexes (Fig. 5a), indicating a lack of order in these aggregates. Similar behaviour is observed for $C_{12}E_5Ac$, with peaks slightly shifted towards lower q (Fig. 5e). The arise of order can also be noticed in the effective structure factor shown in Fig. S7 in the ESI.† In detail, the scattering profiles fully ionized $C_{12}E_{10}Ac$ present peaks at $q \approx 0.4$ and 0.82 nm^{-1} in αCD complexes and, for βCD, at $q \approx 0.6$ and 1.2 nm^{-1}, corresponding to a periodicity of 15.8 and 10.5 nm, respectively. Not only the spacing between the layers of $C_{12}E_{10}Ac$-αCD complexes is higher, but they are also more ordered, with even third-order peaks visible for $\alpha > 0.5$. This difference can be, at least partly, ascribed to the different sizes of the CD cavities, having an outer diameter of 1.52 and 1.66 nm, corresponding to an area per molecule of 1.81 and 2.16 nm^2 for α and βCD, respectively.[40] A higher charge density in the αCD system implies stronger repulsion between the layers. Finally, the effect of the degree of ionization on later packing of the inclusion complexes is probed at high q and evidenced in the insets of Fig. 5b and e. In particular, no effect on the degree of ionization of the packing is observed for complexes formed with βCD system, while a reorganization of the structure takes place in mixtures with αCD. In the presence of the nonionized molecules, two peaks can be observed at $q \approx 3.45$ and 5.25 nm^{-1}, with corresponding distances of 1.82 and 1.20 nm. By increasing the ionic molecules' predominance, the peaks gradually evolve to a singular signal at 4.31 nm^{-1} (Fig. 5b). We ascribe this finding to the larger spacing in the βCD system. The area per molecule of the charged $C_{12}E_{10}Ac$ at the air/water interface is 1.3 nm^2,[20] slightly less but still comparable to the area required by a αCD molecule. The effect of the type of cyclodextrin is further probed in Fig. 5c. While an effect is visible on the charged system at the higher concentration, where multilayered structures are formed, no effect is observed at a lower concentration, where the supramolecular aggregates assume a unilamellar structure.

In summary, by employing weakly acidic surfactants the effect of the charge density on the morphology of CD/S inclusion complexes could be probed. On the one hand, the presence of charges does not fundamentally affect the assembly of the inclusion complexes into bilayered structures. This is due to the relatively large spacing between the surfactant head groups. On the other hand, the gradually increasing electrostatic repulsion between the bilayers is required to provide the periodicity in the multilayered structure.

Finally, in Fig. 5f, the effect of the surfactant molecular architecture on the complexes is evidenced. For both cases, the evolution of the aggregate morphology with concentration is very similar. At high concentration, the repeating distance is smaller for $C_{12}E_5Ac$ than for $C_{12}E_{10}Ac$, with 14.8 and 10 nm for $C_{12}E_5Ac$ with αCD and βCD, respectively, and 15.8 nm for $C_{12}E_{10}Ac$-αCD and 14.1 nm for $C_{12}E_{10}Ac$-βCD system.

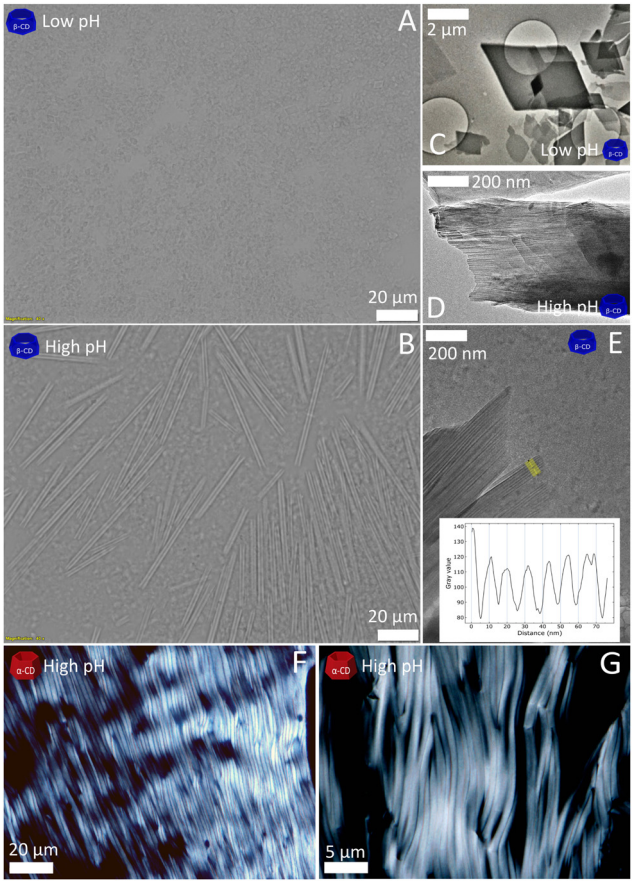

Fig. 6 Morphology of the aggregates observed for $C_{12}E_5Ac$-2βCD inclusion complexes. Optical microscopy overview of the assemblies obtained at (a) $\alpha = 0$ and (b) $\alpha = 1$ (scale bar: 20 μm). (c) TEM picture of the rhombic structures obtained from the assembly with the nonionic surfactant (scale bar: 2 μm). (d) Cryo-TEM pictures of the tubular structure edge obtained from $\alpha = 1$ (scale bar: 200 nm) and (e) cryo-TEM picture zoom-in of the multi-layered tube wall (scale bar: 200 nm). Polarized optical microscopy images of αCD systems: (f) ionized $C_{12}E_5Ac$-αCD (scale bar: 20 μm) and (g) Ionized $C_{12}E_{10}Ac$-αCD (scale bar: 5 μm).

The lack of the Guinier domain in the SANS curves precludes the determination of the dimension and entire morphology of the assemblies. Hence, microscopic analysis was employed to unveil this aspect. The μm morphology of the inclusion complexes formed by $C_{12}E_5Ac$ with α and βCD at low and high degree of ionization is illustrated in Fig. 6. As shown in Fig. 6a, an appreciable amount of rhombic aggregates can be observed in the nonionic system. Although polydispersed in size, the crystals present the remarkable 104° obtuse angle characteristic of this type of cyclodextrin that can be clearly verified in the TEM image (Fig. 6c). Such structures were also reported in other βCD inclusion complexes with SDS,[12] DTAB[14] and Tween-20,[13] and it is closely related to the macrocycle symmetry. In contrast, well-defined hollow cylinders are formed in mixtures of α and βCD with the ionized surfactants (Fig. 6b, d and e for mixtures with βCD and Fig. 6f and g for mixtures with αCD). The statistical distribution of the cylinders diameters was determined from the optical microscopy image and confirms a monodispersed distribution with an average diameter equal to 2.70 μm (standard deviation 0.24 μm) and the visible length polydispersity. However, they present distinct rigidity probed by the straightness of the tube, their positions and the absence of curvatures/bending. Cryo-EM images of a tube edge were acquired (Fig. 6e), aiming for detailed information about those structures.

Differently, for αCD systems (Fig. 6f and g), 3D network structures of long flexible fibers, often entangled, were observed. The fibers present an average diameter of 1.50 μm (standard deviation 0.25 μm) for $C_{12}E_5Ac$ (Fig. 6f), whereas slightly enlarged diameters are observed for $C_{12}E_{10}Ac$ (Fig. 6g). Although the tubular aggregates can be clearly observed for the systems with both cyclodextrins, the nature of their formation, either by the bending of the aligned layered structure[12] or by the mechanism of nucleation and growth proposed by Landman *et al.*,[21] could not be resolved.

4 Conclusions

This study delivers a thermodynamic and structural complementary approach of the interaction between the weakly anionic alkyl ether carboxylates and α and β-cyclodextrins. An analysis of the behaviour of the systems in aqueous solutions demonstrated the ability to spontaneously interact, forming inclusion complexes that can further self-assemble into supramolecular aggregates. The evaluation of the systems' behaviour as a function of the degree of ionization confirmed the role of the electrostatic repulsion in directing the assembly of the inclusion complexes. In this context, the present pH responsiveness of the system provided by the alkyl ethylene oxide carboxylic acids differs from the previously investigated cyclodextrin-surfactant inclusion complexes, in which only ionic or nonionic surfactants were applied mainly with β-cyclodextrin.[18,29,42] To employ a weakly acidic alkyl ether carboxylic acid, which combines the characteristics of both ionic and nonionic surfactants, allowed us the possibility to systematically change the degree of charge of the surfactant without changing the chemical nature of the guest molecule. In particular, small-angle scattering evidenced that the presence of charges is required for the spontaneous assembly of the inclusion complexes into well-ordered, multilayered structures with periodicity of ~10 nm. This long range order, arising from the electrostatic repulsion between the inclusion complex layers, can be further tuned by the CD cavity size. Finally, optical and electron microscopy revealed that the tubular structures formed with αCD are more flexible than those formed by βCD. A schematic representation of these findings is given in Fig. 7.

In contrast to the significant effect of the degree of ionization on the morphology of the supramolecular assemblies, calorimetric and densitometry results show that the complexation interaction between host and guest, is not affected by the electrostatic interactions. In addition, it hints toward the cyclodextrin binding to the alkyl chain of the surfactant rather than the ethylene oxide units of the heads, as differences in the parameters at various pH were no t observed. This seems valid even in the case of αCD, which shows a very high affinity

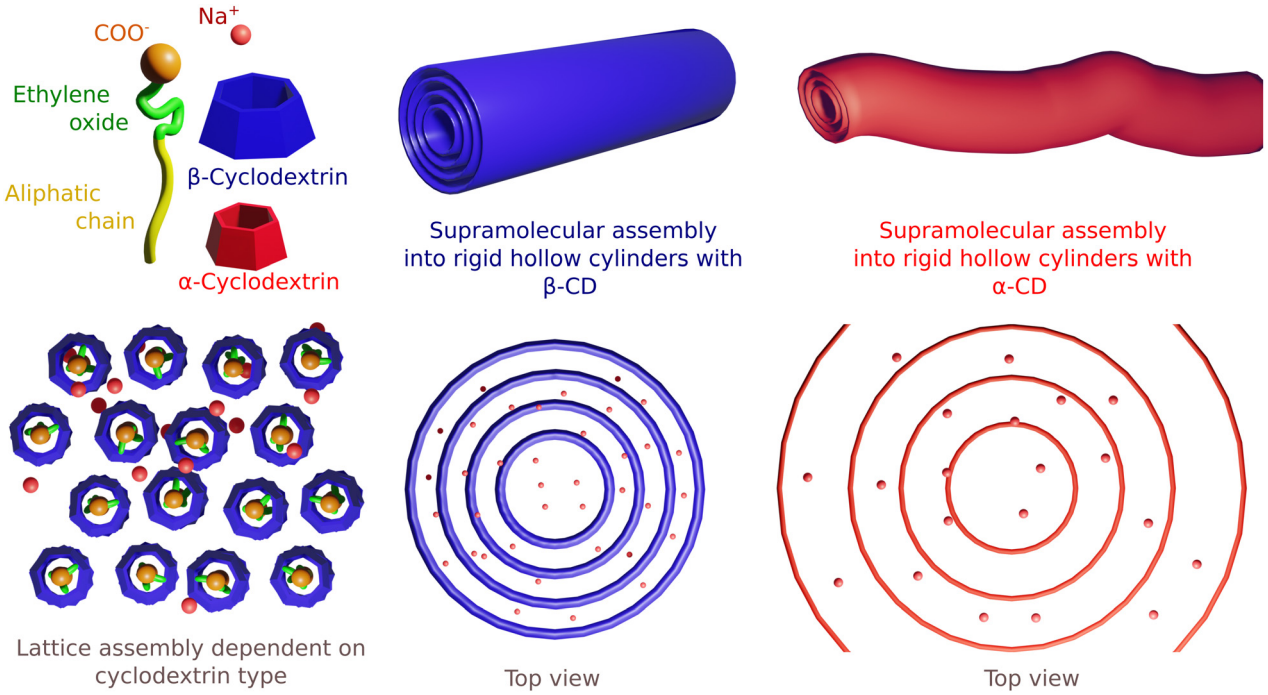

Fig. 7 Schematic representation of the components used in this work and their assembly into rigid and flexible hollow multilayered cylinders for the case of β and α cyclodextrins, respectively. The representations are not at scale and refer to the case of the fully ionized surfactant.

towards the polyethylene glycole headgroup.[10] For the latter case, a significant effect of the pH on the complexation thermodynamics was expected, as the changes in the charge density directly affects the EO units hydration state and conformation.

Controlling the electrostatic repulsion in cyclodextrin inclusion complexes systems has demonstrated to be an essential tool for not only directing the assembly, envisioning the modulation of the long-range interactions but also highlights the importance of studying the impact of the tuning parameters from the short to the long-range interactions in the hierarchical assembly process.

Conflicts of interest

There are no conflicts to declare.

Acknowledgements

We would like to acknowledge the University of Palermo and the ILL for the financial support and the Partnership for Condensed Soft Matter (PSCM), which provided the densitometer, the turbidimeter, the optical microscopy, as well as the preparation facilities. We also would like to acknowledge the assistance of the Core Facility BioSupraMol supported by the DFG. We thank Dr Kai Ludwig for the assistance with the Cryo-EM. This work also used the EM facilities at the Grenoble Instruct-ERIC Center (ISBG; UMS 3518 CNRS CEA-UGA-EMBL) with support from the French Infrastructure for Integrated Structural Biology (FRISBI; ANR-10-INSB-05-02) and GRAL, a project of the University Grenoble Alpes graduate school (Ecoles Universitaires de Recherche) CBH-EUR-GS (ANR-17-EURE-0003) within the Grenoble Partnership for Structural Biology. The IBS Electron Microscope facility is supported by the Auvergne Rhône-Alpes Region, the Fonds Feder, the Fondation pour la Recherche Médicale and GIS-IBiSA. We thank Caroline Mas for assistance and/or access to the Biophysical platform.

References

1 A. J. Valente and O. Söderman, *Adv. Colloid Interface Sci.*, 2014, **205**, 156–176.
2 W. C. Geng, J. L. Sessler and D. S. Guo, *Chem. Soc. Rev.*, 2020, **49**, 2303–2315.
3 R. De Lisi, G. Lazzara and S. Milioto, *Phys. Chem. Chem. Phys.*, 2011, **13**, 12571–12577.
4 M. Mariano, O. D. Bernardinelli, R. Pires-Oliveira, G. A. Ferreira and W. Loh, *ACS Omega*, 2020, **5**, 9517–9528.
5 C. Perry, P. Hébraud, V. Gernigon, C. Brochon, A. Lapp, P. Lindner and G. Schlatter, *Soft Matter*, 2011, **7**, 3502–3512.
6 M. Benko and Z. Király, *J. Chem. Thermodyn.*, 2012, **54**, 211–216.
7 J. Zhang, Z. Yang, H. Zhang, Z. Hua, X. Hu, C. Liu, B. Pi and Y. Han, *Langmuir*, 2019, **35**, 16893–16899.
8 H. Dodziuk, *Cyclodextrins and Their Complexes: Chemistry, Analytical Methods, Applications*, Wiley Online Library, 2006, pp. 1–473.
9 M. Valero, I. Grillo and C. A. Dreiss, *J. Phys. Chem. B*, 2012, **116**, 1273–1281.
10 G. Lazzara, S. Prevost and M. Gradzielski, *Soft Matter*, 2011, **7**, 6082–6091.

11 J. Joseph, C. A. Dreiss, T. Cosgrove and J. S. Pedersen, *Langmuir*, 2007, **23**, 460–466.
12 S. Yang, Y. Yan, J. Huang, A. V. Petukhov, L. M. Kroon-Batenburg, M. Drechsler, C. Zhou, M. Tu, S. Granick and L. Jiang, *Nat. Commun.*, 2017, **8**, 1–7.
13 C. Zhou, X. Cheng, Q. Zhao, Y. Yan, J. Wang and J. Huang, *Langmuir*, 2013, **29**, 13175–13182.
14 J. Carlstedt, A. Bilalov, E. Krivtsova, U. Olsson and B. Lindman, *Langmuir*, 2012, **28**, 2387–2394.
15 J. Wang, W. Qi, N. Lei and X. Chen, *Colloids Surf., A*, 2019, **570**, 462–470.
16 K. Gruhle, S. Müller, A. Meister and S. Drescher, *Org. Biomol. Chem.*, 2018, **16**, 2711–2724.
17 L. Jiang, Y. Peng, Y. Yan and J. Huang, *Soft Matter*, 2011, **7**, 1726–1731.
18 L. Jiang, Y. Peng, Y. Yan, M. Deng, Y. Wang and J. Huang, *Soft Matter*, 2010, **6**, 1731–1736.
19 H. Wang, J. C. Wagner, W. Chen, C. Wang and W. Xiong, *Proc. Natl. Acad. Sci. U. S. A.*, 2020, **117**, 23385–23392.
20 L. Chiappisi, *Adv. Colloid Interface Sci.*, 2017, **250**, 79–94.
21 J. Landman, S. Ouhajji, S. Prévost, T. Narayanan, J. Groenewold, A. P. Philipse, W. K. Kegel and A. V. Petukhov, *Sci. Adv.*, 2018, **4**, 1–8.
22 D. W. Hayward, L. Chiappisi, J. H. Teo, S. Prévost, R. Schweins and M. Gradzielski, *Soft Matter*, 2019, **15**, 8611–8620.
23 L. Chiappisi, I. Hoffmann and M. Gradzielski, *Soft Matter*, 2013, **9**, 3896–3909.
24 J. Hernandez-Pascacio, A. Pineiro, J. M. Ruso, N. Hassan, R. A. Campbell, J. Campos-Terán and M. Costas, *Langmuir*, 2016, **32**, 6682–6690.
25 P. Lindner and R. Schweins, *Neutron News*, 2010, **21**, 15–18.
26 Laue-Langevin, *D22 – Large dynamic range smallangle diffractometer*, Institut Laue-Langevin, 2003, **https://www.ill.eu/users/instruments/instrumentslist/d22/description/instrument-layout**.
27 W. Saenger and T. Steiner, *Acta Crystallogr., Sect. A: Found. Crystallogr.*, 1998, **A54**, 798–805.
28 L. E. Briggner and I. Wadsö, *J. Chem. Thermodyn.*, 1990, **22**, 1067–1074.
29 D. Ondo, *J. Mol. Liq.*, 2020, **311**, 113172.
30 I. Araujo Marques, A. J. Patino-Agudelo, Y. L. Coelho, P. D. Santos Moreau, L. Neves Santa Rosa, A. C. dos Santos Pires and L. H. Mendes da Silva, *J. Mol. Liq.*, 2021, **338**, 116647.
31 B. K. Müller and H. Ritter, *J. Inclusion Phenom. Macrocyclic Chem.*, 2012, **72**, 157–164.
32 L. Liu and Q. X. Guo, *J. Inclusion Phenom.*, 2002, **42**, 1–14.
33 R. De Lisi, G. Lazzara, S. Milioto and N. Muratore, *J. Phys. Chem. B*, 2003, **107**, 13150–13157.
34 I. V. Terekhova, R. De Lisi, G. Lazzara, S. Milioto and N. Muratore, *J. Therm. Anal. Calorim.*, 2008, **92**, 285–290.
35 K. Spildo and H. Høiland, *J. Solution Chem.*, 2002, **31**, 149–164.
36 M. Manabe, T. Ochi, H. Kawamura, H. Katsu-Ura, M. Shiomi and M. S. Bakshi, *Colloid Polym. Sci.*, 2005, **283**, 738–746.
37 L. D. Wilson and R. E. Verrall, *J. Phys. Chem. B*, 1997, **101**, 9270–9279.
38 K. Liu, C. Ma, T. Wu, W. Qi, Y. Yan and J. Huang, *Curr. Opin. Colloid Interface Sci.*, 2020, **45**, 44–56.
39 S. Ouhajji, J. Landman, S. Prévost, L. Jiang, A. P. Philipse and A. V. Petukhov, *Soft Matter*, 2017, **13**, 2421–2425.
40 L. dos Santos Silva Araújo, G. Lazzara and L. Chiappisi, *Adv. Colloid Interface Sci.*, 2021, **289**, 102375.
41 L. Jiang, Y. Yan and J. Huang, *Adv. Colloid Interface Sci.*, 2011, **169**, 13–25.
42 A. Mahata, D. Bose, D. Ghosh, B. Jana, B. Bhattacharya, D. Sarkar and N. Chattopadhyay, *J. Colloid Interface Sci.*, 2010, **347**, 252–259.

Appendix C

Paper III: Thermoresponsive behavior of cyclodextrin inclusion complexes with weakly anionic alkyl ethoxy carboxylates

Soft Matter

PAPER

View Article Online
View Journal | View Issue

Cite this: *Soft Matter*, 2023, **19**, 1523

Thermoresponsive behavior of cyclodextrin inclusion complexes with weakly anionic alkyl ethoxy carboxylates†

Larissa dos Santos Silva Araújo, [ab] Giuseppe Lazzara [a] and Leonardo Chiappisi *[b]

Received 9th December 2022,
Accepted 26th January 2023

DOI: 10.1039/d2sm01621d

rsc.li/soft-matter-journal

This study investigates the temperature responsive behavior of inclusion complexes formed by weakly anionic alkyl ethoxy carboxylates and α (αCD) and β-cyclodextrins (βCD). Small-angle neutron scattering (SANS) was performed to probe the structural behaviour at the 1–100 nanometer scale of the hierarchical assemblies at different temperatures. The phase transitions and thermodynamics were systematically monitored as a function of the degree of ionization of the surfactant by differential scanning calorimetry (DSC). Herein, we investigate the effect of the surfactant degree of ionization on the thermoresponsive properties of the inclusion complex supramolecular assemblies. Inclusion complexes formed with the ionized surfactant spontaneously assemble into multilayered structures, which soften with increasing temperature. We also found that the presence of charges is not only required to impart order to the supramolecular assemblies, but also induced in-plane crystallization of the inclusion complexes. Finally, the use of a weakly anionic surfactant allows us to probe the interplay between the charge density and temperature on the assembly of surfactant-cyclodextrin inclusion complexes. This study helps to improve the design of multi-responsive supramolecular systems based on cyclodextrins.

1 Introduction

Cyclodextrins (CD) are cyclic oligosaccharides able to form inclusion complexes with various molecules. α-cyclodextrin (αCD), β-cyclodextrin (βCD) and γ-cyclodextrin (γCD) are the most commonly used types, containing six, seven and eight α-D-glucopyranose units, linked by α-1,4 glycoside bonds forming a truncated cone-shaped ring. The hydrophilic rims decorated with the primary hydroxyl groups and a hydrophobic cavity containing high-energy water provide these molecules with unique features which are at the origin of their very rich supramolecular assembly behavior.[1] Because of their versatility, cyclodextrins are widely used as hosts to build functionalized supramolecular materials, with polymers,[2–4] and surfactants.[1,5,6]

Cyclodextrin–surfactant inclusion complexes systems exhibit particular physicochemical properties, remarkable versatility, and enriched structural behaviour arising from a delicate balance of repulsive interactions of electrostatic or steric origin between surfactants and hydrogen-bond mediated interactions between cyclodextrins.[5,7–10] Non-covalent interactions are at the basis of the reversible and stimuli-responsive behaviour of cyclodextrin–surfactant systems. Moreover, chemical modifications of CDs and the large variety of surfactants available allow the experimentalist to integrate the system with the desired functionalities. In a reversible process, the assembly of inclusion complexes into highly-ordered structures relies on directional hydrogen bonding between adjacent CDs and CD–water interactions. Hydrogen bonding also plays a critical role in the balance of the electrostatic interactions and macro phase stability, therefore, also influencing the assemblies' morphologies.[9,11]

The knowledge of a system's thermodynamic and structural behaviour and its particular characteristics provide essential tools to regulate and modulate the interactions involved in the assembly.[12] It can also provide essential information on the role of the guests and hosts and their characteristics' effect on the structure and responsiveness.

The complex interplay of interactions governing the supramolecular assembly of surfactant–CD inclusion complexes is a widely exploited strategy to design responsive materials relying on environmental conditions. For instance, inclusion complexes which respond to light,[13–15] pH,[16] redox potential,[17–19] solvent exchanges[20,21] or temperature[22,23] have been prepared for the design of stimuli-responsive assembled materials.[12,24]

[a] *Dipartimento di Fisica e Chimica, Università degli Studi di Palermo, Viale delle Scienze pad 17, 90128, Palermo, Italy*
[b] *Institut Max von Laue-Paul Langevin, 71 avenue des Martyrs, 38042, Grenoble, France. E-mail: chiappisil@ill.eu*

† Electronic supplementary information (ESI) available. See DOI: https://doi.org/10.1039/d2sm01621d

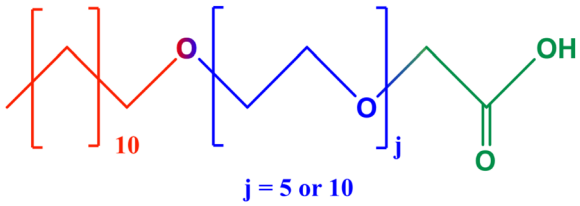

Fig. 1 Schematic representation of representative chemical formula of an alkyl ether carboxylic acid composed by a hydrophobic alkyl chain containing 12 carbons, 5 or 10 ethylene oxide units and terminal carboxylic group. See Experimental section for further details.

Because of the large effect on the solubility, molecular vibrational states and strength of interactions, particularly hydrogen bonds, temperature is one of the most common and efficient stimuli employed in controlling molecular conformation and self-assembly processes.[24] Temperature-controlled phase transitions of highly ordered assemblies of mixtures of CD with dimethyl tetrammonium bromide,[9] tetradecyl dimethylammonium propane sulfonate,[25] sodium 6-(4-((4-(dimethylamino)phenyl)diazenyl)phenoxy)hexanoate,[26] 1-decyl-3-methylimidazolium bromide[27] and sodium dodecyl sulphate (SDS)[28,29] have been investigated before. For these mixtures, thermo-switchable phases of microtubes, lamellas, hydrogels and vesicles have been reported, and the microco-confinement potential *via* a co-assembly process by SDS@2βCD has also been reported.[30,31]

In a recent study, we described the properties of inclusion complex formed by cyclodextrins with weakly anionic alkyl ether carboxylic acids (AEC).[16] In particular, the possibility offered by the weakly anionic head group allowed us to probe the effect of surfactant charge density on the formation of inclusion complexes through the pH of the solution without any change in the chemistry of the system. Very interestingly, multilayered aggregates are formed irrespective of the surfactant charge. However, electrostatic repulsion is essential for the formation of well-defined, ordered structures.

The aim of the present work is to investigate the effect of surfactant ionization on the thermoresponsiveness of the surfactant/CD supramolecular assemblies. We investigated the structural behaviour of the inclusion complexes assemblies between two alkyl ether carboxylic acids, the pentaoxyethylene dodecyl ether carboxylic acid ($C_{12}E_5Ac$) and the decaoxyethylene dodecyl ether carboxylic acid ($C_{12}E_{10}Ac$) (chemical structure in Fig. 1), with αCD and βCD by small-angle neutron scattering (SANS) over a wide temperature range of 15–70 °C. The temperature-induced phase transitions and thermodynamics were monitored by differential scanning calorimetry (DSC). We report the differences in the thermal responses of the structures resultant of the chemical architecture of surfactants, cyclodextrins, and the surfactant's degree of ionization, given as the sodium hydroxide and surfactant molar ratio ($\alpha = [NaOH]/[S_{tot}]$).

This study delivers a micro and nanometer perspective on the temperature responsiveness of the microstructure and CD–surfactant inclusion complexes' lattice assembly, opening the prospects on the guest role and evaluation of the host exchange in cyclodextrin complexes and also in the development of stimuli-responsive materials in the cosmetic, food, and pharmaceutical fields.

2 Experimental section

2.1 Materials

Pentaoxyethylene dodecyl ether carboxylic acid ($C_{12}E_5Ac$) and decaoxyethylene dodecyl ether carboxylic acid ($C_{12}E_{10}Ac$) are technical surfactants provided by KAO chemicals under the commercial names AKYPO RLM45CA (444 g mol^{-1}, 92% purity) and AKYPO RLM100 (686 g mol^{-1}, 90% purity), with 7.3 and 9.8 wt% water content, respectively.[16] The hydrophobic part of the surfactants is a mixture of C_{12}, C_{14} and C_{16} in approx. Ratio 2 : 1 : 0.25. The ethylene oxide units (EO) are Gaussian distributed over a mean of 4.6 and 9.4 for AKYPO RLM45CA and AKYPO RLM100, respectively, and a degree of carboxymethylation of 0.95 for both surfactants determined by NMR.[32,33] αCD and βCD were acquired from TCI Europe. The water content of the cyclodextrins was determined from thermo-gravimetry and it is 10.1 for α and 11.5 wt% for βCD. Sodium hydroxide (Fluka, puriss) was used to adjust the pH of the solutions. The water content in the reagents was considered for sample preparation. All mentioned chemicals were used as received. All the solutions were prepared with D_2O (D content > 99.8%) from Eurisotop (Gif-sur-Yvette, France).

2.2 Sample preparation

The samples were prepared by mixing aqueous solutions of the respective components, adding the cyclodextrin to the surfactant solution to obtain the desired concentrations in the samples at ambient conditions. Samples were heated for 30 minutes at 60 °C and left to stabilize for 24 hours.

2.3 SANS

SANS patterns were recorded using 1 mm path quartz cells on D22[34] at the Institut Laue-Langevin (Grenoble, France), with a two ^{3}He detector setup, one fixed at 1.4 m sample-to-detector distance and, the second, used in two sample-to-detectors centre distance configurations of 5.6 and 17.6 m distance with corresponding collimation of 5.6 and 17.6 m, covering a total q-range of 0.03 to 6.5 nm^{-1}, where $q = 4\pi \sin(\theta/2)/\lambda$. The samples were measured at temperatures 15, 25, 45 and 70 °C.

2.4 DSC

DSC measurements were performed with a sensitive multicell DSC (micro-DSC, TA instruments) under nitrogen flow in the range from 10 to 95 °C with scan rate of 1 °C min^{-1}. The hastelloy sample cells of 1 cm^3 contained approximately 500 mg of sample solution. The ΔH is expressed in J g^{-1} of surfactant. It is noteworthy that no signal was detected for the pure CD solutions, *i.e.*, in the absence of surfactant. The analysis consisted in two heating and cooling cycles. The data were analysed using the freely available tool pyDSC.[35]

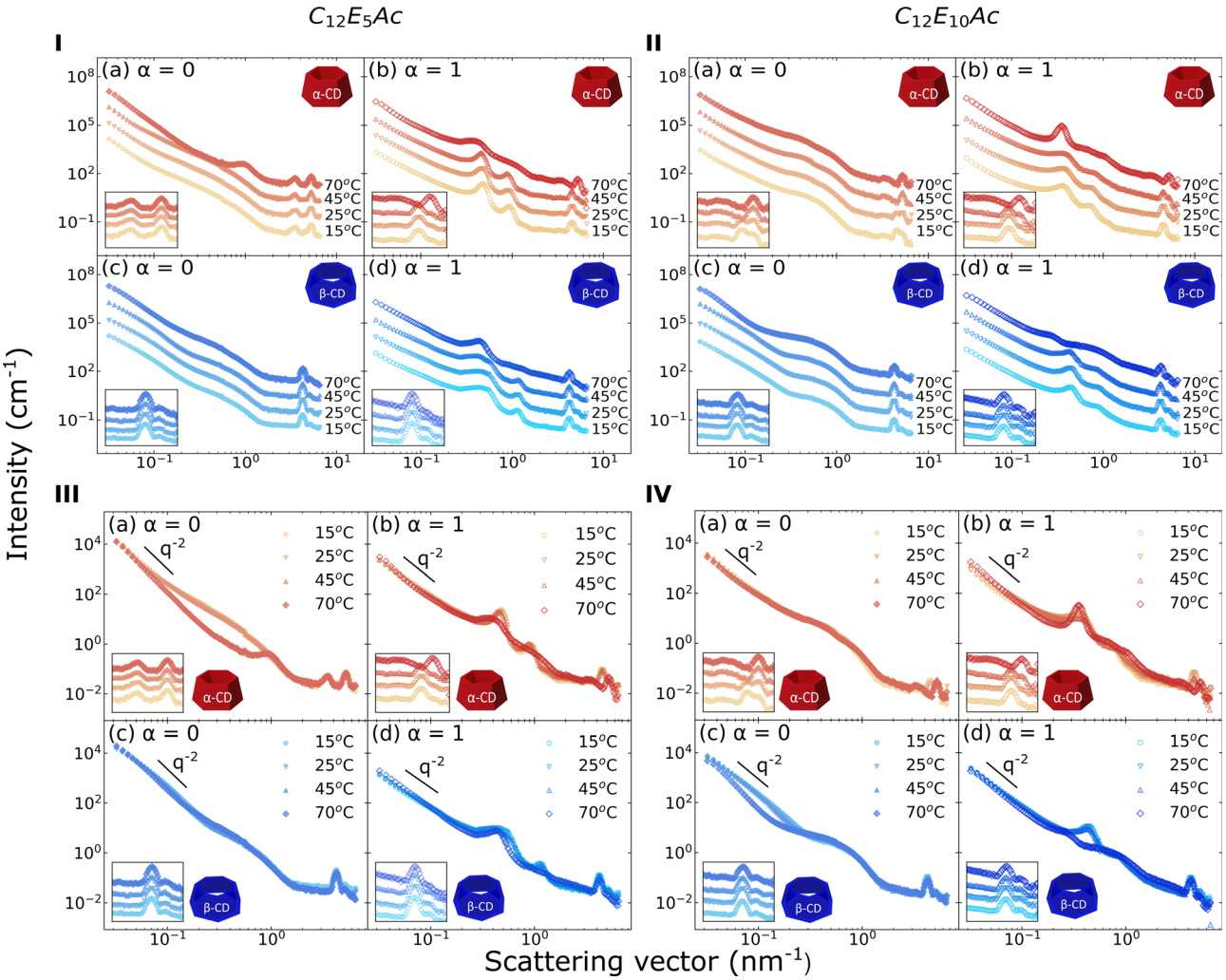

Fig. 2 SANS intensity as a function of scattering vector (q) covering 0.03–6.5 nm^{-1}. The measurements of (I) $C_{12}E_5Ac$ systems and (II) $C_{12}E_{10}Ac$ systems at $\alpha = 0$ and $\alpha = 1$ with αCD (a and b) and βCD (c and d) were performed at 15, 25, 45 and 70 °C, at ratio CD/surfactant = 2, (surfactant = 5 wt%). Curves are scaled by successive factors of 10 to improve readability. Non scaled SANS curves are depicted in III and IV. The insets represent an enlargement of the high q region.

3 Results and discussion

3.1 SANS

In order to elucidate the microstructural aspects of the aggregates' responsiveness to changes in temperature, small-angle neutron scattering (SANS) measurements were performed. SANS curves of nonionized ($\alpha = 0$) and ionized ($\alpha = 1$) surfactant–CD systems at different temperatures are depicted in Fig. 2. We opted for showing in the main text both the intensity-scaled and non-scaled scattering curves: the former allows to highlight of structural features such as correlation peaks and slope changes, and the latter provides a comparison of the evolution of the scattering intensity, proportional to the mass of the aggregates. A further $I(q)q^2$ *vs.* q representation of the data is given in the ESI† (Fig. S3).

Most scattering curves exhibit a q^{-2} power law, the characteristic signature of locally flat structures (Fig. 2. III and IV). The increase of the degree of ionization (α), *e.g.* increase in charge density, provides order to the multilayered structure but without affecting the overall shape and mass of the supramolecular aggregates, as evidenced by the presence of the peaks at mid-q in the SANS curves with a peak-to-peak ratio $q_1/q_2 = 2$ and by the fact that the data exhibit the same scattering intensity at low-q values. Depending on the molecular architecture of the host and guest, the typical spacing of the CD–surfactant layers is 10–15 nm. A table summarizing the different characteristic distances observed in the systems is given in the ESI.† It is important to note that the pure CD solutions are featureless at the given experimental conditions and that the surfactant assembles into simple vesicles ($C_{12}E_5Ac$) and globular micelles ($C_{12}E_{10}Ac$) (see ref. 32 and Fig. S2 in the ESI†).

At $\alpha = 0$, no particular effect of the temperature was observed, except for $C_{12}E_5Ac$-αCD. For this system, the SANS patterns at 15, 25, and 45 °C are equivalent, exhibiting an extended q^{-2} power law at mid q, a decay of the scattering intensity at $\sim$0.6 nm^{-1}. Such scattering patterns, which closely

resemble that of the aqueous solutions of the surfactant,[32] indicate the presence of CD-decorated vesicles in the solution. At 70 °C, a q^{-4} power-law at low-q values is observed, and a pronounced correlation peak appears at q = 0.98 nm^{-1} corresponding to a characteristic size of 6.4 nm. This value corresponds to the length of the surfactant chain, and a correlation peak at $q \sim 1$ nm^{-1} is found in several dense-packed $C_{12}E_5Ac$ systems.[36–38] Moreover, $C_{12}E_5Ac$ was shown to undergo liquid-liquid phase separation around 55 °C.[32] Accordingly, the presence of αCD does not prevent phase separation of the surfactant from the solution. Interestingly, upon the addition of βCD, no temperature-induced structural changes are observed by raising the sample temperature up to 70 °C.

Temperature effects are more marked at $\alpha = 1$, where increasing the temperature from 15 to 45 °C causes the correlation peaks – characteristic of the multilayer structure – to broaden. The broadening of the correlation peak can be ascribed either to a reduction of number of layers in the supramolecular aggregate, or by reducing the long-range order, *i.e.*, by increasing the flexibility of the layer. Both interprepations are consistent with the recorded SANS data. However, a weakening of the later, CD–CD hydrogen bonds which are at the origin of the high rigidity of the inclusion complex layer, is better supported by the endothermic peak observed by differential scanning calorimetry (see next section). Further heating the $C_{12}E_{10}Ac$-αCD and $C_{12}E_5Ac$-βCD complexes at 70 °C, causes the peaks characteristic of the multilayered structure to fully disappear, and a strong single peak appears at $q \approx 0.36$ and 0.44 nm^{-1}, respectively. Such changes in the scattering pattern are consistent with a transition from multilayered aggregates to unilamellar ones, such as disks or vesicles, as found in similar systems.[28,29] In detail, while the two structure peaks at temperatures $\leq$45 °C arise from intra-aggregate correlations, the peak found at 70 °C arises from a typical inter-particle distance of 18 and 14 nm. Similarly, inclusion complexes between sodium dodecyl sulfate and βCD show a structural phase transition from tubular structures to vesicles between 40 and 43 °C.[28,29] The values of the repeating distances found in the investigated complexes are summarized in Table S1 in the ESI.†

Generally, no changes are observed in the CD packing upon the temperature increase for βCD. However, the temperature effect on the CD–CD and CD–water interactions in the lattice assembly can be observed in the high q region for $C_{12}E_{10}Ac$-αCD systems, at $\alpha = 0$ and $\alpha = 1$, and $C_{12}E_5Ac$-αCD ionized systems. For $C_{12}E_5Ac$-αCD, the singular peak observed at q = 4.43 nm^{-1} at low temperatures diverges in two peaks at 3.6 and 5.3 nm^{-1} as the temperature increase indicates changes in the packing lattice. Interestingly, the positions of the peaks at 70 °C are equivalent to the scattering profile observed for the respective nonionic system. Similar transitions are observed for $C_{12}E_{10}Ac$ systems with the same CD at $\alpha = 0$ and $\alpha = 1$.

The structural effect of the different ethylene oxide units and the different behaviour upon thermal stimulus is evidenced at the high q region of $\alpha = 0$ with α-CD of both surfactants in Fig. 2I-a and II-a. Whereas in Fig. 2I-a the scattering curves point to no temperature responsive of the surfactant with smaller number of EO and similar profile for all the temperatures, in Fig. 2II-a, it is possible to observe the lattice phase transition evidenced by the changes in the CD–CD organization.

3.2 Differential scanning calorimetry

Calorimetric methods are well-established techniques to characterize thermodynamically supramolecular structures of surfactants, polymers, inclusion complexes and self-assembled structures. DSC allows to characterize the enthalpic change associated with the structural reorganization observed by small-angle scattering experiments. The DSC thermograms of the different mixtures are shown in Fig. 3, and the obtained enthalpic changes (ΔH) and temperature of the melting peak are given in Fig. 4.

The general trend in the systems is the increase of ΔH with the increase of the surfactants' degree of ionization α. This observation well correlates with the increased crystallinity previously found in self-assembled supramolecular complexes of CD and alkyl ether carboxylic acids with increasing degree of ionization.[16] The values of ΔH are very similar for all mixtures, varying from a basically undetectable transition at low degree of ionization to a value of ΔH of 40 J mol^{-1} of surfactant. An exception is made by the complex formed between $C_{12}E_{10}Ac$ and αCD, which shows a significant endothermic peak also for the surfactant in the nonionic state. The temperature of the transition increases for mixtures of $C_{12}E_5Ac$ with increasing degree of ionization, while an almost constant value of $\approx$40 °C is found for $C_{12}E_{10}Ac$. The increasing melting temperature observed indicates a higher crystal stability with increasing degree of ionization. The fact that this phenomenon is observed for the surfactant with the shorter ethylene oxide spacer only, points towards the importance of the location of the charge in the crystallization of surfactant/CD inclusion complexes.

A further interesting point is given by the fact that the thermograms of αCD complexes show the same onset, except for the mixture at a full degree of ionization. This indicates that for a given surfactant/CD inclusion complex, increasing the degree of ionization causes the amount of structure which are able to melt to increase, but not the energy of the crystal.

Taking into account the results from the SANS analysis, it can be stated that the endothermic peak probed by DSC is correlated with structural changes on the 10–20 nm scale. For all βCD inclusions complexes and the complex of αCD with the non-ionized $C_{12}E_5Ac$, no changes in the CD–CD packing, probed in the high-q region of the scattering pattern could be observed.

Our results agree well with similar studies performed on SDS@2βCD mixtures,[28] where similar values for the melting enthalpy and a melting temperature of approx. 40 °C were found.

4 Conclusions

In summary, we have studied the thermoresponsive behaviour of the hierarchical assemblies of α and β-cyclodextrins and

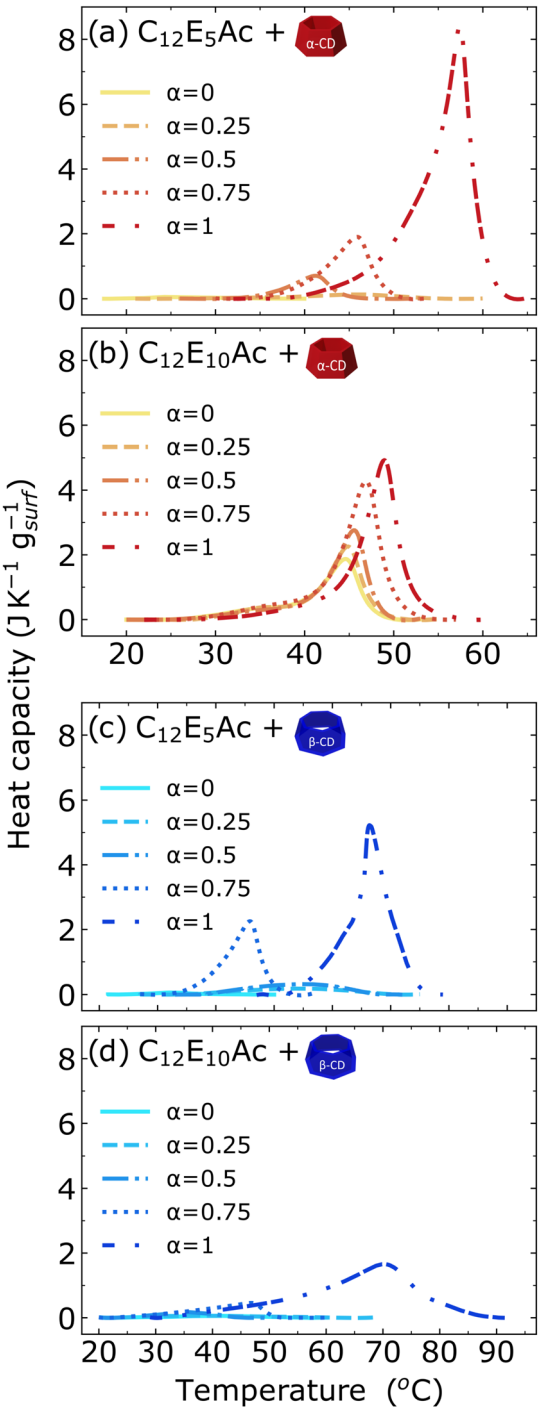

Fig. 3 Thermograms of systems with a CD/Surfactant = 2, ΔH (J K^{-1} g^{-1}) corresponding to the inclusion complexes supramolecular aggregates containing 5 wt% surfactant with αC: (a) $C_{12}E_5Ac$, (b) $C_{12}E_{10}Ac$ and βCD (c) $C_{12}E_5Ac$ and (d) $C_{12}E_{10}Ac$ (exo ↓).

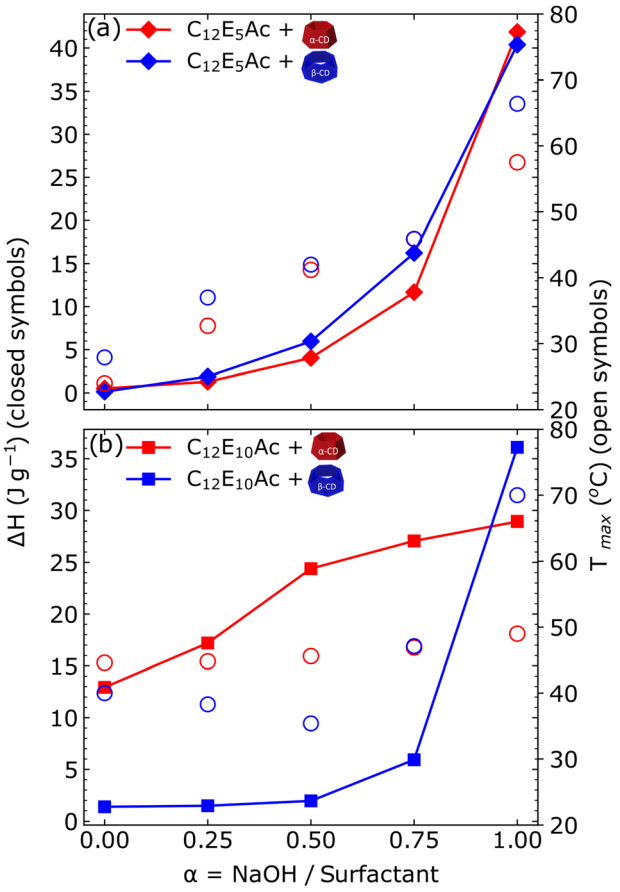

Fig. 4 The enthalpic changes ΔH (J g_{surf}^{-1}) as function of the surfactant's degree of ionization of (a) $C_{12}E_5Ac$ (♦) and (b) $C_{12}E_{10}Ac$ (■) systems and the temperature of the melting peak (○) corresponding to the assembled systems containing 5 wt% surfactant with αCD (red) and βCD (blue).

weakly anionic alkyl oligoethylene oxide carboxylic acids. The presence of a weakly acidic surfactant head group allowed us to probe the effect of the surfactant degree of ionization on the thermoresponsive properties of the inclusion complex supramolecular assemblies. This represents an important advantage with respect to previous studies performed either with strongly ionic or nonionic surfactants.[9,25,27–29]

Small-angle neutron scattering experiments indicate that the presence of electrostatic repulsion is required for the formation of well-defined, ordered supramolecular structures. Increasing the temperature up to 70 °C softens the structures, providing a loss of internal order. The structural data were complemented with differential scanning calorimetry, which allowed us to probe the effect of the surfactant's degree of ionization on the inclusion complex crystal stability. In particular, the experiments evidenced the importance of the presence of charges to induce the crystallization of the layered inclusion complexes. In our previous investigation on the effect of surfactant charge density on the structure of the supramolecular assemblies,[16] we pointed out that a certain degree of ionization of the surfactant is required for the formation of ordered aggregates. We rationalized the finding in terms of electrostatic repulsion between the layers, which promotes the transition from a disordered multilayered structure to a more ordered one. The novel results presented herein point towards a more complex situation. Not only the presence of charges provides electrostatic repulsion to the bilayers, but it

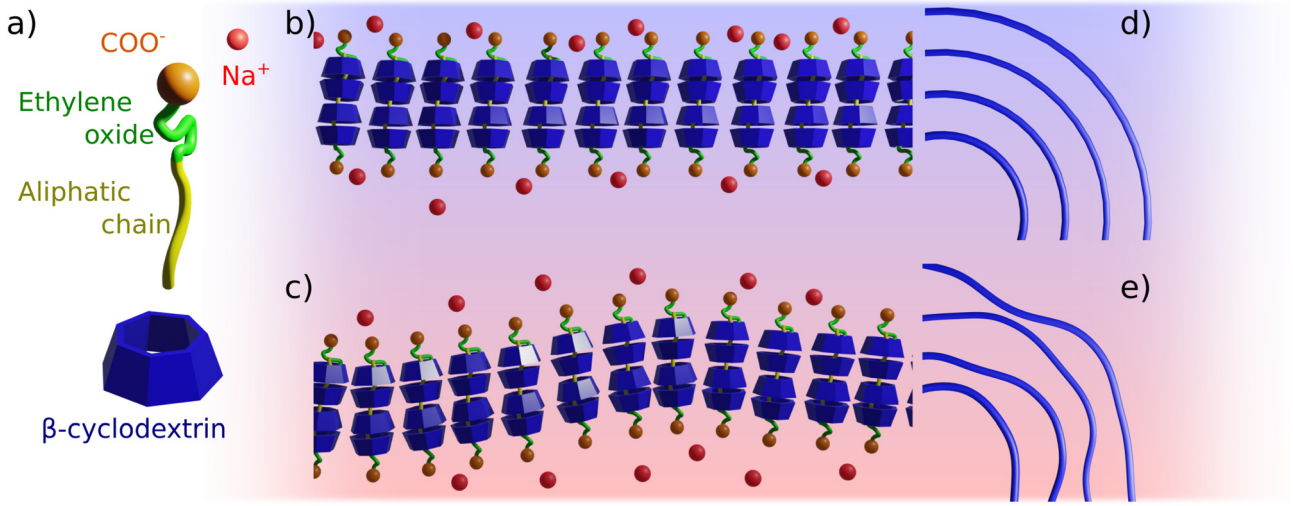

Fig. 5 Schematic representation of the inclusion complex membrane softening induced by increasing temperature, on the example of the fully ionized sodium alkylether carboxylate treaded with β-cyclodextrin. (a) overview on the components of the system; (b and c) represent the bilayer structure at low and high temperature respectively; (d and e) represent the multilayer structure at low and high temperature, respectively.

induces crystallization of the same, thus, very likely, increasing the membrane rigidity.

Temperature might affect the system in many different ways, *e.g.*, by changing the solubility of the cyclodextrins and of the inclusion complexes, it causes a partial dehydration of the surfactant head group, it may cause unthreading events, and, finally, it affects the CD/CD in-plane interactions. It is useful to make some consideration to contextualize the relative importance of the different phenomena. No changes in solubility was detected by visual inspection of the samples, and the fact that the scattering intensity at low-q remains unchanged, allow us to rule out that the observed effects arise from solubility changes in the system and from unthreading events. This observation is in agreement with thermodynamic studies, which show that the equilibrium constant for the formation of CD–surfactant inclusion complexes – albeit decreasing with increasing temperature – remains significant with $K_{eq} \gg 10^4\ M^{-1}$.[39,40,41] At the given experimental conditions, assuming a binding constant of $10^4\ M^{-1}$, only 0.2 mol% of the surfactant would be unthreaded. Furthermore, increasing the temperature causes the oligoethylene oxide units of the surfactant to dehydrate, at least at a low degree of ionization. However, the head group area at low temperature is 58 and 86 Å^2 at low pH and 123 and 130 Å^2 at high pH, for $C_{12}E_5Ac$ and $C_{12}E_{10}Ac$, respectively.[32] The area occupied by α and βCD is 181 and 243 Å^2, respectively. Accordingly, we do not expect any effect of temperature on the geometry of the inclusion complexes, since the packing is determined by the size of the cyclodextrins. Finally, the most likely event to occur is the weakening of the hydrogen bonds between adjacent cyclodextrin molecules, with their partial replacement with CD solvent ones. These bonds represents the weakest interactions in the system, thus the first ones who can be disrupted by increasing the systems' temperature. The weakening of these later, CD–CD bonds is also in agreement with the observed DSC and SANS results. A schematic representation of this phenomenon is given in Fig. 5.

To conclude, cyclodextrin/surfactant complexes have been shown to be extremely versatile systems, owing to the broad variety of stimuli they can respond to. Accordingly, they are excellent candidates for the design of multi-responsive systems. Recent studies have been focused on the characterization of CD inclusion complexes which respond to more than one trigger.[25,26,42] Hence, alkyl oligoethylene oxide carboxylic acids-cyclodextrin complexes and their multiple responsiveness demonstrate the importance of understanding the interplay of interactions and the thermal and ionic effects on the formation and morphology of supramolecular assemblies of cyclodextrin/surfactant complexes. It also reinforces the importance of unveiling fundamental properties and dynamics aiming for the smart use of guests in developing building blocks that can further assemble to finally be able to direct them to the suitable application.

Author contributions

LSSA prepared samples, performed experiments, and wrote the manuscript. GL and LC reviewed the data critically and edited the manuscript. LSSA and LC conceived the experiments. GL and LC contributed to funding acquisition.

Conflicts of interest

There are no conflicts to declare.

Acknowledgements

L. S. S. A. is grateful to the ILL and the University of Palermo for a doctoral fellowship through the ILL PhD program. The ILL is

acknowledged for providing beamtime on the D22 SANS instruments (data available at https://doi.ill.fr/10.5291/ILL-DATA.INTER-532), and the support of Lionel Porcar during the SANS experiments is heartily acknowledged. The partnership for soft condensed matter (PSCM) is acknowledged for providing the calorimeter and the laboratory infrastructure for sample preparation and pre-characterization.

Notes and references

1 A. J. Valente and O. Söderman, The formation of host-guest complexes between surfactants and cyclodextrins, *Adv. Colloid Interface Sci.*, 2014, **205**, 156–176.
2 R. De Lisi, G. Lazzara and S. Milioto, Temperature-controlled poly(propylene) glycol hydrophobicity on the formation of inclusion complexes with modified cyclodextrins. A DSC and ITC study, *Phys. Chem. Chem. Phys.*, 2011, **13**, 12571–12577.
3 A. Harada, Y. Takashima and M. Nakahata, Supramolecular Polymeric Materials via Cyclodextrin-Guest Interactions, *Acc. Chem. Res.*, 2014, **47**, 2128–2140.
4 J. Wankar, N. G. Kotla, S. Gera, S. Rasala, A. Pandit and Y. A. Rochev, Recent Advances in Host-Guest Self-Assembled Cyclodextrin Carriers: Implications for Responsive Drug Delivery and Biomedical Engineering, *Adv. Funct. Mater.*, 2020, **30**, 1909049.
5 L. dos Santos Silva Araújo, G. Lazzara and L. Chiappisi, Cyclodextrin/surfactant inclusion complexes: An integrated view of their thermodynamic and structural properties, *Adv. Colloid Interface Sci.*, 2021, **289**, 1–12.
6 S. Yang, Y. Yan, J. Huang, A. V. Petukhov, L. M. J. Kroon-Batenburg, M. Drechsler, C. Zhou, M. Tu, S. Granick and L. Jiang, Giant capsids from lattice self-assembly of cyclodextrin complexes, *Nat. Commun.*, 2017, **8**, 15856.
7 W. Saenger and T. Steiner, Cyclodextrin Inclusion Complexes: Host-Guest Interactions and Hydrogen-Bonding Networks, *Acta Crystallogr., Sect. A: Found. Crystallogr.*, 1998, **A54**, 798–805.
8 L. Liu and Q. X. Guo, The driving forces in the inclusion complexation of cyclodextrins, *J. Inclusion Phenom.*, 2002, **42**, 1–14.
9 J. Carlstedt, A. Bilalov, E. Krivtsova, U. Olsson and B. Lindman, Cyclodextrin–surfactant coassembly depends on the cyclodextrin ability to crystallize, *Langmuir*, 2012, **28**, 2387–2394.
10 J. Landman, S. Ouhajji, S. Prévost, T. Narayanan, J. Groenewold, A. P. Philipse, W. K. Kegel and A. V. Petukhov, Inward growth by nucleation: Multiscale self-assembly of ordered membranes, *Sci. Adv.*, 2018, **4**, 1–8.
11 H. Wang, J. C. Wagner, W. Chen, C. Wang and W. Xiong, Spatially dependent H-bond dynamics at interfaces of water/biomimetic self-assembled lattice materials, *Proc. Natl. Acad. Sci. U. S. A.*, 2020, **117**, 23385–23392.
12 K. Liu, C. Ma, T. Wu, W. Qi, Y. Yan and J. Huang, Recent advances in assemblies of cyclodextrins and amphiphiles: construction and regulation, *Curr. Opin. Colloid Interface Sci.*, 2020, **45**, 44–56.
13 Y. Wang, N. Ma, Z. Wang and X. Zhang, Photocontrolled reversible supramolecular assemblies of an azobenzene-containing surfactant with α-cyclodextrin, *Angew. Chem., Int. Ed.*, 2007, **46**, 2823–2826.
14 P. Xing, H. Chen, M. Ma, X. Xu, A. Hao and Y. Zhao, Light and cucurbit[7]uril complexation dual-responsiveness of a cyanostilbene-based self-assembled system, *Nanoscale*, 2016, **8**, 1892–1896.
15 X. Zhang, X. Ma, K. Wang, S. Lin, S. Zhu, Y. Dai and F. Xia, Recent Advances in Cyclodextrin-Based Light-Responsive Supramolecular Systems, *Macromol. Rapid Commun.*, 2018, **39**, 1–12.
16 L. dos Santos Silva Araújo, L. Watson, D. A. Traore, G. Lazzara and L. Chiappisi, Hierarchical assembly of pH-responsive surfactant-cyclodextrin complexes, *Soft Matter*, 2022, **18**, 6529–6537.
17 B. Jiang, H. Guo, L. Zhao, B. Xu, C. Wang, C. Liu and H. Fan, Fabrication of a *β*-cyclodextrin-based self-assembly containing a redox-responsive ferrocene, *Soft Matter*, 2019, **16**, 125–131.
18 C. Zuo, X. Dai, S. Zhao, X. Liu, S. Ding, L. Ma, M. Liu and H. Wei, Fabrication of dual-redox responsive supramolecular copolymers using a reducible *β* -cyclodextran-ferrocene double-head unit, *ACS Macro Lett.*, 2016, **5**, 873–878.
19 H. Zhang, W. An, Z. Liu, A. Hao, J. Hao, J. Shen, X. Zhao, H. Sun and L. Sun, Redox-responsive vesicles prepared from supramolecular cyclodextrin amphiphiles, *Carbohydr. Res.*, 2010, **345**, 87–96.
20 C. Zhou, X. Cheng, Q. Zhao, Y. Yan, J. Wang and J. Huang, Self-assembly of nonionic surfactant tween 20@2*β*-CD inclusion complexes in dilute solution, *Langmuir*, 2013, **29**, 13175–13182.
21 A. A. Rafati and F. Safatian, Thermodynamic studies of inclusion complex between cetyltrimethylammonium bromide (CTAB) and β-cyclodextrin (*β* -CD) in water/n-butanol mixture, using potentiometric technique, *Phys. Chem. Liq.*, 2008, **46**, 587–598.
22 C. Perry, P. Hébraud, V. Gernigon, C. Brochon, A. Lapp, P. Lindner and G. Schlatter, Pluronic and β-cyclodextrin in water: From swollen micelles to self-assembled crystalline platelets, *Soft Matter*, 2011, **7**, 3502–3512.
23 G. Lazzara, G. Olofsson, V. Alfredsson, K. Zhu, B. Nyström and K. Schillén, Temperature-responsive inclusion complex of cationic PNIPAAM diblock copolymer and *γ* -cyclodextrin, *Soft Matter*, 2012, **8**, 5043–5054.
24 A. Wang, W. Shi, J. Huang and Y. Yan, Adaptive soft molecular self-assemblies, *Soft Matter*, 2016, **12**, 337–357.
25 L. Jiang, Y. Yan and J. Huang, Zwitterionic surfactant/cyclodextrin hydrogel: microtubes and multiple responses, *Soft Matter*, 2011, **7**, 10417.
26 J. Wang, Q. Li, S. Yi and X. Chen, Visible-light/temperature dual-responsive hydrogel constructed by α-cyclodextrin and an azobenzene linked surfactant, *Soft Matter*, 2017, **13**, 6490–6498.

27 J. Zhang and X. Shen, Temperature-induced reversible transition between vesicle and supramolecular hydrogel in the aqueous ionic liquid-β-cyclodextrin system, *J. Phys. Chem. B*, 2013, **117**, 1451–1457.
28 C. Zhou, X. Cheng, Y. Yan, J. Wang and J. Huang, Reversible transition between SDS@2β -CD microtubes and vesicles triggered by temperature, *Langmuir*, 2014, **30**, 3381–3386.
29 S. Ouhajji, J. Landman, S. Prévost, L. Jiang, A. P. Philipse and A. V. Petukhov, In situ observation of self-assembly of sugars and surfactants from nanometres to microns, *Soft Matter*, 2017, **13**, 2421–2425.
30 J. W. De Folter, P. Liu, L. Jiang, A. Kuijk, H. E. Bakker, A. Imhof, A. Van Blaaderen, J. Huang, W. K. Kegel, A. P. Philipse and A. V. Petukhov, Self-organization of anisotropic and binary colloids in thermo-switchable 1D microconfinement, *Part. Part. Syst. Charact.*, 2015, **32**, 313–320.
31 L. Jiang, J. W. De Folter, J. Huang, A. P. Philipse, W. K. Kegel and A. V. Petukhov, Helical colloidal sphere structures through thermo-reversible co-assembly with molecular microtubes, *Angew. Chem., Int. Ed.*, 2013, **52**, 3364–3368.
32 L. Chiappisi, Polyoxyethylene alkyl ether carboxylic acids: An overview of a neglected class of surfactants with multi-responsive properties, *Adv. Colloid Interface Sci.*, 2017, **250**, 79–94.
33 D. W. Hayward, L. Chiappisi, J. H. Teo, S. Prévost, R. Schweins and M. Gradzielski, Neutralisation rate controls the self-assembly of pH-sensitive surfactants, *Soft Matter*, 2019, **15**, 8611–8620.
34 I. Laue-Langevin, D22-Large dynamic range small-angle diffractometer (Institut Laue-Langevin), 2003, **https://www.ill.eu/users/instruments/instruments-list/d22/description/instrument-layout**.
35 A. Cisse, J. Peters, G. Lazzara and L. Chiappisi, PyDSC: a simple tool to treat differential scanning calorimetry data, *J. Therm. Anal. Calorim.*, 2021, **145**, 403–409.
36 L. Chiappisi, I. Hoffmann and M. Gradzielski, Membrane stiffening in Chitosan mediated multilamellar vesicles of alkyl ether carboxylates, *J. Colloid Interface Sci.*, 2022, **627**, 160–167.
37 L. Chiappisi, S. Prévost, I. Grillo and M. Gradzielski, From crab shells to smart systems: Chitosan-alkylethoxy carboxylate complexes, *Langmuir*, 2014, **30**, 10615–10616.
38 S. Micciulla, D. W. Hayward, Y. Gerelli, A. Panzarella, R. von Klitzing, M. Gradzielski and L. Chiappisi, One-step procedure for the preparation of functional polysaccharide/fatty acid multilayered coatings, *Commun. Chem.*, 2019, **2**, 1–12.
39 M. Benko and Z. Király, Thermodynamics of inclusion complex formation of β-cyclodextrin with a variety of surfactants differing in the nature of headgroup, *J. Chem. Thermodyn.*, 2012, **54**, 211–216.
40 R. Lu, J. Hao, H. Wang and L. Tong, Determination of association constants for cyclodextrin–surfactant inclusion complexes: A numerical method based on surface tension measurements, *J. Colloid Interface Sci.*, 1997, **192**, 37–42.
41 P. Brocos, X. Banquy, N. Díaz-Vergara, S. Pérez-Casas, Á. Piñeiro and M. Costas, A critical approach to the thermodynamic characterization of inclusion complexes: Multiple-temperature isothermal titration calorimetric studies of native cyclodextrins with sodium dodecyl sulfate, *J. Phys. Chem. B*, 2011, **115**, 14381–14396.
42 J. Shen, J. Pang, T. Kalwarczyk, R. Hołyst, X. Xin, G. Xu, X. Luan and Y. Yang, Manipulation of multiple-responsive fluorescent supramolecular materials based on the inclusion complexation of cyclodextrins with Tyloxapol, *J. Mater. Chem. C*, 2015, **3**, 8104–8113.

Bibliography

1. Zandi, R. & Reguera, D. Mechanical properties of viral capsids. *Physical Review E - Statistical, Nonlinear and Soft Matter Physics* **72,** 21917. ISSN: 15393755 (2005).
2. Morin-Crini, N. *et al.* 130 Years of Cyclodextrin Discovery for Health, Food, Agriculture, and the Industry: a Review. *Environmental Chemistry Letters* **19,** 2581–2617. ISSN: 16103661 (2021).
3. Hayward, D. W. *et al.* Neutralisation rate controls the self-assembly of pH-sensitive surfactants. *Soft Matter* **15,** 8611–8620. ISSN: 17446848 (2019).
4. Micciulla, S. *et al.* One-step procedure for the preparation of functional polysaccharide/fatty acid multilayered coatings. *Communications Chemistry* **2,** 1–11. ISSN: 23993669 (2019).
5. Chiappisi, L., Prévost, S., Grillo, I. & Gradzielski, M. From crab shells to smart systems: Chitosan-alkylethoxy carboxylate complexes. *Langmuir* **30,** 10615–10616. ISSN: 15205827 (2014).
6. Valente, A. J. & Söderman, O. The formation of host-guest complexes between surfactants and cyclodextrins. *Advances in Colloid and Interface Science* **205,** 156–176. ISSN: 00018686 (2014).
7. Sabadini, E., Cosgrove, T. & Egídio, F. D. C. Solubility of cyclomaltooligosaccharides (cyclodextrins) in H2O and D2O: A comparative study. *Carbohydrate Research* **341,** 270–274. ISSN: 00086215 (2006).
8. Raffaini, G. & Ganazzoli, F. Hydration and flexibility of α-, β-, γ- and δ-cyclodextrin: A molecular dynamics study. *Chemical Physics* **333,** 128–134. ISSN: 03010104 (2007).
9. Dos Santos Silva Araújo, L., Lazzara, G. & Chiappisi, L. Cyclodextrin/surfactant inclusion complexes: An integrated view of their thermodynamic and structural properties. *Advances in Colloid and Interface Science* **289,** 1–11. ISSN: 00018686 (2021).
10. Liu, L. & Guo, Q. X. The driving forces in the inclusion complexation of cyclodextrins. *Journal of Inclusion Phenomena* **42,** 1–14. ISSN: 09230750 (2002).

11. Dodziuk, H. *Cyclodextrins and Their Complexes: Chemistry, Analytical Methods, Applications* 1–473. ISBN: 3527312803 (Wiley Online Library, 2006).

12. Singh, A., Worku, Z. A. & Van Den Mooter, G. Oral formulation strategies to improve solubility of poorly water-soluble drugs. *Expert Opinion on Drug Delivery* **8,** 1361–1378. ISSN: 17425247 (2011).

13. Loftsson, T. & Brewster, M. E. Cyclodextrins as functional excipients: Methods to enhance complexation efficiency. *Journal of Pharmaceutical Sciences* **101,** 3019–3032. ISSN: 15206017 (2012).

14. Jambhekar, S. S. & Breen, P. Cyclodextrins in pharmaceutical formulations I: Structure and physicochemical properties, formation of complexes, and types of complex. *Drug Discovery Today* **21,** 356–362. ISSN: 18785832 (2016).

15. Muankaew, C. & Loftsson, T. Cyclodextrin-Based Formulations: A Non-Invasive Platform for Targeted Drug Delivery. *Basic and Clinical Pharmacology and Toxicology* **122,** 46–55. ISSN: 17427843 (2018).

16. Szejtli, J. *Medicinal Applications of Cyclodextrins* **3,** 353–386. ISBN: 2610140304 (1994).

17. Shepelytskyi, Y. *et al.* Cyclodextrin-based contrast agents for medical imaging. *Molecules* **25,** 13–17. ISSN: 14203049 (2020).

18. Buschmann, H. J. & Schollmeyer, E. Applications of cyclodextrins in cosmetic products: A review. *Journal of Cosmetic Science* **53,** 185–191. ISSN: 00379832 (2002).

19. Santos, A. C. *et al.* Nanotechnology for the development of new cosmetic formulations. *Expert Opinion on Drug Delivery* **16,** 313–330. ISSN: 17447593 (2019).

20. Parmar, V., Patel, G. & Abu-Thabit, N. Y. *Responsive cyclodextrins as polymeric carriers for drug delivery applications* 555–580. ISBN: 9780081019979 (Elsevier Ltd., 2018).

21. Coleman, A. W., Nicolis, I., Keller, N. & Dalbiez, J. P. Aggregation of cyclodextrins: An explanation of the abnormal solubility of β-cyclodextrin. *Journal of Inclusion Phenomena and Molecular Recognition in Chemistry* **13,** 139–143. ISSN: 09230750 (1992).

22. Vargas, C., Schönbeck, C., Heimann, I. & Keller, S. Extracavity Effect in Cyclodextrin/Surfactant Complexation. *Langmuir* **34,** 5781–5787. ISSN: 15205827 (2018).

23. Junquera, E., Peña, L. & Aicart, E. A Conductimetric Study of the Interaction of β-Cyclodextrin or Hydroxypropyl-β-cyclodextrin with Dodecyltrimethylammonium Bromide in Water Solution. *Langmuir* **11,** 4685–4690. ISSN: 15205827 (Dec. 1995).

24. Maccarrone, S., Magazù, S., Migliardo, F. & Mondio, F. M. Small-angle neutron scattering and inelastic neutron scattering studies on β-cyclodextrins and hydroxypropyl-β-cyclodextrins. *Physica B: Condensed Matter* **350,** 615–618. ISSN: 09214526 (2004).

25. Wu, C., Xie, Q., Xu, W., Tu, M. & Jiang, L. Lattice self-assembly of cyclodextrin complexes and beyond. *Current Opinion in Colloid and Interface Science* **39,** 76–85. ISSN: 18790399 (2019).

26. Carlstedt, J., Bilalov, A., Krivtsova, E., Olsson, U. & Lindman, B. Cyclodextrin-surfactant coassembly depends on the cyclodextrin ability to crystallize. *Langmuir* **28,** 2387–2394. ISSN: 07437463 (2012).

27. Jiang, L. *et al.* "Annular ring" microtubes formed by SDS@2β-CD complexes in aqueous solution. *Soft Matter* **6,** 1731–1736. ISSN: 1744683X (2010).

28. Jiang, L., Yan, Y., Drechsler, M. & Huang, J. Enzyme-triggered model self-assembly in surfactant-cyclodextrin systems. *Chemical Communications* **48,** 7347–7349. ISSN: 1364548X (2012).

29. Benko, M. & Király, Z. Thermodynamics of inclusion complex formation of β-cyclodextrin with a variety of surfactants differing in the nature of headgroup. *Journal of Chemical Thermodynamics* **54,** 211–216. ISSN: 00219614 (2012).

30. Ondo, D. & Costas, M. Complexation thermodynamics of α-cyclodextrin with ionic surfactants in water. *Journal of Colloid and Interface Science* **505,** 445–453. ISSN: 10957103 (2017).

31. Luviano, A. S. *et al.* Highly viscoelastic films at the water/air interface: α-Cyclodextrin with anionic surfactants. *Journal of Colloid and Interface Science* **565,** 601–613. ISSN: 10957103 (2020).

32. Rafati, A. A. & Safatian, F. Thermodynamic studies of inclusion complex between cetyltrimethylammonium bromide (CTAB) and β-cyclodextrin (β-CD) in water/n-butanol mixture, using potentiometric technique. *Physics and Chemistry of Liquids* **46,** 587–598. ISSN: 00319104 (2008).

33. González-Gaitano, G., Crespo, A. & Tardajos, G. Thermodynamic Investigation (Volume and Compressibility) of the Systems β-Cyclodextrin + n-Alkyltrimethylammonium Bromides + Water. *Journal of Physical Chemistry B* **104,** 1869–1879. ISSN: 10895647 (2000).

34. Topchieva, I. & Karezin, K. Self-assembled supramolecular micellar structures based on non-ionic surfactants and cyclodextrins. *Journal of Colloid and Interface Science* **213,** 29–35. ISSN: 00219797 (1999).

35. Popova, E. I. & Topchieva, I. N. Complex formation between polyethylene oxide-containing nonionic surfactants and α-and β-cyclodextrins. *Russian Chemical Bulletin* **50,** 620–625. ISSN: 10665285 (2001).

36. Araujo Marques, I. *et al.* Formation and self-association of host-guest complexes between βCD and nonionic surfactants Brij. *Journal of Molecular Liquids* **338,** 116647. ISSN: 01677322 (2021).

37. Zhou, C. *et al.* Self-assembly of nonionic surfactant tween 20@2β-CD inclusion complexes in dilute solution. *Langmuir* **29,** 13175–13182. ISSN: 07437463 (2013).

38. Alami, E., Abrahmsén-Alami, S., Eastoe, J., Grillo, I. & Heenan, R. K. Interactions between a nonionic gemini surfactant and cyclodextrins investigated by small-angle neutron scattering. *Journal of Colloid and Interface Science* **255,** 403–409. ISSN: 00219797 (2002).

39. Benkö, M., Király, L. A., Puskás, S. & Király, Z. Complexation of β-cyclodextrin with a gemini surfactant studied by isothermal titration microcalorimetry and surface tensiometry. *Langmuir* **30,** 6756–6762. ISSN: 15205827 (2014).

40. Guerrero-Martínez, A. *et al.* Solid Crystal Network of Self-Assembled Cyclodextrin and Nonionic Surfactant Pseudorotaxanes. *The Journal of Physical Chemistry B* **114,** 11489–11495. ISSN: 1520-6106 (Sept. 2010).

41. Nilsson, M., Valente, A. J., Olofsson, G., Söderman, O. & Bonini, M. Thermodynamic and kinetic characterization of host-guest association between bolaform surfactants and α- and β-cyclodextrins. *Journal of Physical Chemistry B* **112,** 11310–11316. ISSN: 15206106 (2008).

42. Cabaleiro-Lago, C., Nilsson, M., Valente, A. J., Bonini, M. & Söderman, O. NMR diffusometry and conductometry study of the host-guest association between β-cyclodextrin and dodecane 1,12-bis(trimethylammonium bromide). *Journal of Colloid and Interface Science* **300,** 782–787. ISSN: 00219797 (2006).

43. Kupfer, R. & De, H. (12) Patent Application Publication (10) Pub. No.: US 2003/0194388A1. **1** (2003).

44. Ohmae, K. (12) United States Patent. **2** (2012).

45. Renoncourt, A. *et al.* Spontaneous vesicle formation of an industrial single-chain surfactant at acidic pH and at room-temperature. *ChemPhysChem* **7,** 1892–1896. ISSN: 14397641 (2006).

46. Chiappisi, L. Polyoxyethylene alkyl ether carboxylic acids: An overview of a neglected class of surfactants with multiresponsive properties. *Advances in Colloid and Interface Science* **250,** 79–94. ISSN: 00018686 (2017).

47. Israelachvili, J. N., Mitchell, D. J. & Ninham, B. W. Theory of self-assembly of hydrocarbon amphiphiles into micelles and bilayers. *Journal of the Chemical Society, Faraday Transactions 2: Molecular and Chemical Physics* **72,** 1525–1568. ISSN: 03009238 (1976).

48. Israelachvili, J. N. *Intermolecular and Surface Forces: Third Edition* 3rd editio, 1–676. ISBN: 9780123919274 (Academic Press, London, 2011).

49. Chiappisi, L. Polyoxyethylene alkyl ether carboxylic acids: An overview of a neglected class of surfactants with multiresponsive properties. *Advances in Colloid and Interface Science* **250,** 79–94. ISSN: 00018686 (2017).

50. Vlachy, N. *et al.* Spontaneous formation of bilayers and vesicles in mixtures of single-chain alkyl carboxylates: Effect of pH and aging and cytotoxicity studies. *Langmuir* **24,** 9983–9988. ISSN: 07437463 (2008).

51. Chiappisi, L., Prévost, S., Grillo, I. & Gradzielski, M. Chitosan/alkylethoxy carboxylates: A surprising variety of structures. *Langmuir* **30,** 1778–1787. ISSN: 07437463 (2014).

52. Rocha, B. C., Paul, S. & Vashisth, H. Role of entropy in colloidal self-assembly. *Entropy* **22,** 1–4. ISSN: 10994300 (2020).

53. De Lisi, R., Lazzara, G., Milioto, S. & Muratore, N. Characterization of the Cyclodextrin-Surfactant Interactions by Volume and Enthalpy. *Journal of Physical Chemistry B* **107,** 13150–13157. ISSN: 15206106 (2003).

54. Bouchemal, K. & Mazzaferro, S. How to conduct and interpret ITC experiments accurately for cyclodextrin-guest interactions. *Drug Discovery Today* **17,** 623–629. ISSN: 13596446 (2012).

55. Cabaleiro-Lago, C., Nilsson, M. & Söderman, O. Self-diffusion NMR studies of the host-guest interaction between β-cyclodextrin and alkyltrimethylammonium bromide surfactants. *Langmuir* **21,** 11637–11644. ISSN: 07437463 (2005).

56. Petek, A., Krajnc, M. & Petek, A. Study of host–guest interaction between ß-cyclodextrin and alkyltrimethylammonium bromides in water. *Journal of Inclusion Phenomena and Macrocyclic Chemistry* **86,** 221–229. ISSN: 15731111 (2016).

57. Jiang, L., Yan, Y. & Huang, J. Versatility of cyclodextrins in self-assembly systems of amphiphiles. *Advances in Colloid and Interface Science* **169,** 13–25. ISSN: 00018686 (2011).

58. Saenger, W. Crystal packing patterns of cyclodextrin inclusion complexes. *Journal of Inclusion Phenomena* **2,** 445–454. ISSN: 01677861 (1984).

59. Saenger, W. & Steiner, T. Cyclodextrin Inclusion Complexes: Host-Guest Interactions and Hydrogen-Bonding Networks. *Acta Crystallographica Section A: Foundations of Crystallography* **A54,** 798–805. ISSN: 01087673 (1998).

60. Landman, J. *et al.* Inward growth by nucleation: Multiscale self-assembly of ordered membranes. *Science Advances* **4,** 1–8. ISSN: 23752548 (2018).

61. Amiel, C., Galant, C. & Auvray, L. Ternary complexes involving a β-cyclodextrin polymer, a cationic surfactant and an anionic polymer. *Progress in Colloid and Polymer Science* **126,** 44–46. ISSN: 0340255X (2004).

62. Galant, C., Amiel, C., Wintgens, V., Sébille, B. & Auvray, L. Ternary complexes with poly(β-cyclodextrin), cationic surfactant, and polyanion in dilute aqueous solution: A viscometric and small-angle neutron scattering study. *Langmuir* **18,** 9687–9695. ISSN: 07437463 (2002).

63. Li, Z. *et al.* Sodium dodecyl sulfate/β-cyclodextrin vesicles embedded in chitosan gel for insulin delivery with pH-selective release. *Acta Pharmaceutica Sinica B* **6,** 344–351. ISSN: 22113843 (2016).

64. Zhou, C., Huang, J. & Yan, Y. Chain length dependent alkane/β-cyclodextrin nonamphiphilic supramolecular building blocks. *Soft Matter* **12,** 1579–1585. ISSN: 17446848 (2016).

65. Ouhajji, S. *et al.* In situ observation of self-assembly of sugars and surfactants from nanometres to microns. *Soft Matter* **13,** 2421–2425. ISSN: 17446848 (2017).

66. Jiang, L., Peng, Y., Yan, Y. & Huang, J. Aqueous self-assembly of SDS@2β-CD complexes: Lamellae and vesicles. *Soft Matter* **7,** 1726–1731. ISSN: 1744683X (2011).

67. Mariano, M., Bernardinelli, O. D., Pires-Oliveira, R., Ferreira, G. A. & Loh, W. Inclusion Complexation between α-Cyclodextrin and Oligo(ethylene glycol) Methyl Ether Methacrylate. *ACS Omega* **5,** 9517–9528. ISSN: 24701343 (2020).

68. Harada, A., Nishiyama, T., Kawaguchi, Y., Okada, M. & Kamachi, M. Preparation and characterization of inclusion complexes of aliphatic polyesters with cyclodextrins. *Macromolecules* **30,** 7115–7118. ISSN: 00249297 (1997).

69. Makedonopoulou, S. & Mavridis, I. M. Structure of the inclusion complex of β-cyclodextrin with 1,12-dodecanedioic acid using synchrotron radiation data; a detailed dimeric β-cyclodextrin structure. *Acta Crystallographica Section B: Structural Science* **56,** 322–331. ISSN: 01087681 (2000).

70. Wang, A., Shi, W., Huang, J. & Yan, Y. Adaptive soft molecular self-assemblies. *Soft Matter* **12,** 337–357. ISSN: 17446848 (2016).

71. Wang, J., Wang, T., Liu, X., Lu, Y. & Geng, J. Multiple-responsive supramolecular vesicle based on azobenzene-cyclodextrin host-guest interaction. *RSC Advances* **10,** 18572–18580. ISSN: 20462069 (2020).

72. Jiang, L., Yan, Y. & Huang, J. Zwitterionic surfactant/cyclodextrin hydrogel: microtubes and multiple responses. *Soft Matter* **7,** 10417. ISSN: 1744-683X (2011).

73. He, Y., Fu, P., Shen, X. & Gao, H. Cyclodextrin-based aggregates and characterization by microscopy. *Micron* **39,** 495–516. ISSN: 09684328 (2008).

74. Schmidtchen, F. P. in *Analytical Methods in Supramolecular Chemistry* (ed Schalley, C. A.) 2nd, 55–78 (2007). ISBN: 9783527315055.

75. Biedermann, F., Nau, W. M. & Schneider, H. J. The Hydrophobic Effect Revisited - Studies with Supramolecular Complexes Imply High-Energy Water as a Noncovalent Driving Force. *Angewandte Chemie - International Edition* **53,** 11158–11171. ISSN: 15213773 (2014).

76. Briggner, L. E. & Wadsö, I. Heat capacities of maltose, maltotriose, maltotetrose and α-, β-, and γ-cyclodextrin in the solid state and in dilute aqueous solution. *The Journal of Chemical Thermodynamics* **22,** 1067–1074. ISSN: 10963626 (1990).

77. Rekharsky, M. V. & Inoue, Y. Complexation thermodynamics of cyclodextrins. *Chemical Reviews* **98,** 1875–1917. ISSN: 00092665 (1998).

78. Okubo, T., Kitano, H. & Ise, N. Conductometric studies on association of cyclodextrin with colloidal electrolytes. *Journal of Physical Chemistry* **80,** 2661–2664. ISSN: 00223654 (1976).

79. Martin, J. V, Turmine, M, Letellier, P & Hemery, P. Study of β-Cyclodextrin / Dodecyltrimethylammonium Bromide Complex Into Water-Isopropanol Mixtures. *Electrochimica Acta* **40,** 2749–2753 (1995).

80. Zhou, C., Cheng, X., Yan, Y., Wang, J. & Huang, J. Reversible transition between SDS@2β-CD microtubes and vesicles triggered by temperature. *Langmuir* **30,** 3381–3386. ISSN: 15205827 (2014).

81. Loh, W., Brinatti, C. & Tam, K. C. Use of isothermal titration calorimetry to study surfactant aggregation in colloidal systems. *Biochimica et Biophysica Acta - General Subjects* **1860,** 999–1016. ISSN: 18728006 (2016).

82. Gharibi, H., Jalili, S. & Rajabi, T. Electrochemical studies of interaction between ceyltrimethylammonium bromide and α-, β-cyclodextrins at various temperature. *Colloids and Surfaces A: Physicochemical and Engineering Aspects* **175,** 361–369. ISSN: 09277757 (2000).

83. Benkő, M., Tabajdi, R. & Király, Z. Thermodynamics of formation of β-cyclodextrin inclusion complexes with four series of surfactant homologs. *Journal of Thermal Analysis and Calorimetry* **112,** 969–976. ISSN: 13886150 (2013).

84. Dos Santos Silva Araújo, L., Watson, L., Traore, D. A., Lazzara, G. & Chiappisi, L. Hierarchical assembly of pH-responsive surfactant-cyclodextrin complexes. *Soft Matter* **18,** 6529–6537. ISSN: 17446848 (2022).

85. Ondo, D. Thermodynamic study on complexation of long-chain fatty acid anions with α-cyclodextrin in water. *Journal of Molecular Liquids* **311,** 113172. ISSN: 01677322 (2020).

86. Pereira, J. C., Valente, A. J. & Söderman, O. α-Cyclodextrin affects the acid-base properties of octanoic acid/sodium octanoate. *Journal of Molecular Liquids* **364,** 119955. ISSN: 01677322 (2022).

87. Rouget, J. B. *et al.* Size and sequence and the volume change of protein folding. *Journal of the American Chemical Society* **133,** 6020–6027. ISSN: 00027863 (2011).

88. Harpaz, Y., Gerstein, M. & Chothia, C. Volume changes on protein folding. *Structure* **2,** 641–649. ISSN: 09692126 (1994).

89. De Lisi, R., Lazzara, G., Milioto, S., Muratore, N. & Terekhova, I. V. Heat capacity study to evidence the interactions between cyclodextrin and surfactant in the monomeric and micellized states. *Langmuir* **19,** 7188–7195. ISSN: 07437463 (2003).

90. Young, T. F. & Smith, M. B. Thermodynamic properties of mixtures of electrolytes in aqueous solutions. *Journal of Physical Chemistry* **58,** 716–724. ISSN: 00223654 (1954).

91. Lazzara, G. & Milioto, S. Copolymer-cyclodextrin inclusion complexes in water and in the solid state. A physico-chemical study. *Journal of Physical Chemistry B* **112,** 11887–11895. ISSN: 15206106 (2008).

92. Inglese, A., Mavelli, F., De Lisi, R. & Milioto, S. Group contributions to the infinite dilution partial molar volumes of alkanes, alcohols, and glycols in polar organic solvents. *Journal of Solution Chemistry* **26,** 319–336. ISSN: 00959782 (1997).

93. Wilson, L. D. & Verrall, R. E. A volumetric study of β-cyclodextrin/hydrocarbon and β-cyclodextrin/fluorocarbon surfactant inclusion complexes in aqueous solutions. *Journal of Physical Chemistry B* **101,** 9270–9279. ISSN: 15206106 (1997).

94. Yang, Z. *et al.* Effect of β-cyclodextrin on the micellar behavior of cetyltrimethylammonium chloride in aqueous solution. *Zeitschrift fur Physikalische Chemie* **221,** 215–224. ISSN: 09429352 (2007).

95. Terekhova, I. V., De Lisi, R., Lazzara, G., Milioto, S. & Muratore, N. Volume and heat capacity studies to evidence interactions between cyclodextrins and nicotinic acid in water. *Journal of Thermal Analysis and Calorimetry* **92,** 285–290. ISSN: 13886150 (2008).

96. Wilson, L. D. & Verrall, R. E. A Volumetric Study of Cyclodextrin-α,ω-Alkyl Dicarboxylate Anion Complexes in Aqueous Solutions. *Journal of Physical Chemistry B* **104,** 1880–1886. ISSN: 15206106 (2000).

97. Saha, S., Roy, A., Roy, K. & Roy, M. N. Study to explore the mechanism to form inclusion complexes of β-cyclodextrin with vitamin molecules. *Scientific Reports* **6,** 1–12. ISSN: 20452322 (2016).

98. Manabe, M. *et al.* Volumetric study on the inclusion complex formation of α- and β-cyclodextrin with 1-alkanols at different temperatures. *Colloid and Polymer Science* **283,** 738–746. ISSN: 0303402X (2005).

99. Hingerty, B. & Saenger, W. Topography of Cyclodextrin Inclusion Complexes. 8. Crystal and Molecular Structure of the α-Cyclodextrin-Methanol-Pentahydrate Complex. Disorder in a Hydrophobic Cage. *Journal of the American Chemical Society* **98,** 3357–3365. ISSN: 15205126 (1976).

100. Steiner, T., M. Moreira da Silva, A., Teixeira-Dias, J. J. C., Mûller, J. & Saege, W. Rapid Water diffusion in a cage-type crystal lattice: β-Cyclodextrin dodecahydrate. *Angewandte Chimie* **34,** 13–14 (1995).

101. Myles, A. M., Barlow, D. J., France, G. & Lawrence, M. J. Analysis and modelling of the structures of β-cyclodextrin complexes. *BBA - General Subjects* **1199,** 27–36. ISSN: 03044165 (1994).

102. Sciortino, F. Entropy in self-assembly. *Rivista del Nuovo Cimento* **42,** 511–548. ISSN: 18269850 (2019).

103. Wang, A., Shi, W., Huang, J. & Yan, Y. Adaptive soft molecular self-assemblies. *Soft Matter* **12,** 337–357. ISSN: 17446848 (2016).

104. Aree, T., Schulz, B. & Reck, G. Crystal structures of β-cyclodextrin complexes with formic acid and acetic acid. *Journal of Inclusion Phenomena* **47,** 39–45. ISSN: 09230750 (2003).

105. Hunt, M. A., Rusa, C. C., Tonelli, A. E. & Balik, C. M. Structure and stability of columnar cyclomaltohexaose (α- cyclodextrin) hydrate. *Carbohydrate Research* **339,** 2805–2810. ISSN: 00086215 (2004).

106. Hunt, M. A., Rusa, C. C., Tonelli, A. E. & Balik, C. M. Structure and stability of columnar cyclomaltooctaose (γ- cyclodextrin) hydrate. *Carbohydrate Research* **340,** 1631–1637. ISSN: 00086215 (2005).

107. Rodríquez-Llamazares, S. *et al.* The structure of the first supramolecular α-cyclodextrin complex with an aliphatic monofunctional carboxylic acid. *European Journal of Organic Chemistry,* 4298–4300. ISSN: 1434193X (2007).

108. Takeo, K. & Kuge, T. Complexes of Starchy Materials with Organic Compounds. *Agricultural and Biological Chemistry* **34,** 1787–1794 (1970).

109. Zhou, C. *et al.* Self-assembly of channel type β-CD dimers induced by dodecane. *Scientific Reports* **4,** 1–6. ISSN: 20452322 (2014).

110. Yue, X., Chen, X., Li, Q. & Qian, Z. Soft aggregates formed by a nonionic phytosterol ethoxylate and β-cyclodextrin in aqueous solution. *Colloids and Surfaces A: Physicochemical and Engineering Aspects* **482,** 79–86. ISSN: 18734359 (2015).

111. Lazzara, G., Prevost, S. & Gradzielski, M. Selectivity of cyclodextrins as a parameter to tune the formation of pseudorotaxanes and micelles supramolecular assemblies. A systematic SANS study. *Soft Matter* **7,** 6082–6091. ISSN: 1744683X (2011).

112. Yang, S. *et al.* Giant capsids from lattice self-assembly of cyclodextrin complexes. *Nature Communications* **8,** 1–7. ISSN: 20411723 (2017).

113. Tsianou, M. & Fajalia, A. I. Cyclodextrins and surfactants in aqueous solution above the critical micelle concentration: Where are the cyclodextrins located? *Langmuir* **30,** 13754–13764. ISSN: 15205827 (2014).

114. Ahlnäs, T., Karlström, G. & Lindman, B. Dynamics and order of nonionic surfactants in neat liquid and micellar solution from multifield 13C NMR relaxation and 13C NMR chemical shifts. *Journal of Physical Chemistry* **91,** 4030–4036. ISSN: 00223654 (1987).

115. Schneider, H. J., Hacket, F., Rüdiger, V. & Ikeda, H. NMR studies of cyclodextrins and cyclodextrin complexes. *Chemical Reviews* **98,** 1755–1785. ISSN: 00092665 (1998).

116. Krueger, S. SANS provides unique information on the structure and function of biological macromolecules in solution. *Physica B: Condensed Matter* **241-243,** 1131–1137. ISSN: 09214526 (1998).

117. Narayanan, G., Boy, R., Gupta, B. S. & Tonelli, A. E. Analytical techniques for characterizing cyclodextrins and their inclusion complexes with large and small molecular weight guest molecules. *Polymer Testing* **62,** 402–439. ISSN: 01429418 (2017).

118. Lindner, P. & Schweins, R. The D11 small-angle scattering instrument: A new benchmark for SANS. *Neutron News* **21,** 15–18. ISSN: 10448632 (Apr. 2010).

119. Laue-Langevin, I. *D22 - Large dynamic range small-angle diffractometer (Institut Laue-Langevin)* 2003. https://www.ill.eu/users/instruments/instruments-list/d22/description/instrument-layout.

120. Dos Santos Silva Araujo, L., Lazzara, G. & Chiappisi, L. Thermoresponsive behavior of cyclodextrin inclusion complexes with weakly anionic alkyl ethoxy carboxylates. *Soft Matter* **18,** 17–19. ISSN: 1744-683X (2023).

121. Stewart, P. L. Cryo-electron microscopy and cryo-electron tomography of nanoparticles. *Wiley Interdisciplinary Reviews: Nanomedicine and Nanobiotechnology* **9,** 1–16. ISSN: 19390041 (2017).

122. Franken, L. E., Grünewald, K., Boekema, E. J. & Stuart, M. C. A Technical Introduction to Transmission Electron Microscopy for Soft-Matter: Imaging, Possibilities, Choices, and Technical Developments. *Small* **16,** 1–15. ISSN: 16136829 (2020).

123. Li, T., Nowell, C. J., Cipolla, D., Rades, T. & Boyd, B. J. Direct Comparison of Standard Transmission Electron Microscopy and Cryogenic-TEM in Imaging Nanocrystals Inside Liposomes. *Molecular Pharmaceutics* **16,** 1775–1781. ISSN: 15438392 (2019).

124. Flammersheim, H. J. *Ca lori metry* 31–63. ISBN: 9783642055935 (2003).

125. Cisse, A., Peters, J., Lazzara, G. & Chiappisi, L. PyDSC: a simple tool to treat differential scanning calorimetry data. *Journal of Thermal Analysis and Calorimetry* **145,** 403–409. ISSN: 15882926 (2021).

126. Wang, Y., Ma, N., Wang, Z. & Zhang, X. Photocontrolled reversible supramolecular assemblies of an azobenzene-containing surfactant with α-cyclodextrin. *Angewandte Chemie - International Edition* **46,** 2823–2826. ISSN: 14337851 (2007).

127. Xing, P. *et al.* Light and cucurbit[7]uril complexation dual-responsiveness of a cyanostilbene-based self-assembled system. *Nanoscale* **8,** 1892–1896. ISSN: 20403372 (2016).

128. Zhang, X. *et al.* Recent Advances in Cyclodextrin-Based Light-Responsive Supramolecular Systems. *Macromolecular Rapid Communications* **39,** 1–12. ISSN: 15213927 (2018).

129. Jiang, B. *et al.* Fabrication of a β-cyclodextrin-based self-assembly containing a redox-responsive ferrocene. *Soft Matter* **16,** 125–131. ISSN: 17446848 (2019).

130. Zuo, C. *et al.* Fabrication of dual-redox responsive supramolecular copolymers using a reducible β-cyclodextran-ferrocene double-head unit. *ACS Macro Letters* **5,** 873–878. ISSN: 21611653 (2016).

131. Zhang, H. *et al.* Redox-responsive vesicles prepared from supramolecular cyclodextrin amphiphiles. *Carbohydrate Research* **345,** 87–96. ISSN: 00086215 (2010).

132. Lazzara, G. *et al.* Temperature-responsive inclusion complex of cationic PNIPAAM diblock copolymer and γ-cyclodextrin. *Soft Matter* **8,** 5043–5054. ISSN: 1744683X (2012).

133. Perry, C. *et al.* Pluronic and β-cyclodextrin in water: From swollen micelles to self-assembled crystalline platelets. *Soft Matter* **7,** 3502–3512. ISSN: 17446848 (2011).

134. De Folter, J. W. *et al.* Self-organization of anisotropic and binary colloids in thermo-switchable 1D microconfinement. *Particle and Particle Systems Characterization* **32,** 313–320. ISSN: 15214117 (2015).

135. Jiang, L. *et al.* Helical colloidal sphere structures through thermo-reversible co-assembly with molecular microtubes. *Angewandte Chemie - International Edition* **52,** 3364–3368. ISSN: 14337851 (2013).

136. Liang, J. *et al.* Hierarchically Chiral Lattice Self-Assembly Induced Circularly Polarized Luminescence. *ACS Nano* **14,** 3190–3198. ISSN: 1936086X (2020).

137. Qi, W., Ma, C., Yan, Y. & Huang, J. Chirality manipulation of supramolecular self-assembly based on the host-guest chemistry of cyclodextrin. *Current Opinion in Colloid and Interface Science* **56,** 101526. ISSN: 18790399 (2021).

138. Wang, J., Qi, W., Lei, N. & Chen, X. Lamellar hydrogel fabricated by host-guest interaction between α-cyclodextrin and amphiphilic phytosterol ethoxylates. *Colloids and Surfaces A: Physicochemical and Engineering Aspects* **570,** 462–470. ISSN: 18734359 (2019).

139. Zhang, J. *et al.* Hydrogels Consisting of Vesicles Constructed via the Self-Assembly of a Supermolecular Complex Formed from α-Cyclodextrin and Perfluorononanoic Acid. *Langmuir* **35,** 16893–16899. ISSN: 15205827 (2019).

140. Jiang, L. *et al.* Special effect of β-cyclodextrin on the aggregation behavior of mixed cationic/anionic surfactant systems. *Journal of Physical Chemistry B* **113,** 7498–7504. ISSN: 15206106 (2009).

141. Schönbeck, C., Gaardahl, K. & Houston, B. Drug Solubilization by Mixtures of Cyclodextrins: Additive and Synergistic Effects. *Molecular Pharmaceutics* **16,** 648–654. ISSN: 15438392 (2019).

142. Jansook, P. & Loftsson, T. γCD/HPγCD: Synergistic solubilization. *International Journal of Pharmaceutics* **363,** 217–219. ISSN: 03785173 (2008).

143. Skiba, M. *Method For Synthesizing Calxarene and/or Cyclodextrin Copolymers, Terpolymers And Tetrapolymers, And Uses Thereof - US 2013/0018164 A1* 2013.

144. Gradzielski, M. & Hoffmann, I. Polyelectrolyte-surfactant complexes (PESCs) composed of oppositely charged components. *Current Opinion in Colloid and Interface Science* **35,** 124–141. ISSN: 18790399 (2018).

145. Guzmán, E., Fernández-Peña, L., Ortega, F. & Rubio, R. G. Equilibrium and kinetically trapped aggregates in polyelectrolyte–oppositely charged surfactant mixtures. *Current Opinion in Colloid and Interface Science* **48,** 91–108. ISSN: 18790399 (2020).

146. Lindman, B., Antunes, F., Aidarova, S., Miguel, M. & Nylander, T. Polyelectrolyte-surfactant association—from fundamentals to applications. *Colloid Journal* **76,** 585–594. ISSN: 1061933X (2014).

147. Schlenoff, J. B., Rmaile, A. H. & Bucur, C. B. Hydration contributions to association in polyelectrolyte multilayers and complexes: Visualizing hydrophobicity. *Journal of the American Chemical Society* **130,** 13589–13597. ISSN: 00027863 (2008).

148. Chiappisi, L., Hoffmann, I. & Gradzielski, M. Complexes of oppositely charged polyelectrolytes and surfactants - Recent developments in the field of biologically derived polyelectrolytes. *Soft Matter* **9,** 3896–3909. ISSN: 17446848 (2013).

149. Piculell, L. *et al.* Controlling structure in associating polymer-surfactant mixtures. *Pure and Applied Chemistry* **79,** 1419–1434. ISSN: 00334545 (2007).

150. Piculell, L. Understanding and exploiting the phase behavior of mixtures of oppositely charged polymers and surfactants in water. *Langmuir* **29,** 10313–10329. ISSN: 07437463 (2013).

151. Chiappisi, L. & Gradzielski, M. Co-assembly in chitosan-surfactant mixtures: Thermodynamics, structures, interfacial properties and applications. *Advances in Colloid and Interface Science* **220,** 92–107. ISSN: 00018686 (2015).

152. Zhou, S. & Chu, B. Assembled Materials : Polyelectrolyte ± Surfactant Complexes **. *Advanced Materials* **12,** 544–556 (2000).

153. Piculell, L. Understanding and exploiting the phase behavior of mixtures of oppositely charged polymers and surfactants in water. *Langmuir* **29,** 10313–10329. ISSN: 07437463 (2013).

154. Janiak, J., Piculell, L., Olofsson, G. & Schillén, K. The aqueous phase behavior of polyion-surfactant ion complex salts mixed with nonionic surfactants. *Physical Chemistry Chemical Physics* **13,** 3126–3138. ISSN: 14639076 (2011).

155. Fegyver, E. & Mészáros, R. The impact of nonionic surfactant additives on the nonequilibrium association between oppositely charged polyelectrolytes and ionic surfactants. *Soft Matter* **10,** 1953–1962. ISSN: 1744683X (2014).

156. Chiappisi, L., David Leach, S. & Gradzielski, M. Precipitating polyelectrolyte-surfactant systems by admixing a nonionic surfactant-a case of cononsurfactancy. *Soft Matter* **13,** 4988–4996. ISSN: 17446848 (2017).

157. Ram-On, M., Cohen, Y. & Talmon, Y. Effect of polyelectrolyte stiffness and solution pH on the nanostructure of complexes formed by cationic amphiphiles and negatively charged polyelectrolytes. *Journal of Physical Chemistry B* **120,** 5907–5915. ISSN: 15205207 (2016).

158. Percebom, A. M. & Loh, W. Controlling the phase structures of polymer/surfactant complexes by changing macromolecular architecture and adding n-alcohols. *Journal of Colloid and Interface Science* **466,** 377–387. ISSN: 10957103 (2016).

159. Ishiguro, M. & Koopal, L. K. Binding of alkylpyridinium chloride surfactants to sodium polystyrene sulfonate. *Colloids and Surfaces A: Physicochemical and Engineering Aspects* **347,** 69–75. ISSN: 09277757 (2009).

160. Nakai, K., Ishihara, K. & Yusa, S. I. Complexes Covered with Phosphorylcholine Groups Prepared by Mixing Anionic Diblock Copolymers and Cationic Surfactants. *Langmuir* **33,** 5236–5244. ISSN: 15205827 (2017).

161. Potaś, J., Szymańska, E. & Winnicka, K. Challenges in developing of chitosan – Based polyelectrolyte complexes as a platform for mucosal and skin drug delivery. *European Polymer Journal* **140,** 110020. ISSN: 00143057 (2020).

162. Mukhtar Ahmed, K. B., Khan, M. M. A., Siddiqui, H. & Jahan, A. Chitosan and its oligosaccharides, a promising option for sustainable crop production-a review. *Carbohydrate Polymers* **227,** 115331. ISSN: 01448617 (2020).

163. Cavallaro, G., Micciulla, S., Chiappisi, L. & Lazzara, G. Chitosan-based smart hybrid materials: A physico-chemical perspective. *Journal of Materials Chemistry B* **9,** 594–611. ISSN: 20507518 (2021).

164. Schatz, C., Viton, C., Delair, T., Pichot, C. & Domard, A. Typical physicochemical behaviors of chitosan in aqueous solution. *Biomacromolecules* **4,** 641–648. ISSN: 15257797 (2003).

165. Rinaudo, M., Kil'Deeva, N. R. & Babak, V. G. Surfactant-polyelectrolyte complexes on the basis of chitin. *Russian Journal of General Chemistry* **78,** 2239–2246. ISSN: 10703632 (2008).

166. Mourya, V. K. & Inamdar, N. N. Chitosan-modifications and applications: Opportunities galore. *Reactive and Functional Polymers* **68,** 1013–1051. ISSN: 13815148 (2008).

167. Guzmán, E., Ortega, F. & Rubio, R. G. Chitosan: A Promising Multifunctional Cosmetic Ingredient for Skin and Hair Care. *Cosmetics* **9,** 1–15. ISSN: 20799284 (2022).

168. Malerba, M. & Cerana, R. Recent advances of chitosan applications in plants. *Polymers* **10,** 1–10. ISSN: 20734360 (2018).

169. Moura, L. I. *et al.* Chitosan-based dressings loaded with neurotensin - An efficient strategy to improve early diabetic wound healing. *Acta Biomaterialia* **10,** 843–857. ISSN: 18787568 (2014).

170. Patrulea, V., Ostafe, V., Borchard, G. & Jordan, O. Chitosan as a starting material for wound healing applications. *European Journal of Pharmaceutics and Biopharmaceutics* **97,** 417–426. ISSN: 18733441 (2015).

171. Dragostin, O. M. *et al.* New antimicrobial chitosan derivatives for wound dressing applications. *Carbohydrate Polymers* **141,** 28–40. ISSN: 01448617 (2016).

172. Ravi Kumar, M. N. A review of chitin and chitosan applications. *Reactive and Functional Polymers* **46,** 1–27. ISSN: 13815148 (2000).

173. Hirano, S. Chitin and chitosan as novel biotechnological materials. *Polymer International* **48,** 732–734. ISSN: 09598103 (1999).

174. Chiappisi, L., Simon, M. & Gradzielski, M. Toward bioderived intelligent nanocarriers for controlled pollutant recovery and pH-sensitive binding. *ACS Applied Materials and Interfaces* **7,** 6139–6145. ISSN: 19448252 (2015).

175. Lichtfouse, E. *et al.* Chitosan for direct bioflocculation of wastewater. *Environmental Chemistry Letters* **17,** 1603–1621. ISSN: 16103661 (2019).

176. Biswas, S., Fatema, J., Debnath, T. & Rashid, T. U. ChitosanClay Composites for Wastewater Treatment: A State-of-the-Art Review. *ACS ES and T Water* **1,** 1055–1085. ISSN: 26900637 (2021).

177. Wang, H., Qian, J. & Ding, F. Emerging Chitosan-Based Films for Food Packaging Applications. *Journal of Agricultural and Food Chemistry* **66,** 395–413. ISSN: 15205118 (2018).

178. Kabanov, V. L. & Novinyuk, L. V. Chitosan Application in Food Technology: a Review of Rescent Advances. *Food systems* **3,** 10–15. ISSN: 2618-9771 (2020).

179. Thongngam, M. & McClements, D. J. Characterization of Interactions between Chitosan and an Anionic Surfactant. *Journal of Agricultural and Food Chemistry* **52,** 987–991. ISSN: 00218561 (2004).

180. Thongngam, M. & McClements, D. J. Influence of pH, ionic strength, and temperature on self-association and interactions of sodium dodecyl sulfate in the absence and presence of chitosan. *Langmuir* **21,** 79–86. ISSN: 07437463 (2005).

181. Jiang, S., Qiao, C., Wang, X., Li, Z. & Yang, G. Structure and properties of chitosan/sodium dodecyl sulfate composite films. *RSC Advances* **12,** 3969–3978. ISSN: 20462069 (2022).

182. Onesippe, C. & Lagerge, S. Study of the complex formation between sodium dodecyl sulfate and chitosan. *Colloids and Surfaces A: Physicochemical and Engineering Aspects* **317,** 100–108. ISSN: 09277757 (2008).